THE FLORIDA STATE UNIVERSITY

COLLEGE OF ARTS AND SCIENCES

THE RELATIONSHIP BETWEEN LOW-FREQUENCY NORTH ATLANTIC SEA SURFACE TEMPERATURES AND EASTERN NORTH AMERICAN CLIMATE

By

ANTHONY ARGUEZ

A Thesis submitted to the
Department of Meteorology
in partial fulfillment of the
requirements for the degree of
Master of Science

Degree Awarded:
Summer Semester, 2002

The members of the Committee approve the

thesis of Anthony Arguez defended on

June 6, 2002

James J. O'Brien
Professor Directing Thesis

James B. Elsner
Committee Member

Henry E. Fuelberg
Committee Member

Kwang-Yul Kim
Committee Member

This thesis is dedicated to my loving mother, Angela Arguez. Your inspiration is the foundation of my success in life. Te quiero, Mima.

ACKNOWLEDGEMENTS

Primary funding for this work was obtained from the Center for Ocean-Atmospheric Prediction Studies, which receives its base funding from NOAA's Office of Global Programs. The American Meteorological Society, DynCorp Information Systems, and the Florida State University's Office of Graduate Studies provided additional support through a pair of graduate fellowships. I would like to thank the Hadley Centre and the UK Met Office for providing the HadISST data set. Additional thanks go to the thesis committee, consisting of H. Fuelberg, K. Kim, and J. Elsner. Special thanks go to Shawn Smith, Kyle Hilburn, and Josh Grant for their valuable advice and support. I would also like to express my heartfelt appreciation for my major professor, Dr. James J. O'Brien. Without his guidance and flexibility, this project could not have succeeded.

TABLE OF CONTENTS

REFERENCES 94

BIOGRAPHICAL SKETCH 97

LIST OF FIGURES

ABSTRACT

A time series of North Atlantic sea surface temperature anomalies is constructed by grid-averaging monthly anomalies from the Labrador Sea to Iceland from 1901-1999. The relationship between this North Atlantic SST Index (NASSTI) and temperature and precipitation anomalies over eastern North America is investigated. The NASSTI is low-pass filtered to isolate low-frequency fluctuations and separated into three parts: a warm phase (top 20%), a neutral phase, and a cold phase (bottom 20%).

The NASSTI is compared to low-pass filtered time series of the Arctic Oscillation (AO) and the North Atlantic Oscillation (NAO), which have been shown to significantly influence the climate regime over eastern North America during the boreal winter (Thompson and Wallace, 2001; Hurrell, 1995). The AO and NAO indices are categorized in a fashion similar to the NASSTI, yielding a high phase, a neutral phase, and a low phase. The NAO and AO, which are well indexed by westerly wind anomalies over the North Atlantic mid-latitudes (Wallace and Thompson, 2002), are negatively correlated with the NASSTI. This may be due to the dominance of the oceanic response to atmospheric forcing, as stronger (weaker) westerlies are associated with increased (decreased) evaporation, leading to cold (warm) SST anomalies. During the low phases of the AO/NAO, a dipole in temperature anomalies exists in which much of eastern Canada is considerably warmer than normal (the neutral phase), while most of the eastern

of the AO/NAO, a dipole in temperature anomalies exists in which much of eastern Canada is considerably warmer than normal (the neutral phase), while most of the eastern

U.S. experiences slightly cooler temperatures. The high phases of the AO and NAO are associated with the reverse conditions.

The cold-neutral deviations reveal a dipole-like pattern in winter temperatures, with considerably colder conditions in Quebec and slightly warmer temperatures in much of the United States. This corresponds well with the impacts of the high phase of the AO/NAO. Precipitation deviations from neutral during the cold phase are not as spatially or temporally coherent, although fall precipitation tends to be marginally wetter than normal over most of the U.S. stations during fall (OND). Precipitation anomalies during the warm phase do not yield any discernible large-scale patterns. Warm phase temperature deviations from neutral reveal a general warming from late fall to early spring over much of eastern North America. The signal arrives in fall in the Ohio River Valley and moves northeastward in time, amplifying as it reaches northern Quebec before subsiding in the spring. This propagating pattern does not appear to correspond to any large-scale AO/NAO impact in the region, but it does agree with low-neutral conditions over eastern Canada.

INTRODUCTION

The expansion of research interest in climate variability, fueled by a great desire to understand the El Niño Southern Oscillation (ENSO), has focused attention on several dominant modes of climate variability. These include, but are not limited to, the North Atlantic Oscillation (NAO), the Arctic Oscillation (AO), and the Pacific Decadal Oscillation (PDO). The AO and NAO describe atmospheric mass fluctuations between the Arctic and the Northern Hemisphere's middle latitudes. The PDO is an interdecadal, ENSO-like fluctuation in sea surface temperature (SST) centered over the North Pacific Ocean. These climate oscillations are well known not only for their aperiodic variability along numerous timescales, but also for the climate impacts they impart on their respective regions of influence.

The present study investigates the relation between low-frequency North Atlantic SST anomalies and eastern North American climate. SST's are used because the ocean plays a large role in determining long-term climate fluctuations, given the ocean's large specific heat and inertia. In addition, several studies have indicated that the North Atlantic Ocean is a region of intense ocean-atmosphere coupling, particularly during winter (Häkkinen, 2000; Mizoguchi et al., 1999). Other studies have shown that prescribed North Atlantic SST's in an atmospheric general circulation model (AGCM) can reproduce the low-frequency variability characterized by the NAO/AO (Rodwell et

can reproduce the low-frequency variability characterized by the NAO/AO (Rodwell et al., 1999; Mehta et al, 2000).

The NAO and AO, which are arguably the same phenomenon (Wallace, 2000), are unique because most of the emerging interest in them can be attributed to upward trends in their indices (Wallace and Thompson, 2002). However, the oscillatory components of the AO and NAO are also important, particularly for the forecasting of Northern Hemisphere climate (Higgins et al., 2000). Over the United States and Canada, low-frequency fluctuations in the AO/NAO explain a significant portion of climate variability. During the low-index phases of the AO and NAO, eastern Canada experiences warmer conditions while negative temperature anomalies reside over the eastern United States. The high-index phase brings the opposite dipole pattern in temperature to eastern North America (Wallace and Thompson, 1998; Hurrell, 1995).

In light of the recent findings mentioned above, it may be possible to find a meaningful relation between North Atlantic SST anomalies and climate change in the eastern United States and Canada. It will be shown that a meaningful link does exist for temperature, but not for precipitation, and that the link is primarily conspicuous during winter. Cold North Atlantic SST anomalies influence eastern North American temperatures in the same manner as the high phases of the AO and NAO. However, warm temperature anomalies engulf most of eastern North America when North Atlantic SST anomalies are warm.

Section 1 discusses recent papers on North Atlantic SST variability, with emphasis on low-frequency variability. Sections 2 and 3 provide additional background on the NAO and AO, respectively. The data sets are introduced in Section 4, while Section 5 describes the methodology. The results of the SST Index analyses are

Section 5 describes the methodology. The results of the SST Index analyses are presented in Section 6. Section 7 interprets the results with respect to the AO and NAO.

A summary and a discussion are offered in Section 8. Finally, the appendices include a description of the running sum filter, as well as auxiliary figures that are not referenced in the text.

NORTH ATLANTIC SST VARIABILITY

The North Atlantic Ocean plays an important role in the global ocean-atmosphere system. It is home to the Gulf Stream and a significant branch of the global Thermohaline Circulation. The North Atlantic is also a significant source of deep-water formation. In addition, the majority of the sea ice that forms in the Arctic Ocean makes its way into the North Atlantic. On a more practical note, the Atlantic Ocean is particularly informative for climate studies because it is one of few basins with a relatively long observation record.

The North Atlantic exhibits numerous modes of low-frequency variability in SST. The dominant mode is multidecadal, while significant modes also exist at quasi-decadal and inter-annual timescales. Kushnir (1994) investigated interdecadal variability in the North Atlantic, pointing out that there were cold anomalies before 1920, warm anomalies between 1930 and 1960, and a return to cold anomalies in this region in the 1970s and 1980s. Delworth et al. (1993) described a 50-year oscillation in the North Atlantic Ocean's thermohaline circulation, which resembled the patterns found by Kushnir. Using a real EOF analysis of North Atlantic SSTs, Deser and Blackmon (1993, hereafter DB) also found a multidecadal mode, with a period of 25 years. More recently, Kerr (2000) described a 65-80 year mode in the North Atlantic obtained from proxy records (tree rings) that he termed the Atlantic Multidecadal Oscillation (AMO). Delworth and Mann

rings) that he termed the Atlantic Multidecadal Oscillation (AMO). Delworth and Mann

(2000) were able to reproduce a 50-60 year mode in the GFDL model, which they attributed to the AMO.

DB also described a secondary mode that corresponded to a 12-14 year oscillation. This quasi-decadal mode lagged decadal sea ice anomalies in the region by 2 years, prompting Deser and Blackmon to suggest that the 12-14 year SST fluctuation arises from sea ice variability in the Arctic. Mizoguchi et al. (1999) utilized complex EOF analysis (or propagating EOFs) to investigate low frequency modes in North Atlantic SST. The dominant mode has a 42-year period with centers of action that are associated with deep-water formation, namely the Labrador Sea, off the Newfoundland coast, and South of Greenland. Mizoguchi et al. combined the second and third modes, describing a roughly 14-year propagating pattern similar to the mode found in DB.

Delworth (1996) investigated interannual SST variability in the North Atlantic, using a coupled model. The SST variability resembled the NAO footprint in this region, and Delworth suggested that North Atlantic interannual SST variability is primarily a result of atmospheric (wind stress) forcing. These findings agree with the critical conclusions made by Bjerknes (1964) in which the atmosphere forces the interannual variability in the North Atlantic, whereas longer timescales of variability derive from intrinsic oceanic processes.

THE NORTH ATLANTIC OSCILLATION (NAO)

The North Atlantic Oscillation is an atmospheric signature of general circulation anomalies over the North Atlantic Ocean. Sir Gilbert Walker discovered the signal in the 1930s, as he investigated the global teleconnectivity of the Indian monsoon (Walker, 1924). The NAO is essentially a fluctuation in the meridional pressure gradient over the North Atlantic Ocean. The NAO imparts a great deal of influence on the North Atlantic wind regime, transports of heat and moisture, extratropical and tropical storm tracks, and even marine and land ecosystems (Hurrell et al., 2001).

The NAO Index is usually defined as the normalized difference in Mean Sea Level Pressure (MSLP) between stations near the climatological Subtropical (Azores) High and the Sub-polar (Icelandic) Low. The northern station is usually a station in Iceland. The southern station is not as fixed, with different indices using stations in Lisbon (Portugal), Ponta Delgada (Azores Islands, Portugal), and Gibraltar (a British territory in southern Spain). Large positive values indicate an anomalously intense pressure gradient, while weak pressure gradients translate into a negative index. Thus, the NAO can be considered a metric of westerly winds across the mid-latitudes of the North Atlantic basin.

The NAO exhibits several low frequency modes, including quasi-biennial, quasi-decadal, and interdecadal modes (Deser and Blackmon 1993). These low-frequency

decadal, and interdecadal modes (Deser and Blackmon 1993). These low-frequency

modes have been associated with oceanic variability (Rodwell et al., 1999; Mehta et al.,

2000), since the heat capacity of the ocean dwarfs that of the atmosphere. The low-frequency component of the NAO is speculated to be amplifying (Hurrell and van Loon, 1997). The NAO has also exhibited a significant positive trend in the past 40 years, prompting some scientists to use this as evidence of global warming (Shindell et al., 1999). It may be premature, though, to extract the notion of global warming from what may be natural variability.

THE ARCTIC OSCILLATION (AO)

The Arctic Oscillation is a hemisphere-wide, dominant mode of atmospheric variability. It is defined as the leading empirical orthogonal function (EOF) north of 20° N of sea level pressure, geopotential height, or zonal wind (Thompson and Wallace, 1998). The AO pattern is characterized by strong zonal symmetry and a dominant Arctic action center, giving it an annular appearance. Deser (2001) showed that the annular appearance of the AO is a consequence of this principal Arctic action center, as opposed to longitudinal teleconnectivity between its Pacific and Atlantic sectors.

The Arctic Oscillation pattern is also known as the Northern Hemisphere Annular Mode (NAM). The Southern Hemisphere Annular Mode (also known as the Antarctic Oscillation) is the NAM's austral counterpart (Gong and Wang, 1999). Both modes are well indexed by the strength of the westerlies at 55° in their respective hemispheres.

The NAO, on the other hand, has been characterized as the Atlantic manifestation of the broader AO. Their spatial signals are essentially the same. However, their time series are only distinguishable if a crude, station-based index is used for the NAO, which is common practice (Wallace 2000).

The Arctic Oscillation is associated with a pronounced coupling between the stratosphere and the troposphere. Baldwin and Dunkerton (2000) showed that the AO's tropospheric signature is linked to the strength of the stratospheric polar vortex. Using

tropospheric signature is linked to the strength of the stratospheric polar vortex. Using

lag correlations, they demonstrate that the AO pattern first appears at stratospheric levels

and propagates downward, reaching the surface in roughly 3 weeks. Thus, the Arctic Oscillation signal is conspicuous throughout the troposphere and it is apparently maintained by atmospheric forcing.

DATA

The data for this project are extracted from four data sets. North Atlantic SSTs are from the Hadley Centre Sea Ice and Sea Surface Temperature Data Set (HadISST). Temperature and Precipitation from select stations in the Eastern United States and Canada are retrieved from the Global Historical Climatology Network (GHCN) data set. In addition, indices of the AO and the NAO are used. Each of the data sets consists of monthly values between 1901 and 1999.

The HadISST contains SSTs, including values for sea ice, on a 1° by 1° resolution over the globe for all months between 1871 and 1999. HadISST incorporates data from numerous different sources and utilizes rigorous quality control techniques, accounting for biases inherent in other data sets such as COADS (Woodruff et al., 1987). Grid boxes that contained sea ice during a particular month are defined by an SST of –1.8°C (Parker and Rayner, 2000). Although the HadISST does contain missing values, the North Atlantic (in middle latitudes at least) is not as susceptible to data voids because ships routinely traversed this region during the last century.

The GHCN data set (Peterson and Vose, 1997) is a compilation of station climate data, made available through collaboration between the National Climatic Data Center, Arizona State University, and the Carbon Dioxide Information Analysis Center. Version 2 of the data set, released in 1997, includes monthly temperature (mean, maximum, and

2 of the data set, released in 1997, includes monthly temperature (mean, maximum, and
minimum) and precipitation (monthly total) data from over 7,000 different stations

worldwide. A considerable number of stations are substantially incomplete, and not all stations report data for each variable. The data are plentiful over the United States and southern Canada; however, the spatial coverage and data completeness over Northeast Canada is not as ideal, given the region's low population density. All forms of precipitation are included in the totals, i.e. snow and rainfall are not distinguished.

The Arctic Oscillation time series utilized in the present study was defined by Thompson and Wallace (2000). They use SLP from two sources: monthly anomalies before 1958 are obtained from Trenberth and Paolino (1980), while the anomalies from 1958 to the present come from the NCEP/NCAR Reanalysis. They define the AO (pattern) as the leading empirical orthogonal function (EOF) of SLP north of 20° N, using monthly SLP anomalies from January 1958 to April 1997. The AO index is calculated by projecting the leading EOF onto the SLP anomalies. The index is then normalized, such that the resulting units are arbitrary (Thompson and Wallace, 2000).

The NAO index (Jones et al., 1997) is obtained from the Climate Research Unit of the University of East Anglia (UK). It consists of the normalized pressure difference between Gibraltar and Reykjavik. By using these two stations, the NAO Index was extended back to 1821. Using Gibraltar as the southern station (instead of Lisbon or Ponta Delgada), the wintertime (DJF) correlations are marginally more negative, although this does not hold for the remainder of the year.

METHODOLOGY

The North Atlantic SST Index (NASSTI) was calculated from data in the HadISST data set. All monthly SST values in the box bounded by 51° N, 65° N, 23° W, and 65°W are averaged, yielding a monthly time series. For simplicity, the grid boxes were not weighted by the cosine of the latitude. This may inject bias into the time series since sea ice is often present in the northern extent of the SST box, although the effect is not considered significant. Subsequently, the monthly SST series was detrended and the monthly climatology (over the 99-year period) was removed. The time series was then low-pass filtered with a 145-point binomial filter, or 72 consecutive 1-2-1 hannings. This filtering scheme reduces three-year periods by 50%, while lower frequencies retain most of their spectral energy and the highest frequencies are essentially removed (Figure 1). Filtering over the series ends was accomplished by extending the series symmetrically, thereby reducing the degrees of freedom of these points.

Following the ENSO convention, the NASSTI is separated into three parts: a warm phase, a neutral phase, and a cold phase (see Figure 2a). The warm and cold phases represent the top and bottom 20% of the SST anomaly values, respectively. The 20% threshold is selected as a compromise between station data completeness (specifically the data voids in Canada) and a desire to isolate extreme events. Note that there is no persistence criterion, although intensive filtering generally tends to impart persistence to time series.

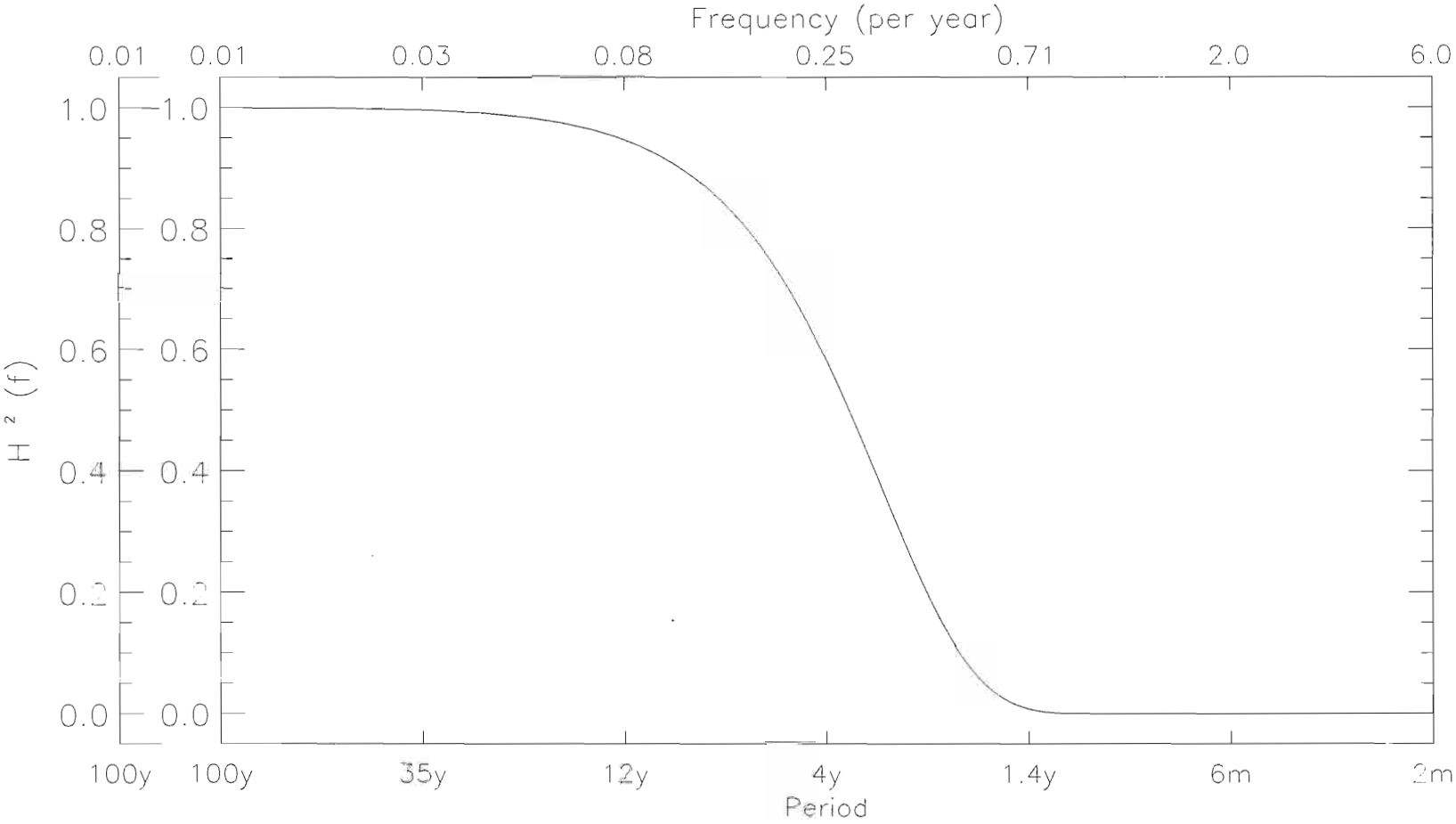

Figure 1. The F 1. The Power Transfer Function of a 145-point Gaussian filter. The x-axis is plotted on a logarithmic scale to highlight lower frequencfrequencies.

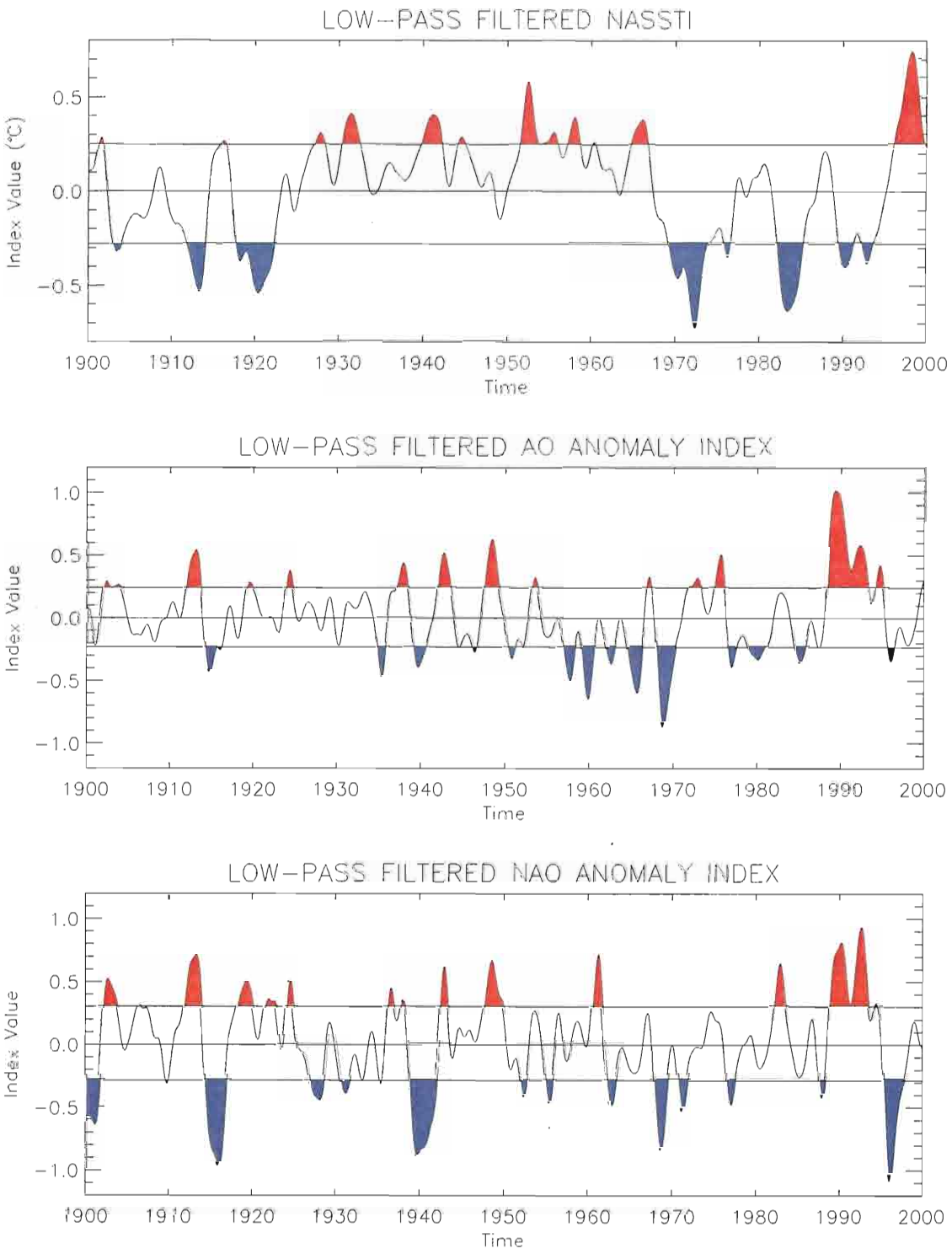

Figure 2. Time series of the (a) NASSTI, (b) the AO Index, and (c) the NAO Index. All three indices were passed through the 145-point Gaussian filter. Red shading

Figure 2. Time series of the (a) NASSTI, (b) the AO Index, and (c) the NAO Index. All three indices were passed through the 145-point Gaussian filter. Red shading indicates the top 20% of the anomaly values, defined as the warm phase for the NASSTI and the high phases for the AO and NAO. Blue shading corresponds to the cold NASSTI phase and the AO and NAO's low phase.

Fifty-one GHCN stations are used for the temperature analysis, whereas 43 stations were utilized in assessing precipitation impacts. The stations were selected with an explicit desire to maximize spatial coherence and data completeness. Total deviations (from neutral) in mean monthly temperature and monthly precipitation are obtained for each station during the warm and cold phases of the NASSTI. Deviations are also evaluated on a monthly basis, reported as three-month seasonal averages. For precipitation, the deviations are also divided by the mean neutral phase value, yielding percent deviations. All comparisons are made with respect to the neutral phase, as opposed to the total mean, because the neutral value is isolated from extreme phase values, whereas the mean incorporates all 3 phases.

We compare the NASSTI to time series of the AO and NAO to assist in the interpretation of the impacts of low frequency SST anomalies in the North Atlantic. The AO and NAO series are filtered with the same 145-point binomial filter (Figure 2bc). Cross-correlations are calculated among the AO, NAO, and NASSTI. Monthly variances and sample spectra (periodograms) are also computed for these three indices. Next, the indices are passed through a running sum filter (see Appendix A) to further analyze lower frequencies. The total and seasonal deviations are also computed using the filtered AO and NAO indices in place of the NASSTI. For the NAO and AO, we distinguish the extreme phases, the top and bottom 20% of the distributions, as the high polarity phase and the low polarity phase, respectively.

Hypothesis testing is utilized to ascertain whether the seasonal deviations in temperature or precipitation are significant. Every seasonal deviation is associated with a

temperature or precipitation are significant. Every seasonal deviation is associated with a
two-tailed t-means test (a difference in means test using the t-statistic) at the 95%

confidence level. For simplicity, an adjustment for simultaneous t-tests, such as the Bonferroni or Tukey adjustments, is not employed. However, such an adjustment would be necessary to claim 95% confidence over all stations simultaneously.

The t-statistic is proportional to the inverse square root of the combined sample size. Thus, extreme-neutral deviations where the sample sizes are relatively small (e.g. a hand full of the Canadian stations) must be somewhat larger in magnitude for the null hypothesis (a difference of zero) to be rejected. Although robustness is a concern due to a few cases of small sample size, preliminary analysis showed that the resulting p-values are resistant to outliers. In addition, it must be noted that the independence assumption is not obeyed precisely because of the inherent autocorrelation of atmospheric time series. The 20% threshold used to define extreme values in the NASSTI, AO, and NAO series was chosen with the above issues (robustness and independence) in mind. Furthermore, results obtained when using 25% and 33.3% as the threshold values suggest that using 20% is acceptable, given the similarity of outcomes.

RESULTS

a. Temperature

Surface temperature deviations from neutral during the NASSTI's warm phase reveal a general warming over much of eastern North America (Figure 3). Seasonal composites indicate that this pattern is most intense during winter. Positive temperature anomalies first appear in the Ohio River Valley (ORV) and the Great Lakes (GL) region in the fall (Figure 4). During DJF, the largest deviations are located over eastern Canada (Figure 5), while the temperature anomalies in ORV and GL have also increased in magnitude. By early spring (FMA), the temperature anomalies in ORV and GL have disappeared, while the withdrawal of the eastern Canadian anomalies has commenced (Figure 6). Animations confirm the existence of a propagating signal in temperature anomalies from southwest to northeast during the warm phase of the NASSTI. This propagation can also be seen using a seasonal Hovmöller diagram (Figure 7).

During the cold phase, a dipole-like pattern exists (Figure 8). Eastern Canada, which borders the SST domain, experiences colder than neutral conditions, while most of the eastern U.S. experiences warm anomalies. Again, the amplitude of the anomalies peak during the winter (Figure 9). The gradient pattern appears to be stationary, with both poles amplifying from fall to winter and fading as spring arrives. It is important to

both poles amplifying from fall to winter and fading as spring arrives. It is important to note that the cold phase and warm phase deviations are not converse patterns.

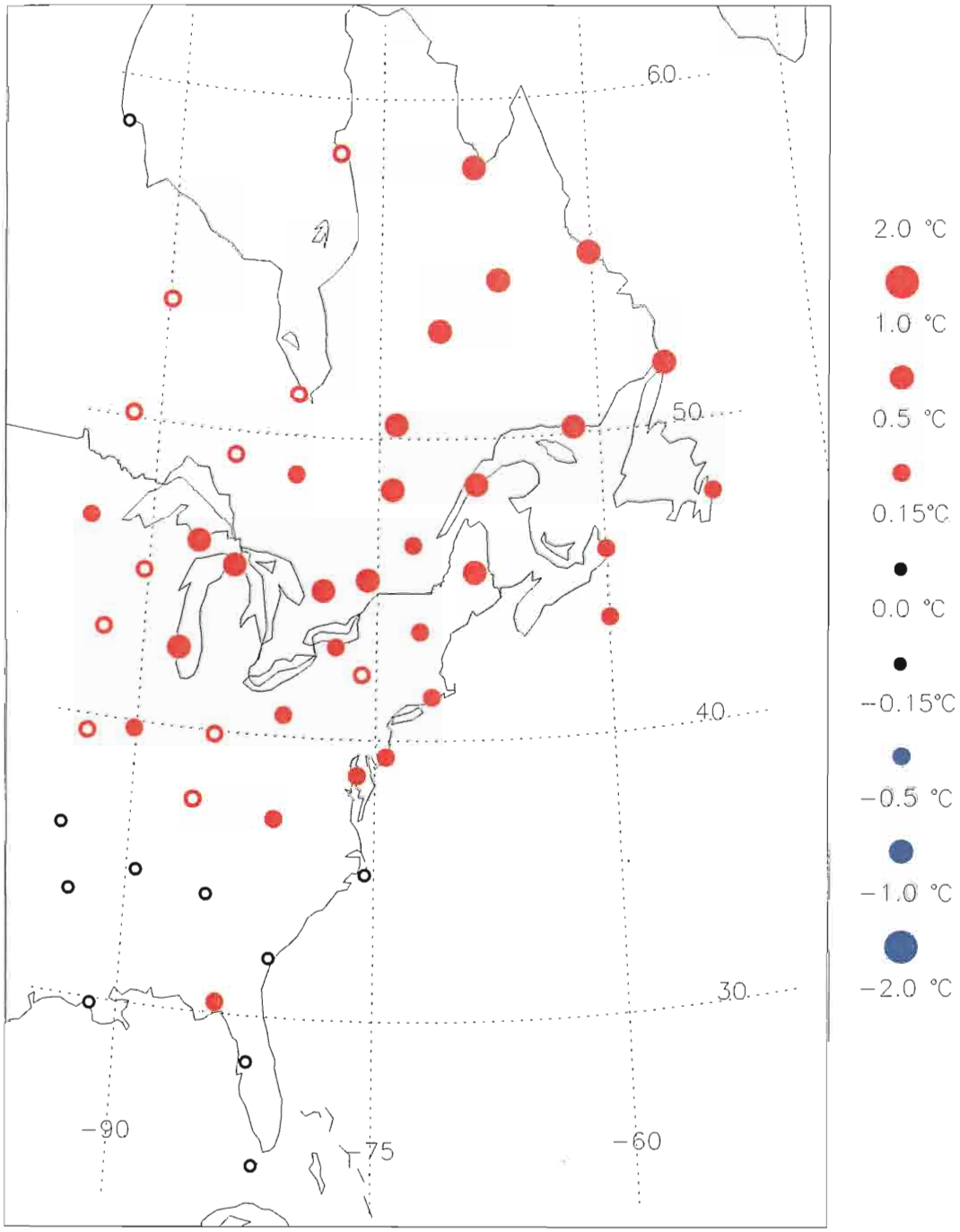

Figure 3. Mean temperature anomalies during the NASSTI warm phase, with respect to the neutral phase. Completely filled circles indicate deviations that are

Figure 3. Mean temperature anomalies during the NASSTI warm phase, with respect to the neutral phase. Completely filled circles indicate deviations that are statistically significant at the 95% confidence level.

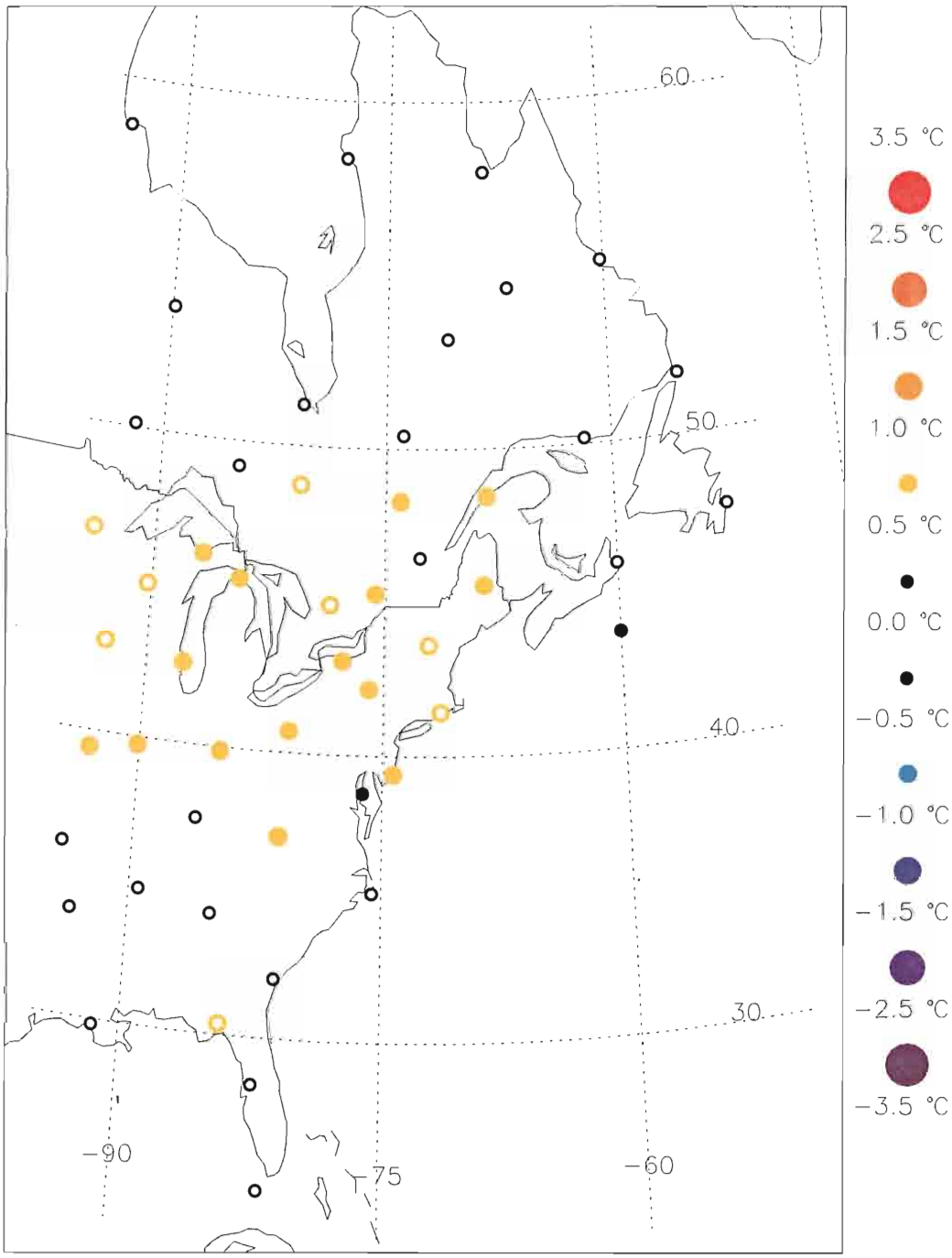

Figure 4. Warm-Neutral NASSTI temperature anomalies during OND.

Figure 4. Warm-Neutral NASSTI temperature anomalies during OND.

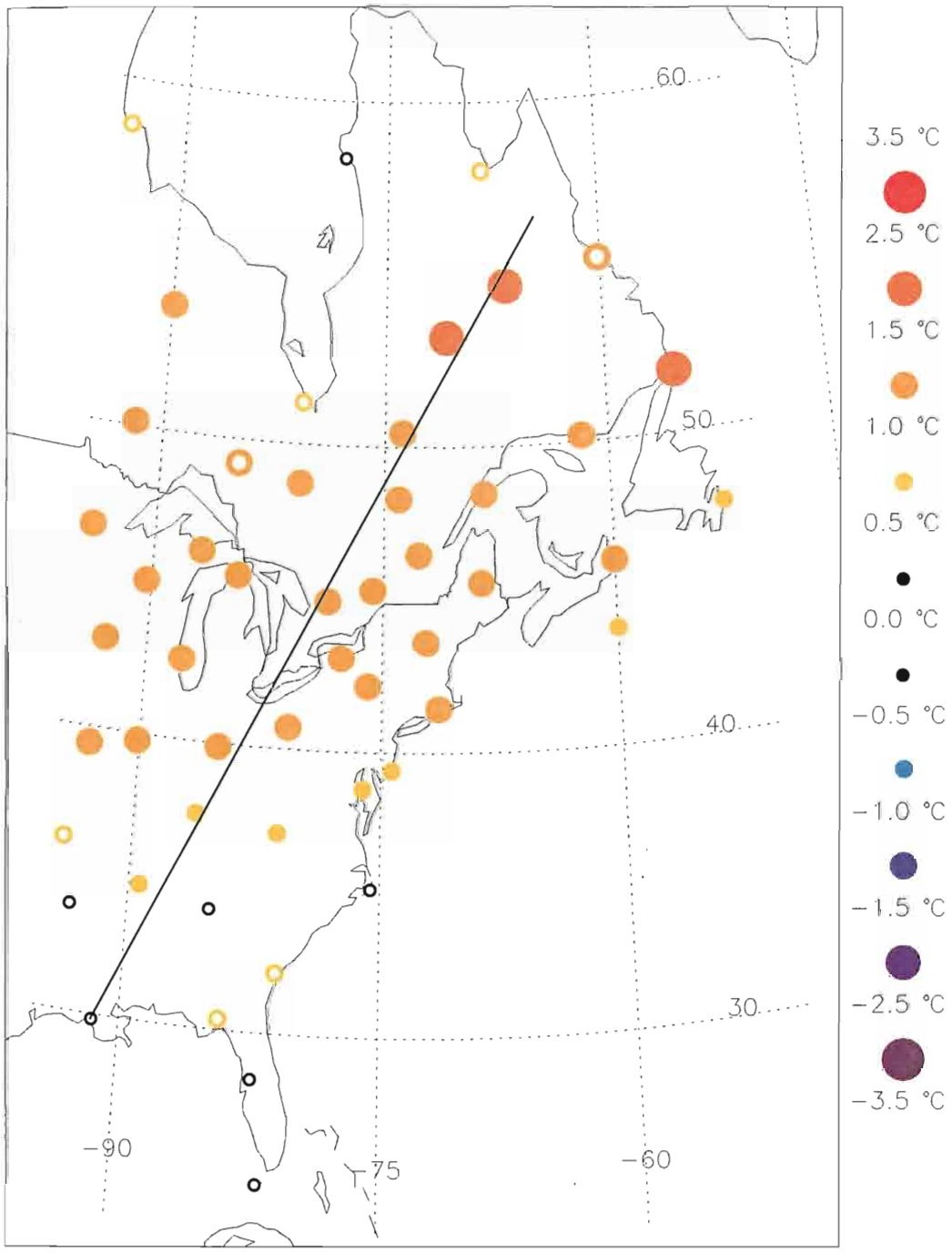

Figure 5. Warm-Neutral NASSTI temperature anomalies during DJF. The straight line is the propagation axis used in Figure 7.

Figure 5. Warm-Neutral NASSTI temperature anomalies during DJF. The straight line is the propagation axis used in Figure 7.

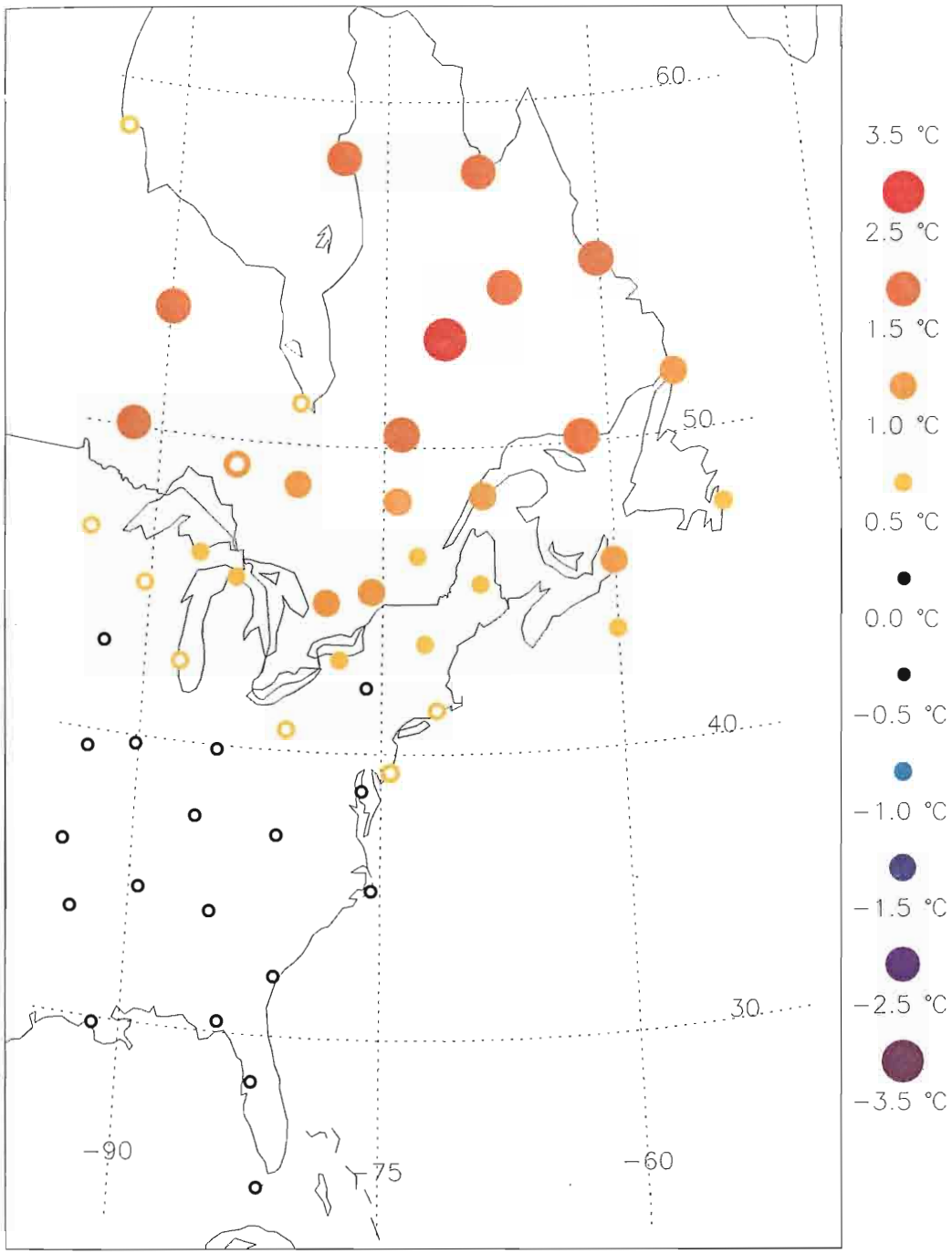

Figure 6. Warm-Neutral NASSTI temperature anomalies during FMA.

Figure 6. Warm-Neutral NASSTI temperature anomalies during FMA.

Figure 7. Hovm 7. Hovmoller diagram of seasonal Warm-Neutral NASSTI temperature anomalies. The propagation axis is the great circle connecting the cting the points (91.6W, 29.8N) and (64.6W, 56.8N). The axis is drawn in Figure 5 and consists of 51 evenly-spaced points. Station. Stations within 500 km of the axis are collapsed onto its closest axis point. The resulting space by time grid is interpolated, smoothed, and contoured.

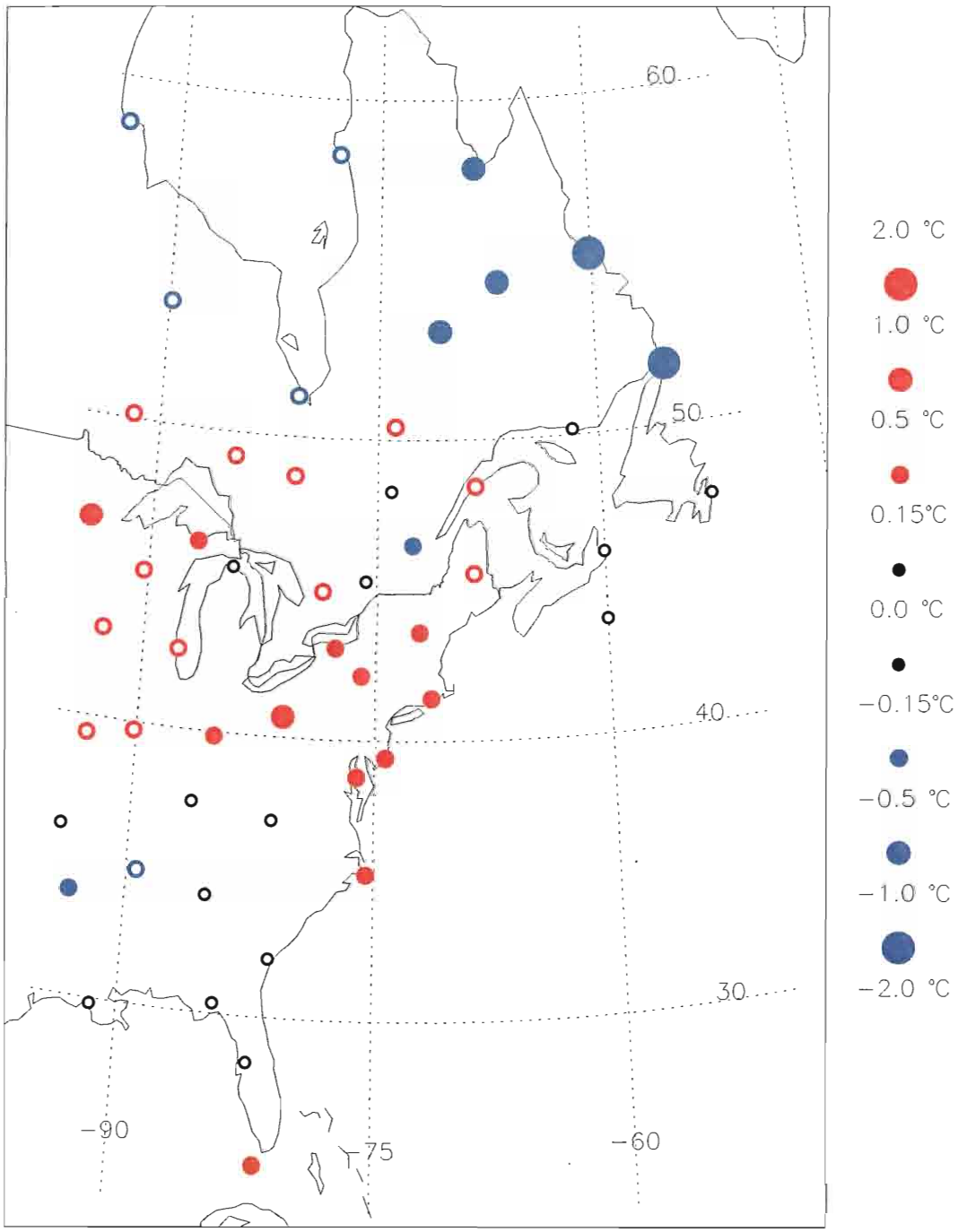

Figure 8. Mean temperature anomalies during the NASSTI cold phase, with respect to the neutral phase

Figure 8. Mean temperature anomalies during the NASSTI cold phase, with respect to the neutral phase.

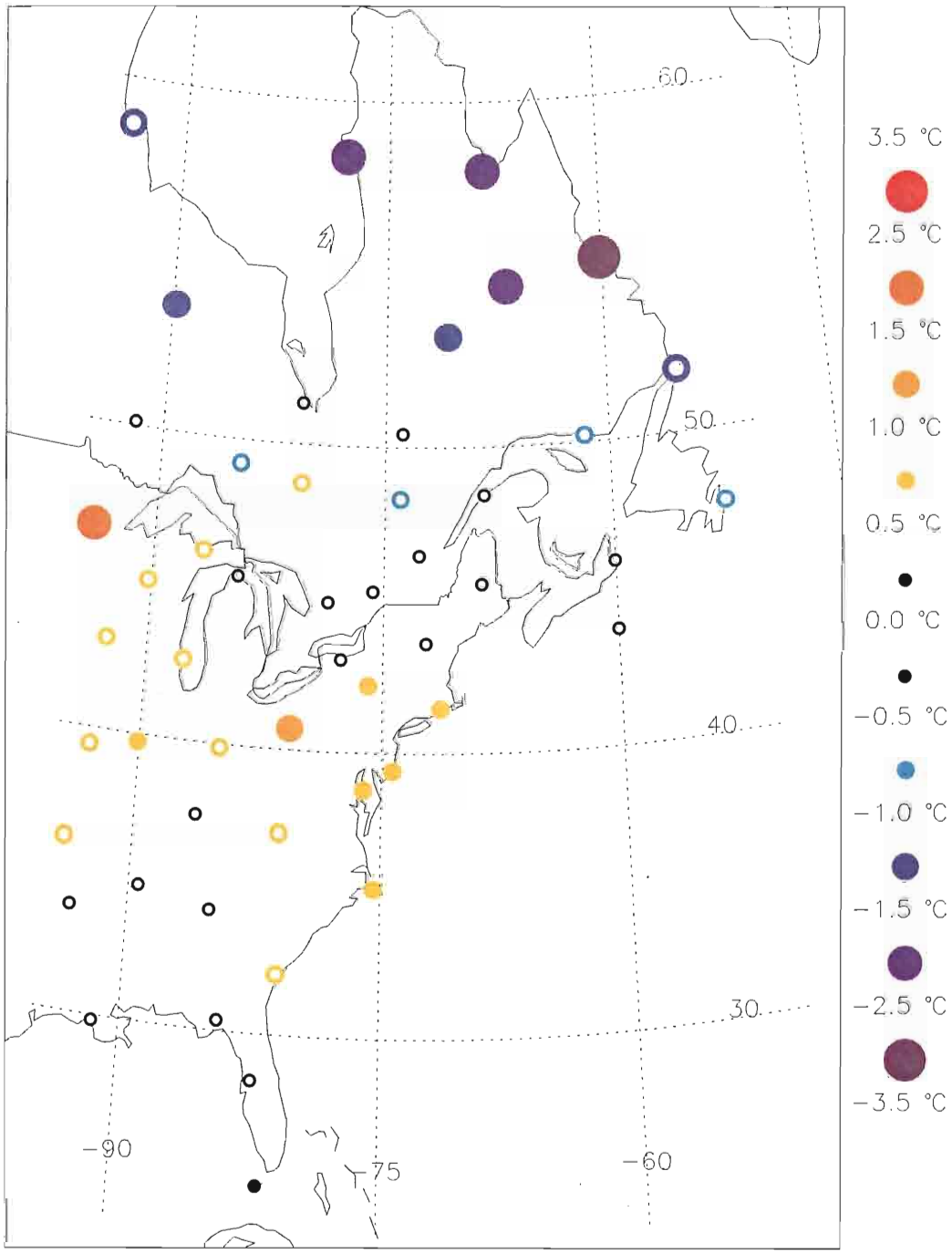

Figure 9. Cold-Neutral NASSTI temperature anomalies during DJF.

Figure 9. Cold-Neutral NASSTI temperature anomalies during DJF.

b. Precipitation

Variations in precipitation are not as clearly defined. Unlike air temperature, which tends to be spatially coherent, precipitation is highly dependent on local effects. In general, the stations tend to be slightly wetter than neutral during the NASSTI's warm phase, although a small concentration of New England stations exhibits somewhat drier conditions (Figure 10). During the cold phase, the northeastern United States and southern Canada tend to receive a little more precipitation than normal (Figure 11). The neutral phase anomalies are marginally drier than mean conditions (Figure 12).

Many stations demonstrate considerable variability in precipitation from season to season during the different NASSTI phases. However, the seasonal precipitation anomalies lack clear spatial signals. A close inspection reveals a few weak, short-lived patterns. During the transition from summer to fall in the warm phase, weak dry anomalies stretch from Alabama to Maine (Figure 13). In autumn of the warm phase, wet anomalies are located around Florida, the Great Lakes, and Quebec (Figure 14). Shifting to the cold phase, fall precipitation anomalies reveal wetter conditions over most of the U.S. stations, including some stations that receive over 20% more precipitation than normal (Figure 15). While this is the most coherent pattern for precipitation, it is rather short-lived, and only 3 stations exhibit deviations that are statistically different from zero at the 95% confidence level. There are no spatially coherent dry anomalies during the cold phase. In general, North Atlantic SST anomalies are spatially and temporally uncorrelated with precipitation variability over eastern North America.

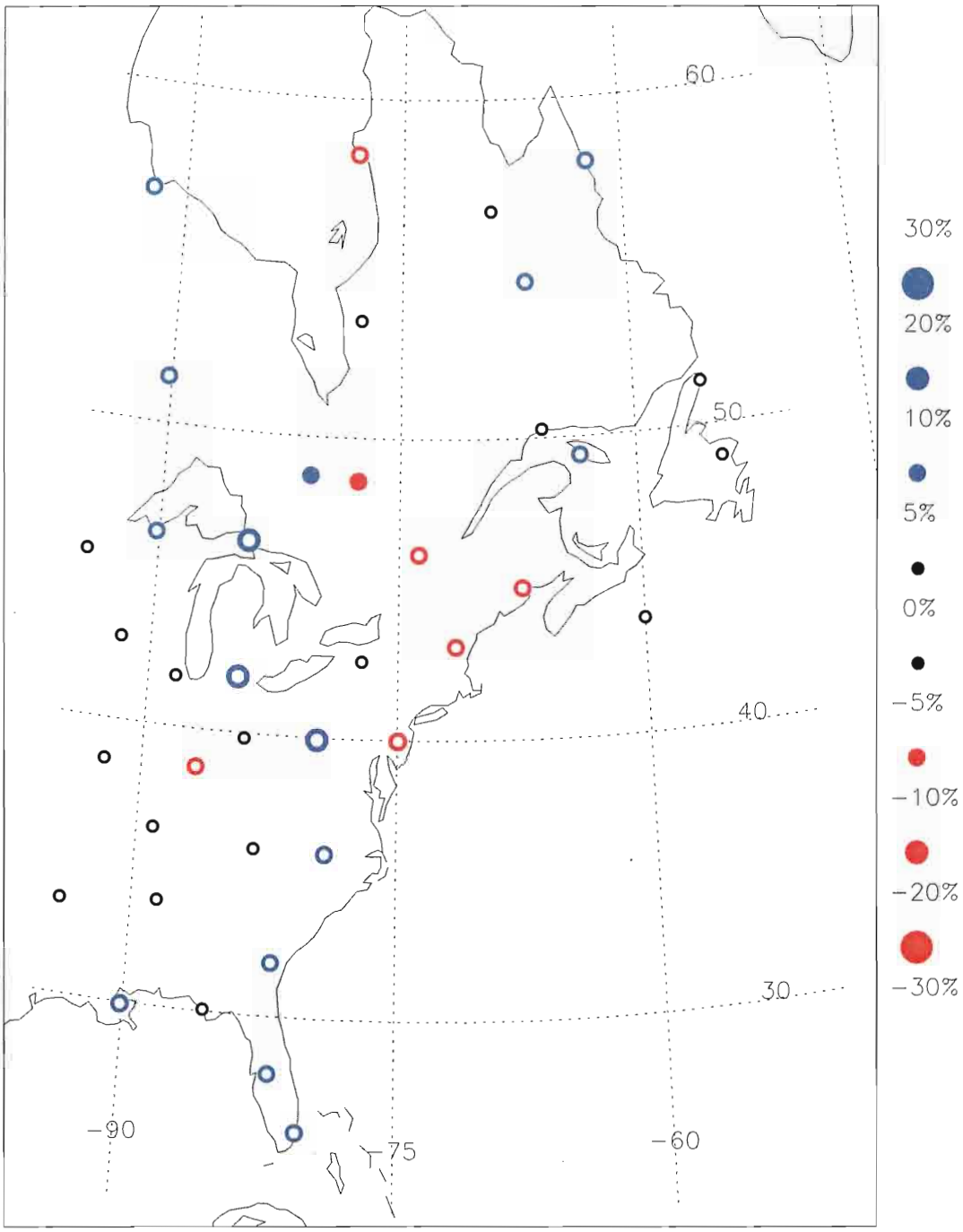

Figure 10. Percent deviation in precipitation during the NASSTI warm phase, with respect to the neutral phase.

Figure 10. Percent deviation in precipitation during the NASSTI warm phase, with respect to the neutral phase.

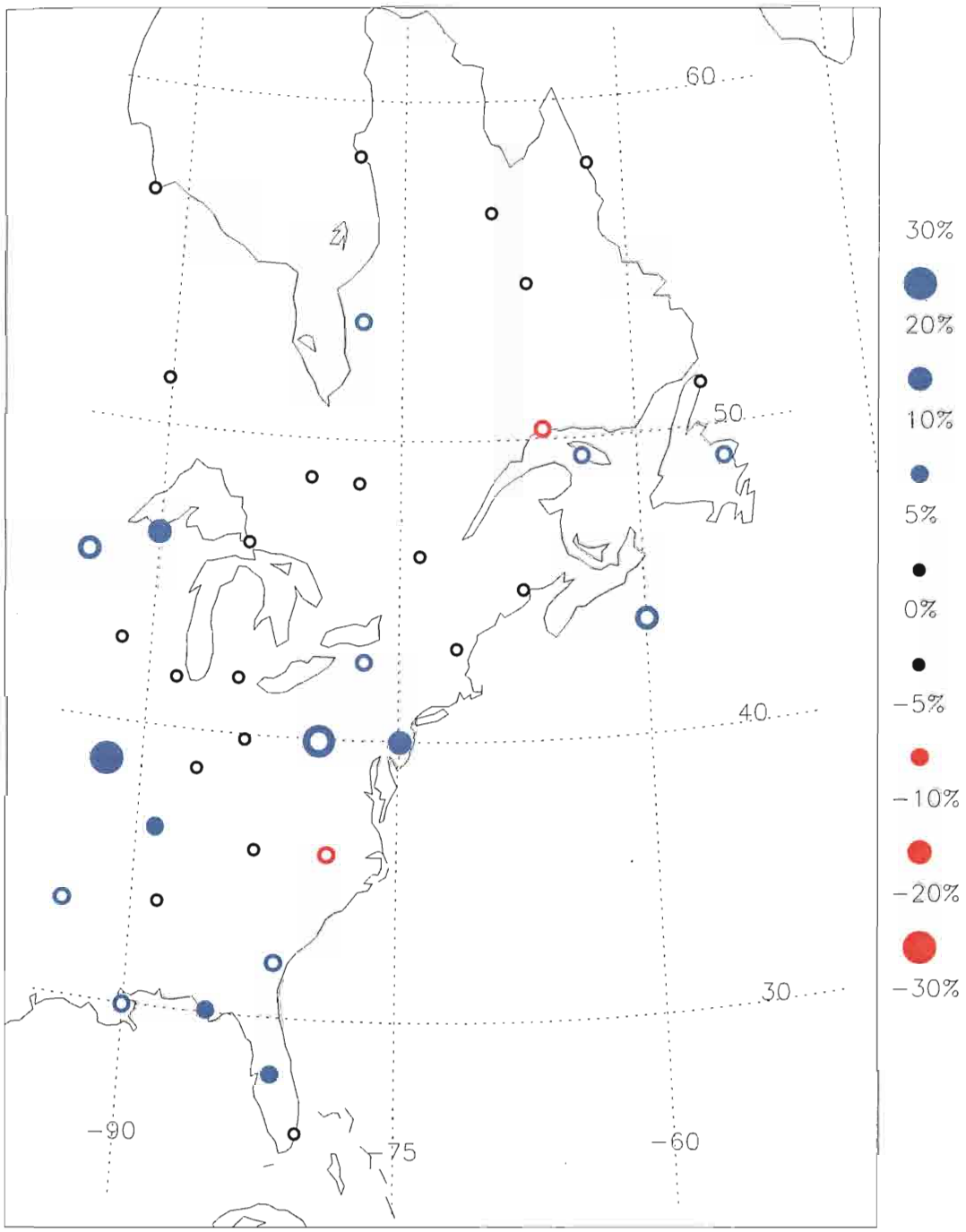

Figure 11. Percent deviation in precipitation during the NASSTI cold phase, with respect to the neutral phase

Figure 11. Percent deviation in precipitation during the NASSTI cold phase, with respect to the neutral phase.

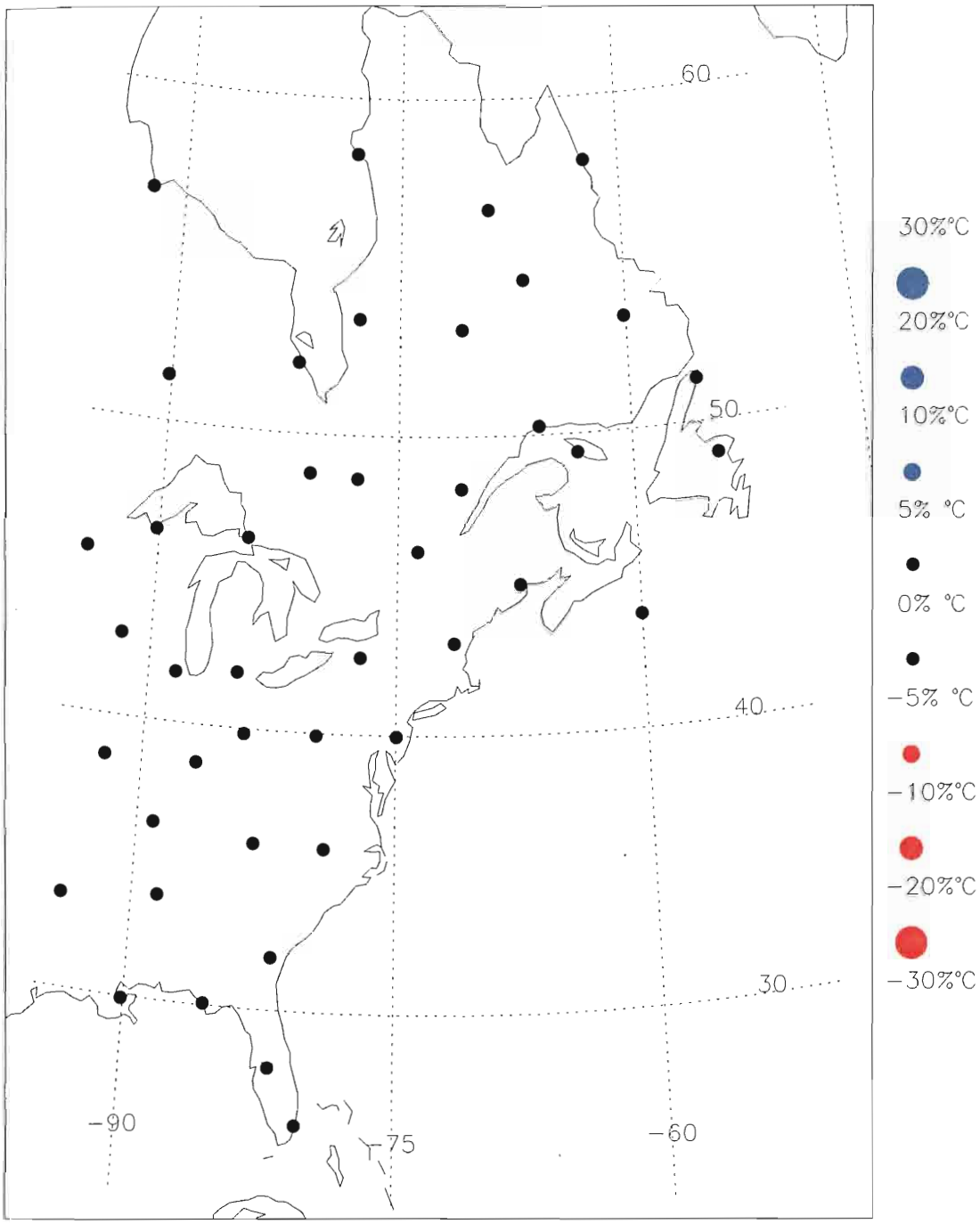

Figure 12. Percent deviation in precipitation during the NASSTI neutral phase, with respect to the total mean

Figure 12. Percent deviation in precipitation during the NASSTI neutral phase, with respect to the total mean.

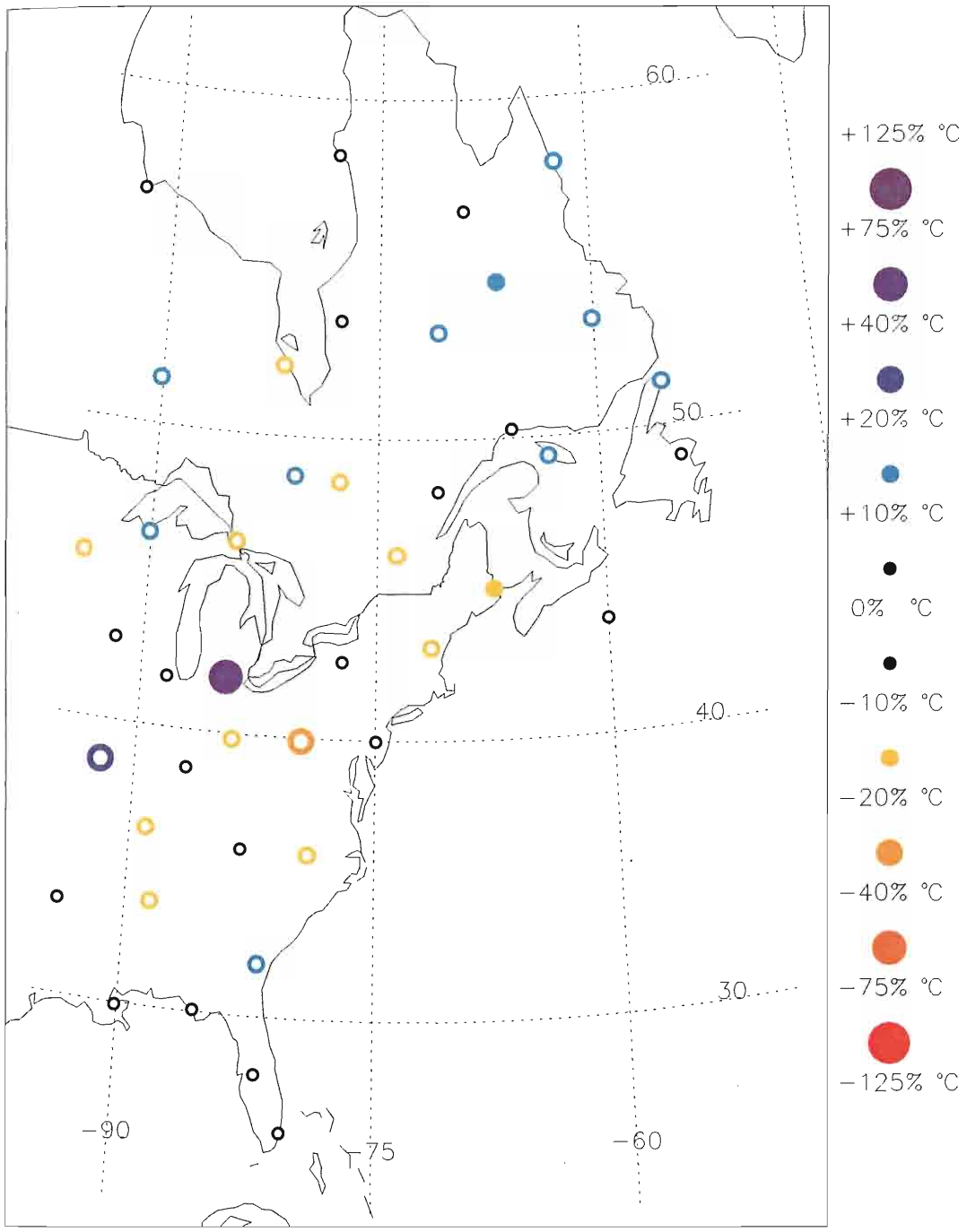

Figure 13. Warm-Neutral NASSTI precipitation anomalies during ASO.

Figure 13. Warm-Neutral NASSTI precipitation anomalies during ASO.

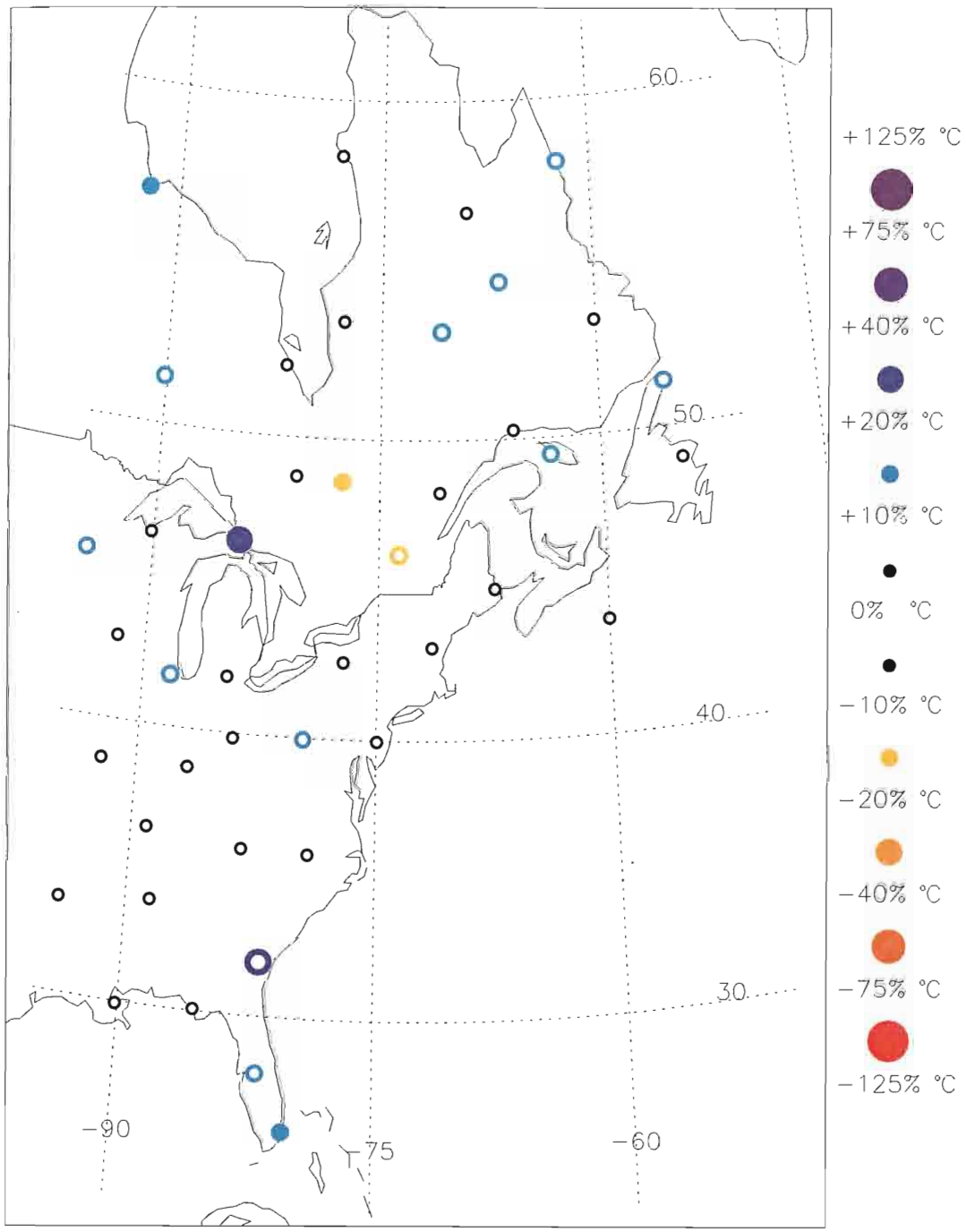

Figure 14. Warm-Neutral NASSTI precipitation anomalies during NDJ.

Figure 14. Warm-Neutral NASSTI precipitation anomalies during NDJ.

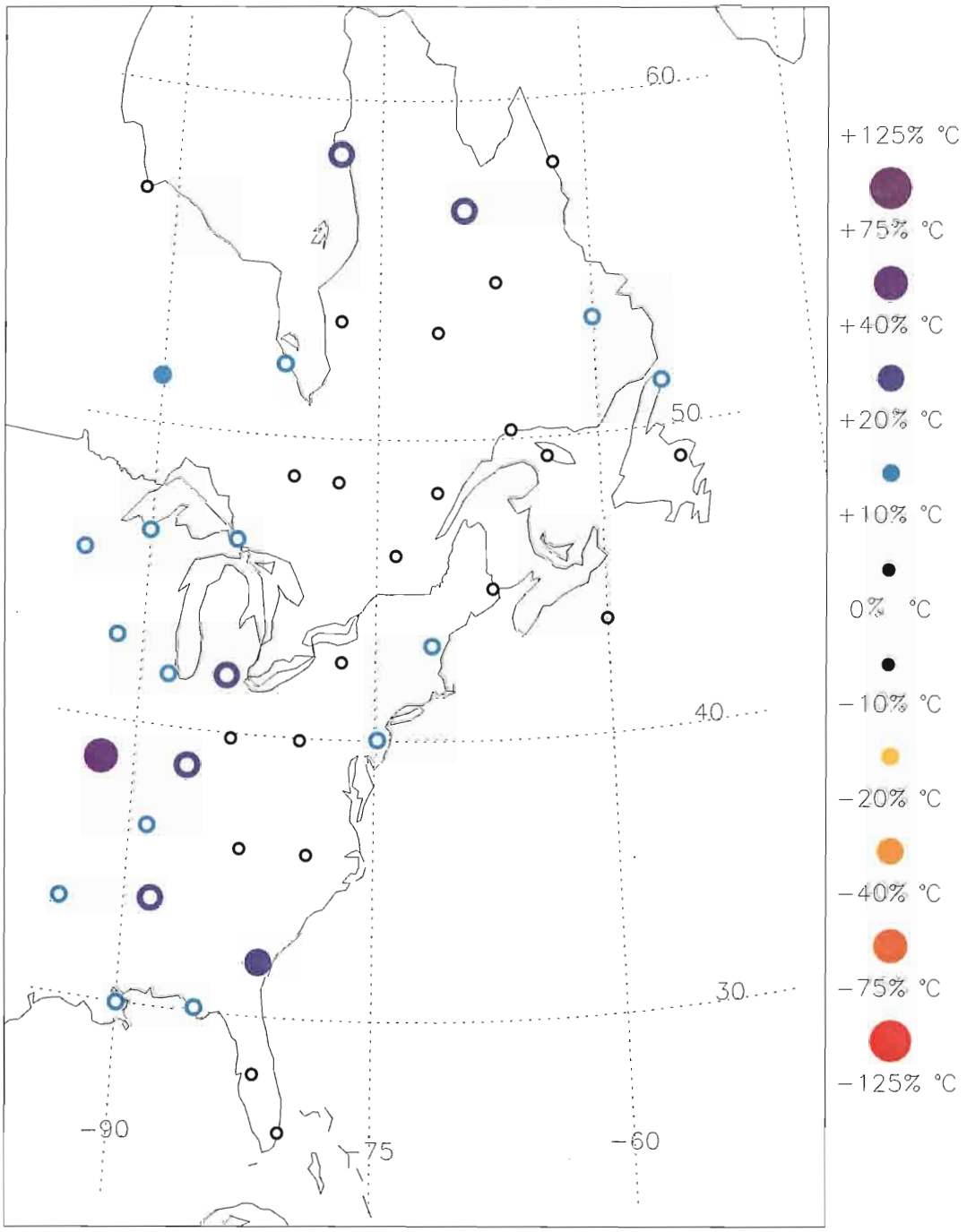

Figure 15. Cold-Neutral NASSTI precipitation anomalies during OND.

Figure 15. Cold-Neutral NASSTI precipitation anomalies during OND.

COMPARISONS OF THE NASSTI WITH THE AO AND NAO SERIES

The relationship between the NASSTI and eastern North American temperatures is compared with temperature deviations associated with low-frequency AO and NAO variability over the same land stations. The three indicator series are compared to each other to assist in the interpretation of using different climate indices to assess eastern North American temperature anomalies. The AO, NAO, and NASSTI are compared by calculating their monthly variances, spectra, running sum series, and cross-correlations. Finally, the AO and NAO series are used instead of the NASSTI to calculate high-neutral and low-neutral temperature anomalies. As before, these anomalies are obtained in terms of total mean deviations and three-month seasonal mean deviations. Only temperature deviations are considered because of the lack of a meaningful relationship between precipitation and the NASSTI.

Lag correlations indicate that the AO and the NAO lead the NASSTI by 7 and 5 months, respectively, while the NAO lags the AO by one month over low frequencies (Table 1). Negative maximum cross-correlations between the North Atlantic SST anomalies and AO/NAO anomalies arise because intense surface winds are associated with increased evaporation, which cools sea surface temperature. However, the cross-correlations remain negative when the ocean leads, suggesting that a feedback relation exists between ocean and atmosphere over the North Atlantic sector. A similar result was

exists between ocean and atmosphere over the North Atlantic sector. A similar result was

found by Czaja and Frankignoul (2002).

Table 1. Correlation Analysis. The lower left values are maximum lag correlations of the monthly series. The index that leads appears in parentheses, followed by the lag. The upper right values are maximum lag correlations for three-month averaged yearly indices. The index that leads is written first.

	NASSTI	AO	NAO
NASSTI	———	**-0.50** AO NDJ vs. NASSTI FMA (+3)	**-0.49** NAO DJF vs. NASSTI FMA (+2)
AO	**-0.43** (AO, 7 months)	———	**0.84** AO DJF vs. NAO JFM (+1)
NAO	**-0.48** (NAO, 5 months)	**0.65** (AO, 1 month)	———

The AO and the NAO anomalies have considerably larger variances during winter and reduced variance during the summer (Figure 16). Also noteworthy is the AO's sharp decline from winter to summer and rapid increase when winter resumes, as opposed to the noisier monthly variances of the NAO. The NASSTI, in contrast, has maximum variance during the summer. The summer maximum is perhaps related to sea ice formation during wintertime in the SST domain, since the large latent heat of fusion acts as a variance cap. This may also arise since HadISST parameterizes sea ice as –1.8°C. The roughly six-month difference in maximum variance is equivalent to the lag of maximum cross-correlation between the NASSTI and the AO/NAO series. However, this does not provide a definitive answer to the lead-lag relationship of the ocean and atmosphere over the North Atlantic.

Plotting the $f \cdot \Gamma$ (the frequency multiplied by the spectral density) versus the logarithm of frequency provides an area-preserving representation that allows a closer inspection of lower frequencies (Figure 17). The amount of spectral energy in a frequency band, say between f_1 and f_2, is simply the area under the curve between these two frequencies. Note that the mean (f_0), which is very close to zero because the monthly climatologies were removed, is not shown for any of the indices. The NASSTI has considerable spectral energy in quasi-decadal and multidecadal timescales, with a peak near 10 years. The AO and NAO series primarily exhibit spectral energy in inter-annual and quasi-decadal timescales, with significant peaks near 5 years. However, both the AO and NAO also demonstrate a considerable amount of area under multidecadal frequencies. It is noteworthy that the AO contains appreciably more spectral energy in

frequencies. It is noteworthy that the AO contains appreciably more spectral energy in multidecadal timescales than the NAO.

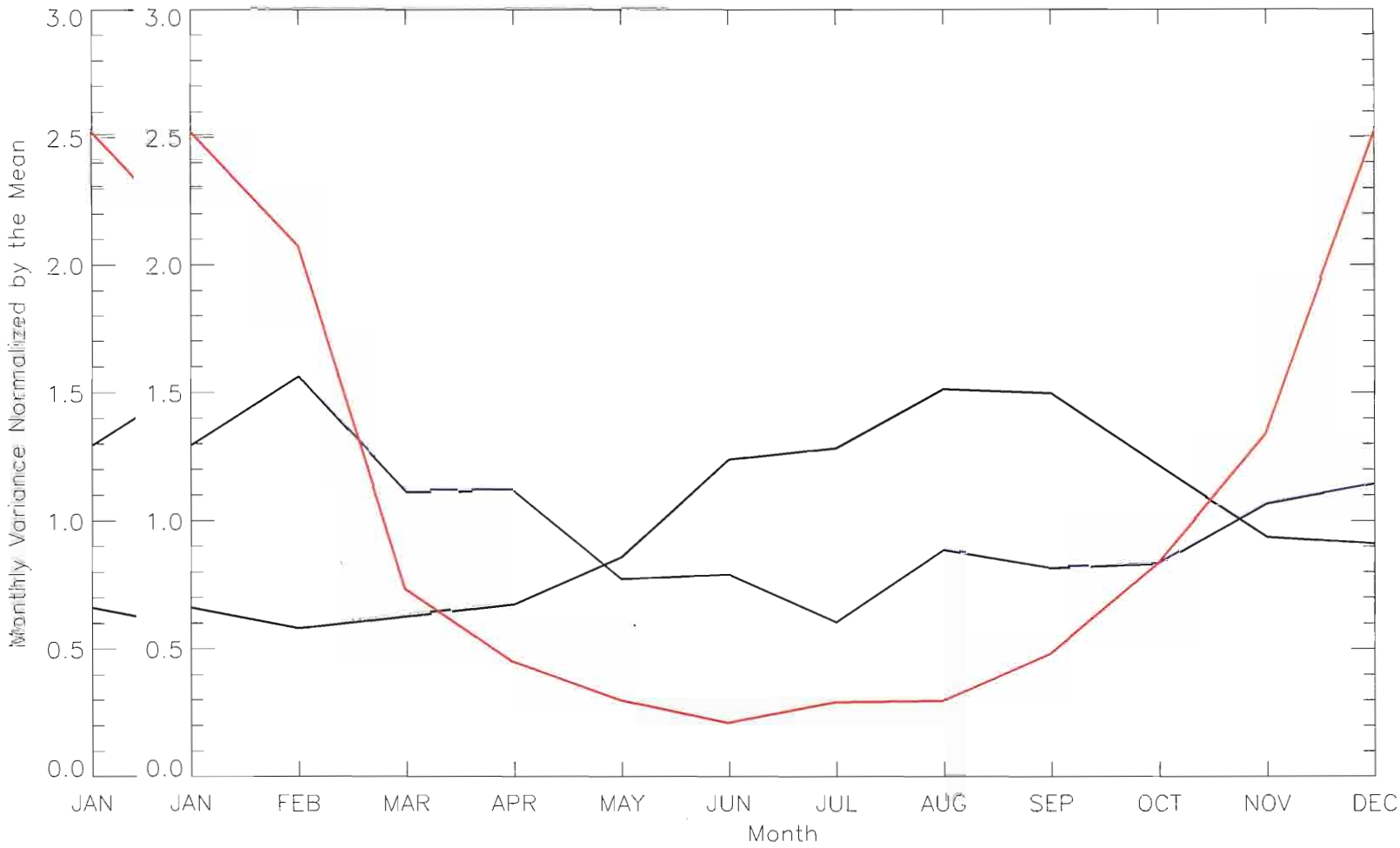

Figure 16. Mor 16. Monthly variance for the NASSTI (black), AO (red), and NAO (blue), scaled by the respective means.

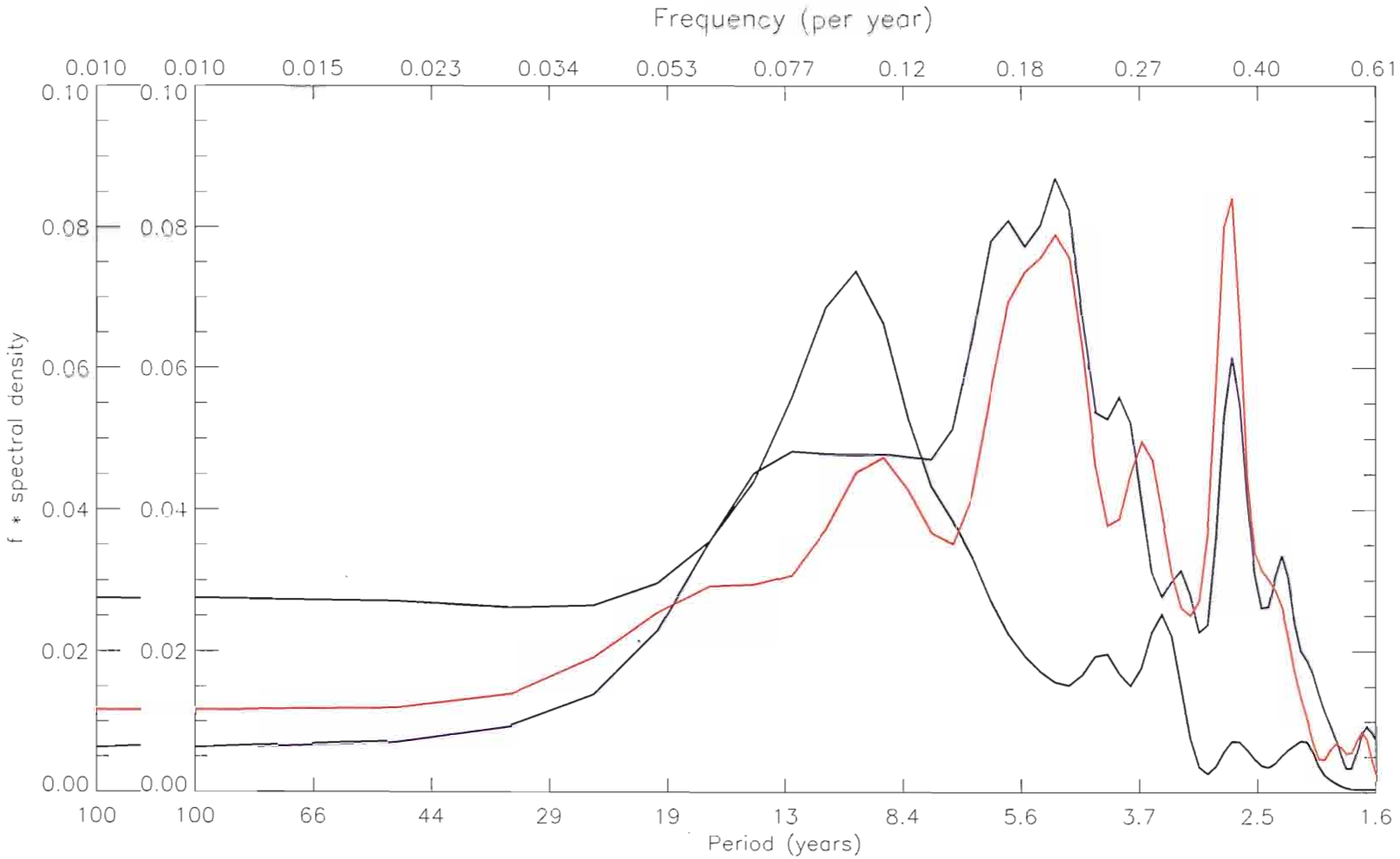

Figure 17. Raw 17. Raw spectra for the NASSTI (black), AO (red), and NAO (blue) time series after filtering. The x-axis is plotted on a logarithmic srithmic scale.

A running sum filter is used to visually inspect low-frequency oscillations (Figure 18). Given this filters' similarity to discrete integration, the slope of the resulting series reveals eras where anomalies tended to be positive or negative. Note that the negative of the NASSTI is plotted, since it is negatively correlated with the AO and NAO. Three clear periods emerge in the NASSTI: 1900-1925 (cold anomalies), 1925-1965 (warm anomalies), and 1965-1995 (cold anomalies). These three episodes are essentially the same as the periods described by Kushnir (1994). There is a hint of a positive upswing in the NASSTI toward the end of the century. Time will tell whether these conditions persist. The quasi-decadal cycle in SST is also evident, especially after 1965, as it modulates the multidecadal frequencies in this plot. Running sums of the AO and NAO are more variable. The AO tended to be in its high phase between 1900 and 1955, while it tended toward its low phase from 1955 to 1970. In addition, the early 1990s were marked by very positive anomalies, as indicated by a very sharp slope. No discernible long-term swings can be found in the running sum of the NAO.

Using the filtered AO and NAO series in place of the NASSTI in our analysis, a set of surface temperature maps was created to compare to the NASSTI results found in Figure 7a. The AO and NAO temperature regimes over eastern North America are comparable during winter, so they will be described jointly. High phase winter temperature deviations from the neutral phase bring positive anomalies to the eastern U.S. and colder conditions to eastern Canada, with substantial cooling in north and central Quebec (Figures 19 and 20). This pattern compares favorably with the findings of Hurrell (1995, hereafter H95) and Thomson and Wallace (1998, hereafter TW98). In

Hurrell (1995, hereafter H95) and Thomson and Wallace (1998, hereafter TW98). In addition, the high - neutral temperature anomalies correspond well with the cold - neutral

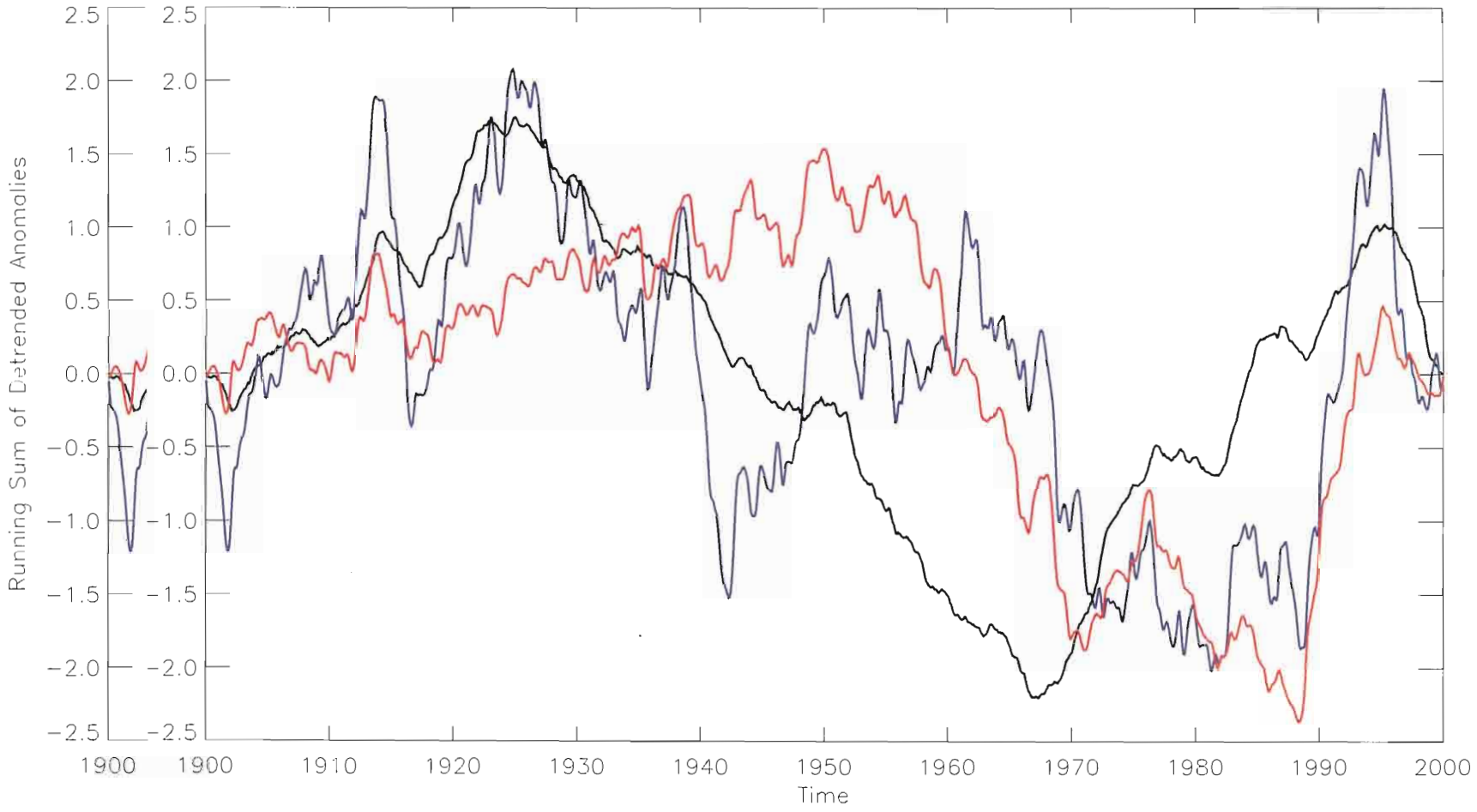

Figure 18. Run 18. Running sums of the NASSTI (black), AO (red), and NAO (blue). The negative of the NASSTI is plotted.

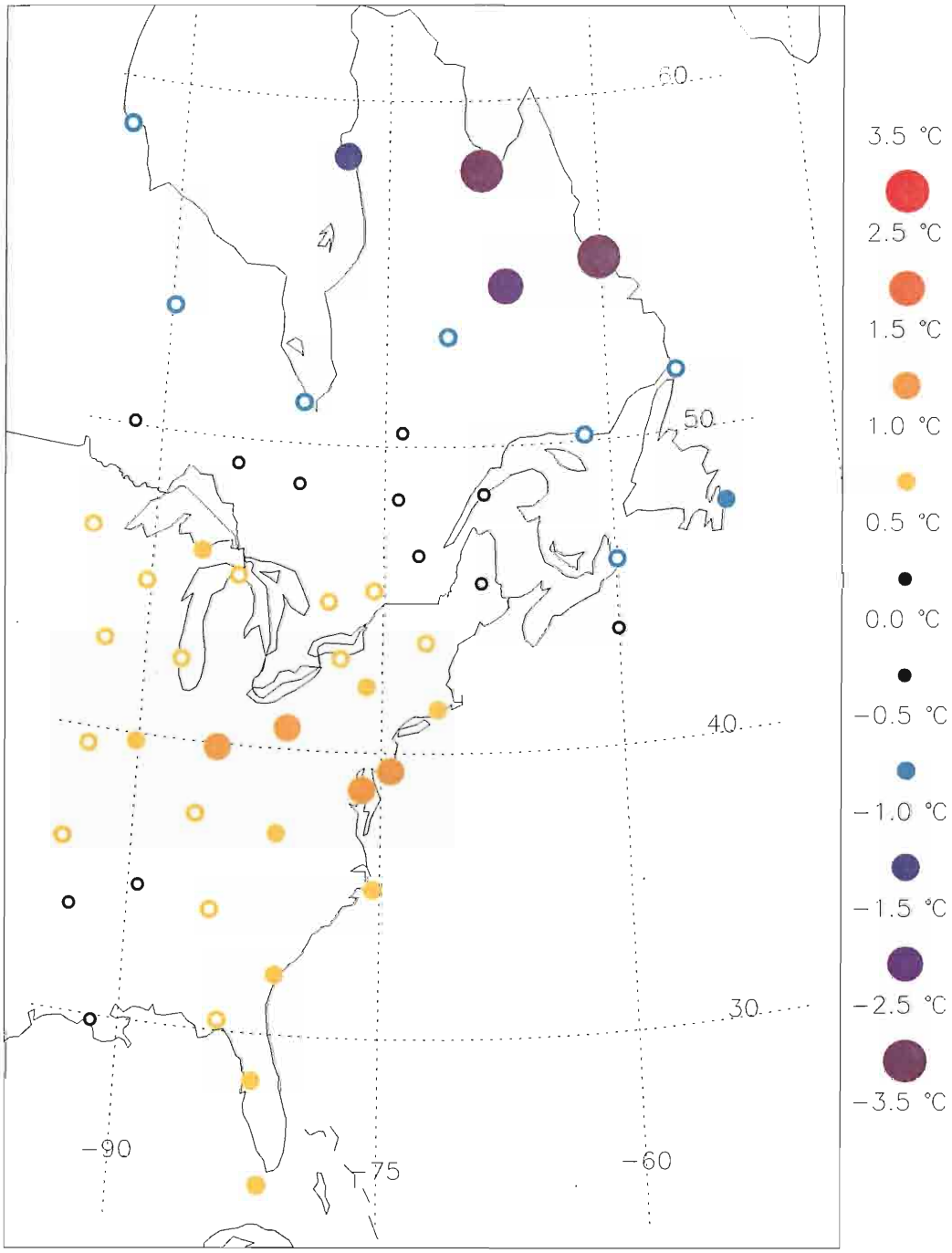

Figure 19. High-Neutral AO temperature anomalies during DJF.

Figure 19. High-Neutral AO temperature anomalies during DJF.

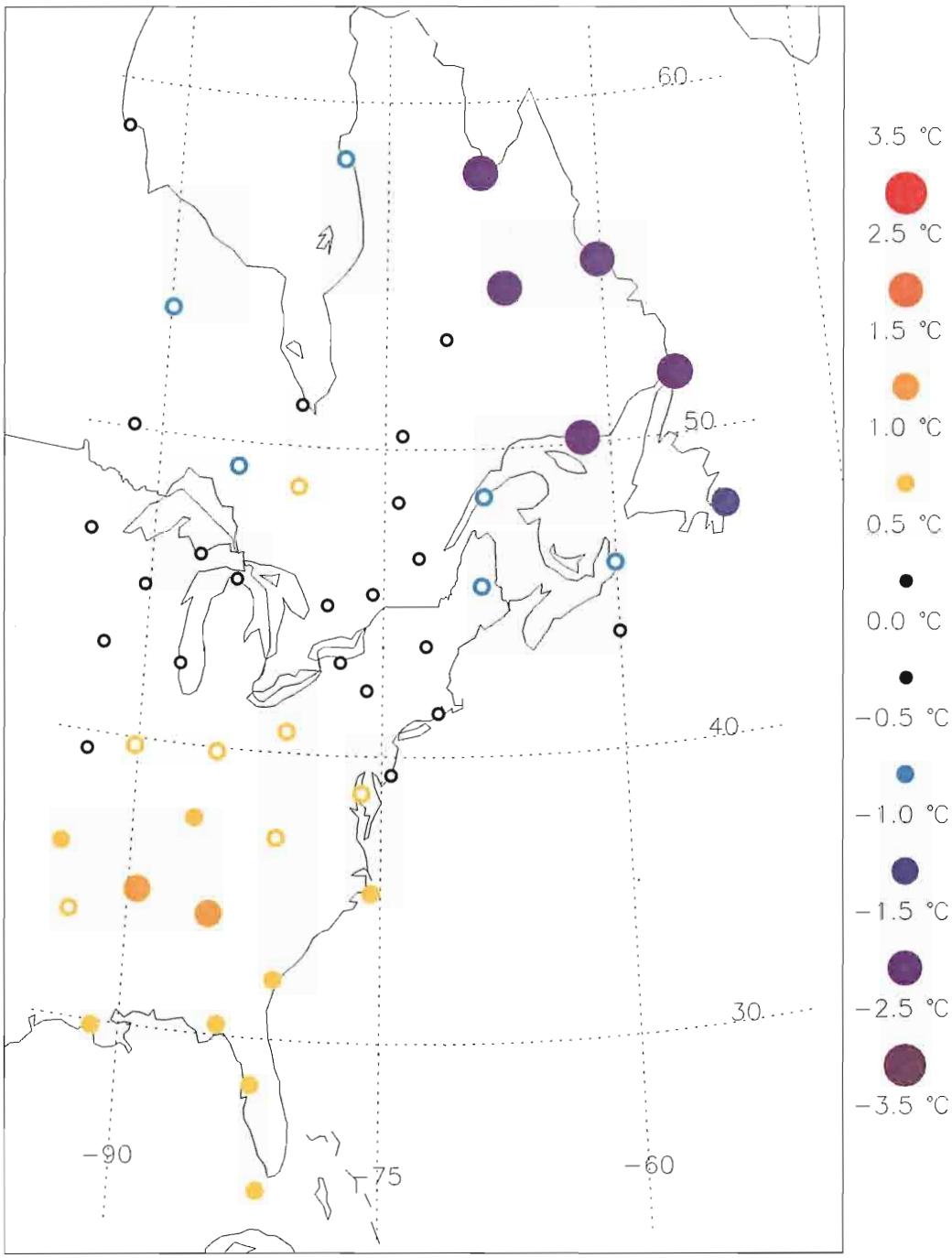

Figure 20. High-Neutral NAO temperature anomalies during DJF.

Figure 20. High-Neutral NAO temperature anomalies during DJF.

temperature anomalies associated with the NASSTI. Recall that the AO and NAO are negatively correlated with the NASSTI, which may account for the high phase's correspondence to the NASSTI's cold phase. Moreover, both H95 and TW98 indicate colder surface air temperatures over the NASSTI's domain during the high phase winter. In summary, the NASSTI's cold phase temperature regime over eastern North America is indistinguishable from the AO/NAO high phase dipole pattern.

Low-neutral anomalies display the reverse of the high-neutral dipole patterns, with considerably warmer conditions in Quebec and cooler temperatures in the U.S. (Figures 21 and 22). The high and low phases are therefore converse events with respect to their associated temperature anomalies over eastern North America, as also indicated by H95 and TW98. The low phase temperature anomaly pattern, however, does not correspond to the signal associated with the warm phase, as might be expected. Although the low phase and warm phase are both associated with positive temperature anomalies over eastern Canada, they do not match up over the United States.

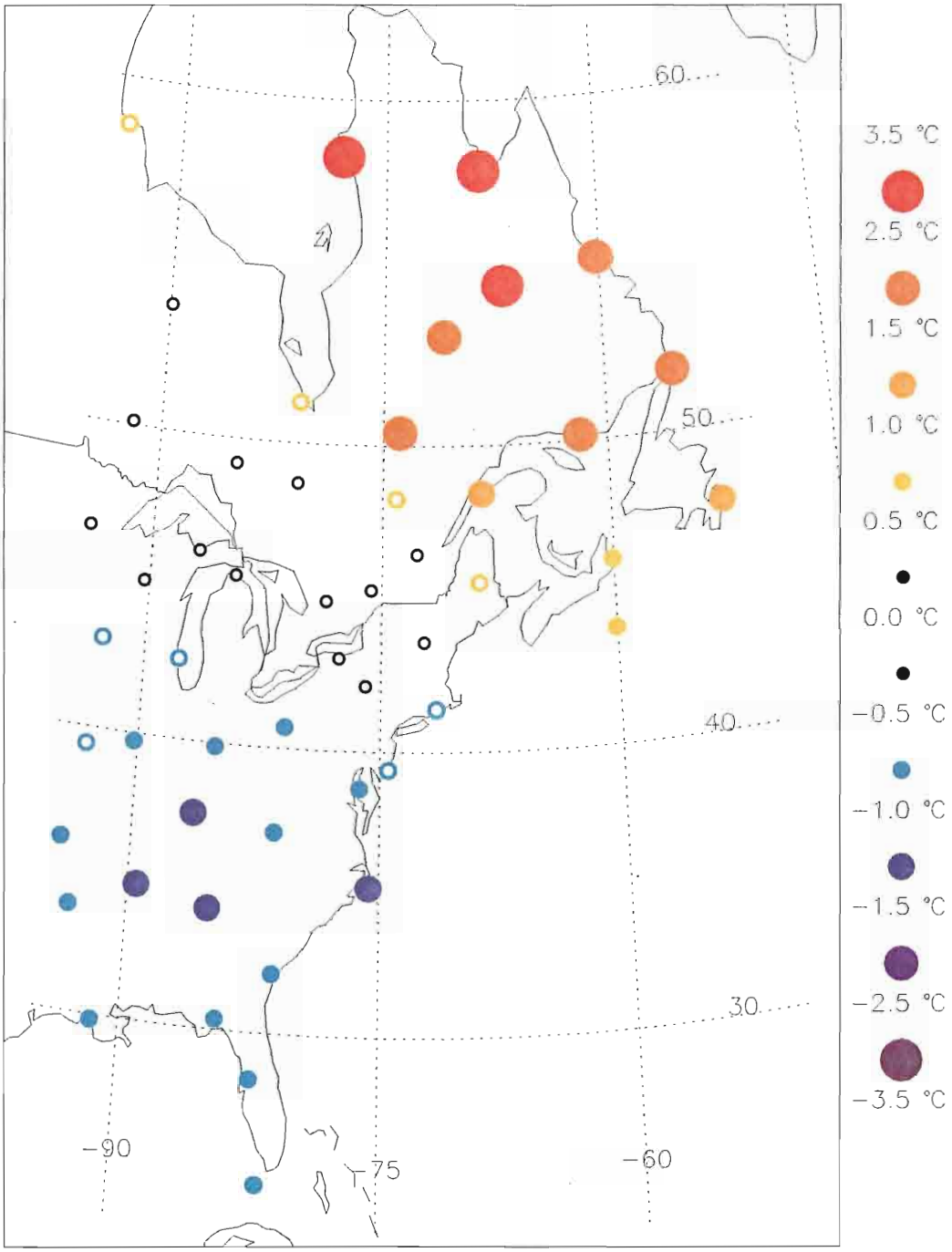

Figure 21. Low-Neutral AO temperature anomalies during JFM.

Figure 21. Low-Neutral AO temperature anomalies during JFM.

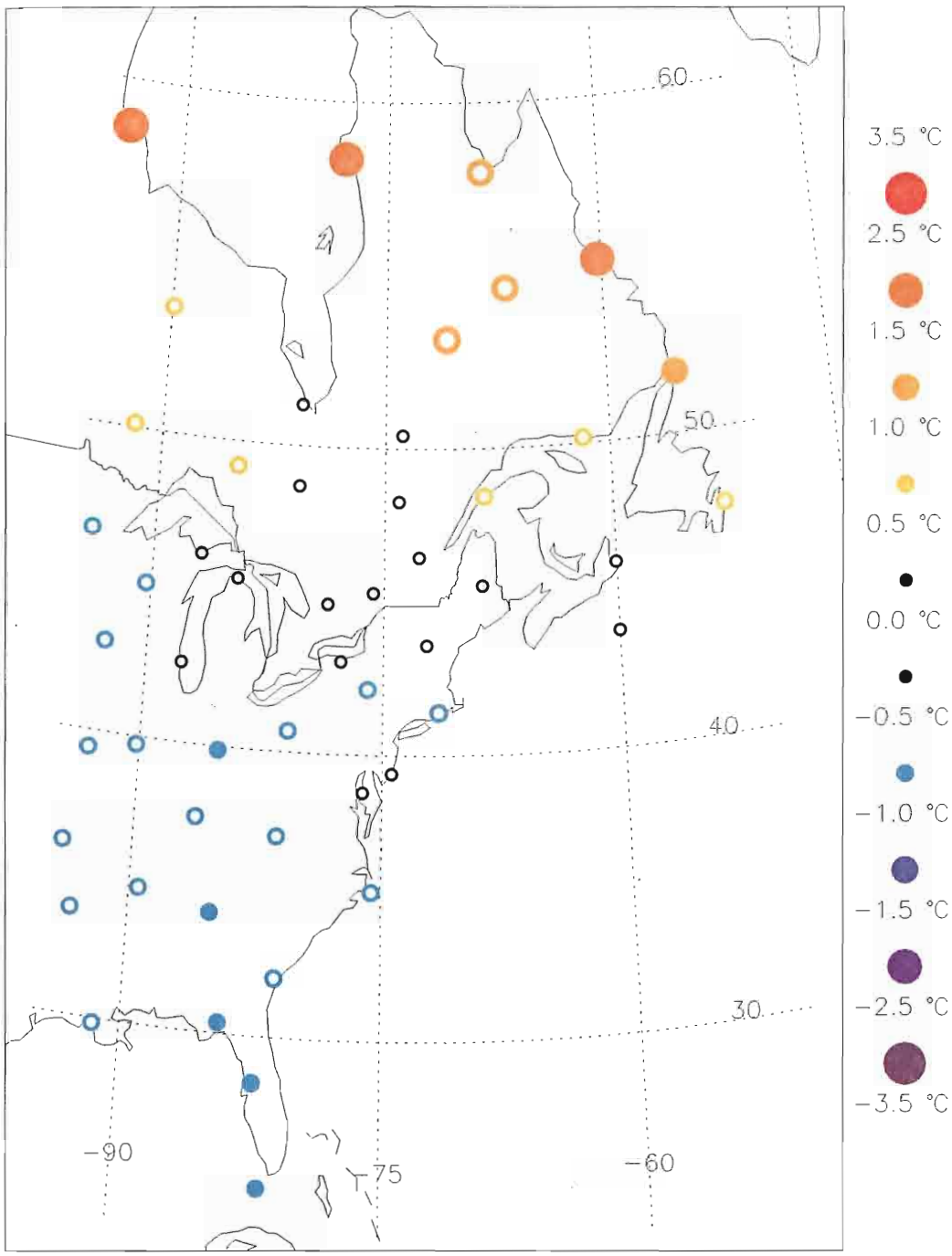

Figure 22. Low-Neutral NAO temperature anomalies during JFM.

Figure 22. Low-Neutral NAO temperature anomalies during JFM.

SUMMARY AND DISCUSSION

The present study investigated the link between monthly North Atlantic SST anomalies and precipitation and temperature changes over eastern North America. The SST anomalies were domain-averaged over a narrow box stretching from the Labrador Sea to Iceland. The SST region was selected because it is an action center of the atmospheric AO (Thompson and Wallace, 1998) and NAO (Hurrell, 1995), but also because of its important role in low- frequency variability over the North Atlantic (Mizoguchi et al., 1999). After low- pass filtering the NASSTI, NAO, and AO, we found that the NASSTI is negatively correlated with the AO and NAO. This indicates that cooler SSTs are associated with stronger westerlies across the SST domain, perhaps due to increased evaporation as suggested by other authors (Rodwell et al., 1999). The physical connection between the three indices motivated a comparison of the relationship between the NASSTI with eastern North American climate to the low-frequency AO and NAO footprints over the same land stations.

Precipitation anomalies during the different NASSTI phases do not reveal many discernible climate signals. Although the deviations from the neutral phase can be quite sharp for particular stations during certain seasons, there is no consistent temporal or spatial coordination between the anomalies. Of the few weak signals that do emerge, the most conspicuous signal is in the fall (OND) cold-neutral deviation chart, in which most of the eastern U.S. experiences marginally wetter conditions. However, this signal is
most conspicuous signal is in the fall (OND) cold-neutral deviation chart, in which most of the eastern U.S. experiences marginally wetter conditions. However, this signal is short-lived. In general, precipitation anomalies over eastern North America are not

correlated with low-frequency North Atlantic SST anomalies in a spatially coherent manner.

The NASSTI is, however, associated with coherent temperature anomaly patterns over eastern North America. The temperature deviations are most pronounced, and typically only present, during the winter months. Cold-neutral is characterized by a gradient pattern with cooler temperatures in northeastern Canada and warmer conditions over the eastern United States. This pattern is virtually identical to the high-neutral temperature patterns in this region of the AO and NAO. The warm-neutral signal, on the other hand, embodies a warming over all of eastern North America during winter. The positive temperature anomalies propagate northeastward towards the NASSTI's domain, amplifying in time. The warm-neutral pattern does not correspond adequately to the large-scale AO/NAO impact in this region, and demonstrates that extreme phases of the NASSTI are not associated with converse temperature anomaly patterns over eastern North America.

If we only consider eastern Canada, however, the AO/NAO fingerprint here matches up well with the NASSTI patterns. This fact is encouraging, considering eastern Canada borders the NASSTI's domain. The warm-neutral signal corresponds to the low-neutral pattern. During these phases, the AO/NAO is associated with a weaker Icelandic Low during winter, and thus weaker westerlies on its southern flank. SST anomalies between Canada and Iceland tend to be warmer, perhaps due to heat flux anomalies. However, recall that recent modeling studies have shown that prescribed SST forcing can reproduce NAO/AO variability over long timescales. Anomalously weaker northerlies

reproduce NAO/AO variability over long timescales. Anomalously weaker northerlies

reside on the western flank of the Icelandic Low, which may be responsible for the warm anomalies in eastern Canada because of reduced advection of cold, polar air.

The low-neutral and high-neutral patterns exhibit the opposite configuration. Between Canada and Iceland, cooler SSTs are accompanied by anomalously strong westerlies. The Icelandic low is more intense than normal and is associated with stronger northerly winds on its western periphery. These strong winds on its western flank may be responsible for increased penetration of cold air into eastern Canada during winter.

The above considerations for the eastern Canadian anomalies fail to explain why the warm-neutral pattern originates in the Ohio River Valley. The 'dipole' patterns of cold-neutral, high-neutral, and low-neutral also implicate variability in the polar front position as a possible mechanism. In removing high-frequency fluctuations from the AO, NAO, and NASSTI, we did not distinguish between the low-frequency modes that were retained. The patterns we have found may thus be the interaction of several low-frequency signals. Future work may involve recasting the experiment to isolate the various low-frequency impacts over eastern North America. Furthermore, it is quite possible that the AO and NAO are not stationary features. They are typically calculated using EOF-based techniques that only identify stationary patterns. Future work may also include calculating the AO/NAO using propagating or cyclo-stationary EOF's and reanalyzing their impacts over eastern North America.

It must be emphasized that the warm-neutral and cold-neutral patterns were found using solely SST as an indicator. The similarity of these two patterns to the high-neutral and low-neutral signals of the AO/NAO, which are the dominant modes of Northern

and low-neutral signals of the AO/NAO, which are the dominant modes of Northern Hemisphere variability, is a testament to the strong coupling of the ocean and atmosphere

in the North Atlantic during winter. Häkkinen (2000) also emphasized the importance of air-sea interactions in low-frequency modes, proposing the existence of a coupled system in the North Atlantic in which the quasi-decadal SST variability could be reproduced with knowledge of surface heat fluxes. It is clear that the North Atlantic Ocean actively communicates with the atmosphere above it, and that this relation involves the AO/NAO system (Häkkinen, 2000). A more complete understanding of this communication is necessary to better comprehend low-frequency signals in eastern North America.

APPENDIX A

THE RUNNING SUM FILTER

The running sum filter is a useful tool used to visually inspect low-frequency fluctuations in time series. It can be defined as

$$R(t) = R(t\text{-}1) + X(t), \quad t = 1, 2, 3, \ldots, N, \qquad \text{(A1)}$$

where R(t) is the running sum filter and X(t) is the original series. Alternatively, we can express it as the following summation:

$$R(t) = \sum_{i=1}^{t} X(i) \qquad \text{(A2)}$$

Note that R(1) = X(1).

The running sum filter has several important properties. The first is order-dependence, or recursiveness. This arises from the fact that at a particular time, say t', R(t') is related to R(t'-1), which is in turn tied to R(t'-2), and so on. This is in contrast to non-recursive filters, which only depend on the input series values in X. The actual value of each running sum element is not very meaningful. The slope of the running sum is meaningful, especially if the original data is in the form of anomalies.

The second important property of the running sum filter is non-preservation of the series mean. Unlike most filters, which 'pass' the original series mean to the output series, the running sum filter does not pass the mean as a consequence of its order-dependence. In fact, the mean of the running sum can be related to the mean of the

series, the running sum filter does not pass the mean as a consequence of its order-dependence. In fact, the mean of the running sum can be related to the mean of the original series by the following equation:

$$\overline{R} = (N+1)\,\overline{X} - \frac{1}{N}\sum_{t=1}^{N} tX(t) \qquad \text{(A3)}$$

The running sum filter has special characteristics if the input values are anomalies, i.e. $\overline{X} = 0$. The last value, R(N), must be zero since $R(N) = \sum_{i=1}^{N} X(i) = N\overline{X} = 0$. Secondly, a useful interpretation involving the slope exists. Positive slopes are regions where there are positive anomalies in the original data; conversely, a negative slope indicates ranges in the original data where there are negative anomalies. For anomalies, the running sum mean reduces to

$$\overline{R} = -\frac{1}{N}\sum_{t=1}^{N} tX(t)\,. \qquad \text{(A4)}$$

With the aid of a random number generator, the distribution of $\overline{R}$ is Gaussian with an expected value of zero. The mean of the running sum is often removed so that a plot of it shows equal areas above and below zero. Mean removal also allows comparisons to be made more easily between different sets of running sums. However, mean removal does not aid in the interpretation of a particular running sum, since removing a constant at each point does not alter the slope. In addition, the running sum filter loses the property of being zero at the final value if the mean is removed (unless the mean is zero).

Given the recursive nature of the running sum filter, the frequency response characteristics are considerably different from that of non-recursive filters. The power transfer function, $H^2(f)$, is given by

$$H^2(f) = \frac{1}{2 - 2\cos(2\pi f)} \qquad \text{assuming } \Delta t = 1. \qquad \text{(A5)}$$

$$H^2(f) = \frac{1}{2 - 2\cos(2\pi f)} \qquad \text{assuming } \Delta t = 1. \qquad \text{(A5)}$$

It approaches infinity as f goes to zero and bottoms at 0.25 at the Nyquist frequency. Thus, the running sum filter amplifies frequencies lower than $f = 1/6$, where the power transfer function equals one. Given that H^2 is not defined at $f = 0$, we clearly see that the running sum filter does not maintain the mean.

The running sum filter is related to numerical integration. This is precisely why the slope (derivative) of the running sum filter gives insight into the original series: the derivative of an integral is the integrand itself. The running sum can be related to the trapezoidal rule at a given point by

$$R(t) = Z(t) - \frac{1}{2}[X(1) + X(t)], \qquad (A6)$$

where Z(t) is the discrete trapezoidal rule. Thus, the difference between R(t) and Z(t) is merely the average of 2 points out of N. Provided X(1) is not an outlier of the input series, the running sum filter is an excellent approximation of the discrete integral of X.

APPENDIX B

ADDITIONAL FIGURES

The following are additional figures from the analysis that were not referenced. This includes the total mean temperature deviations for the neutral phase of the NASSTI, as well as the remaining warm-neutral and cold-neutral seasonal temperature anomalies. In addition, the remaining seasonal precipitation deviations are also included.

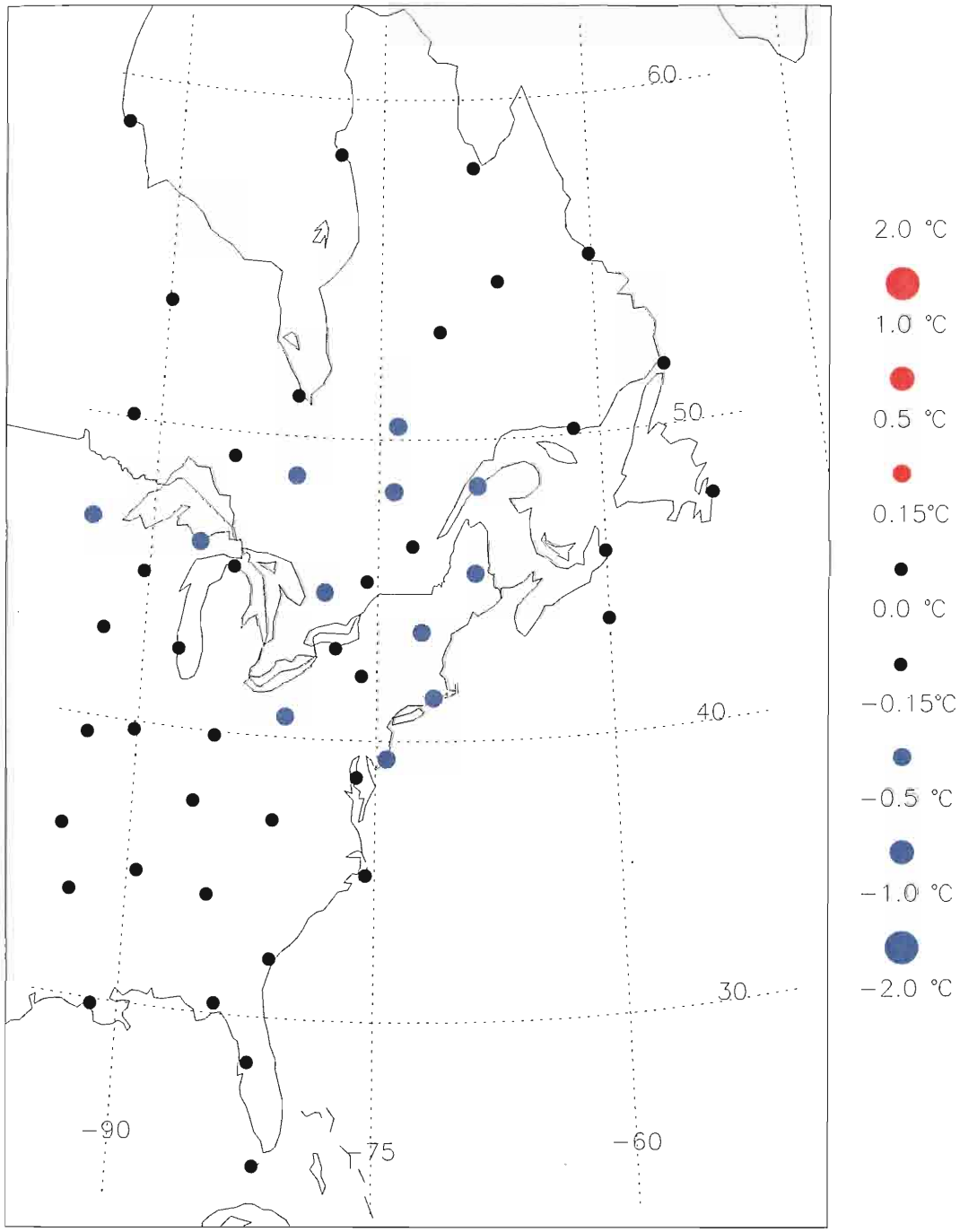

Mean temperature anomalies during the NASSTI neutral phase, with respect to the total mean.

Mean temperature anomalies during the NASSTI neutral phase, with respect to the total mean.

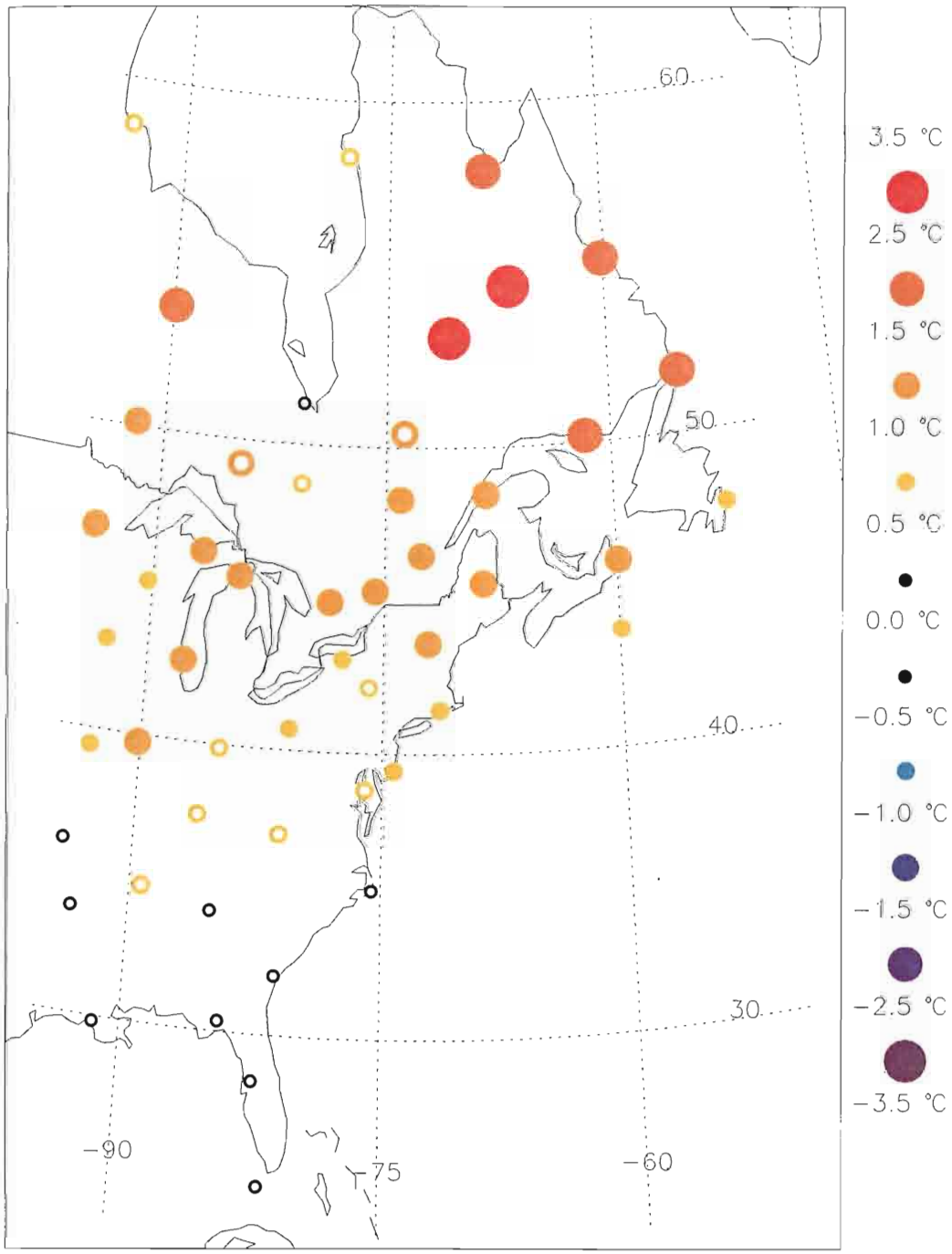

Warm-Neutral NASSTI temperature anomalies during JFM.

Warm-Neutral NASSTI temperature anomalies during JFM.

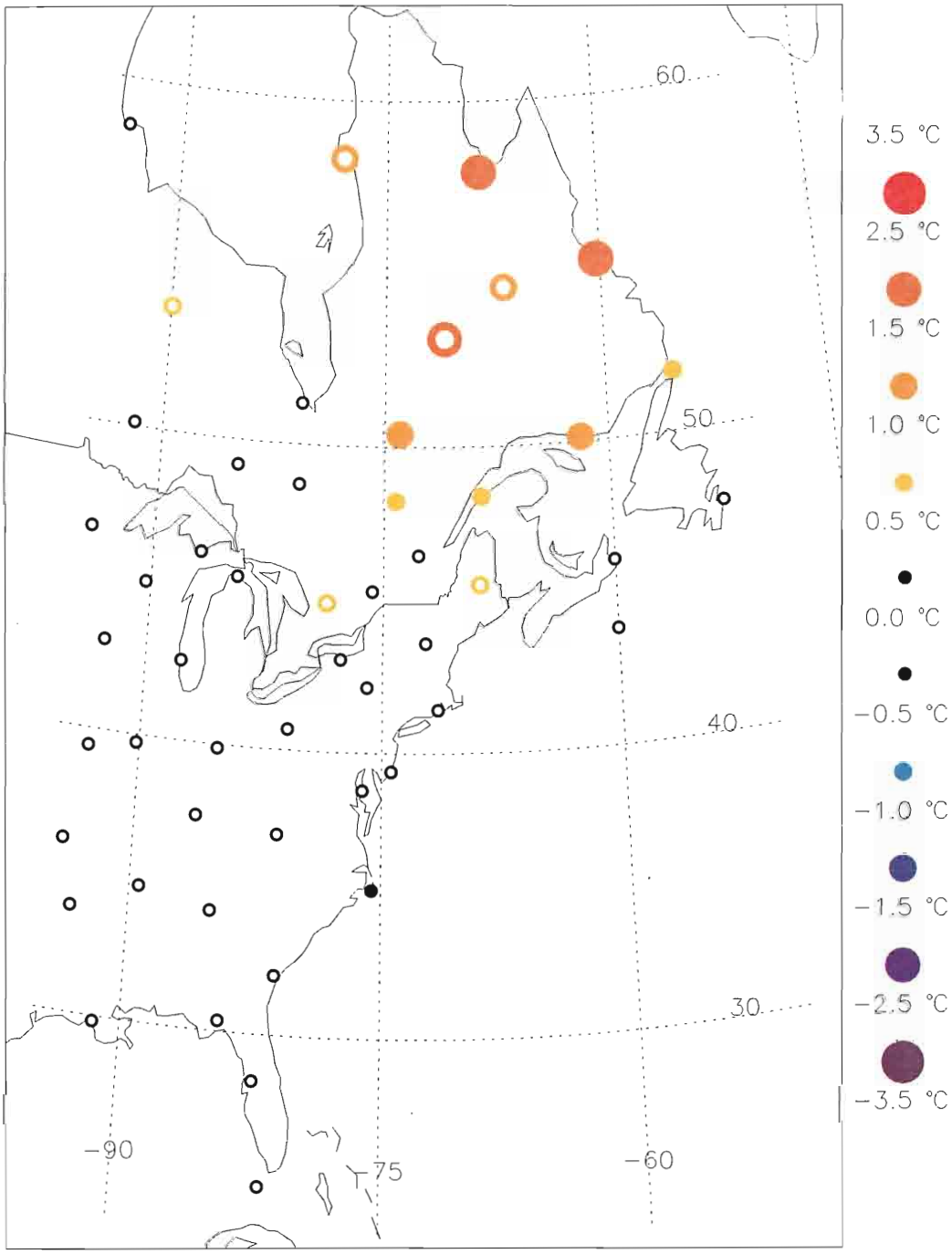

Warm-Neutral NASSTI temperature anomalies during MAM.

Warm-Neutral NASSTI temperature anomalies during MAM.

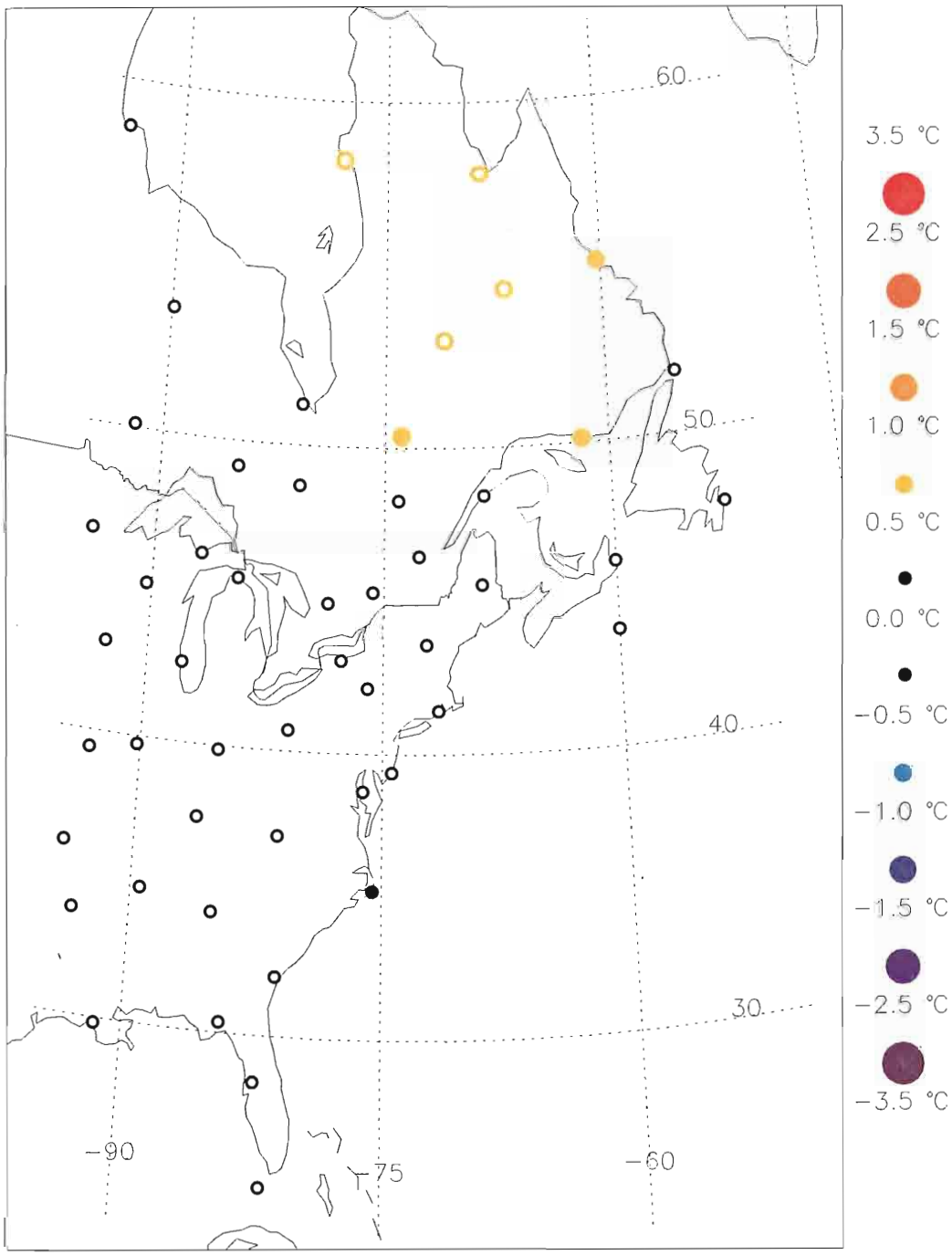

Warm-Neutral NASSTI temperature anomalies during AMJ.

Warm-Neutral NASSTI temperature anomalies during AMJ.

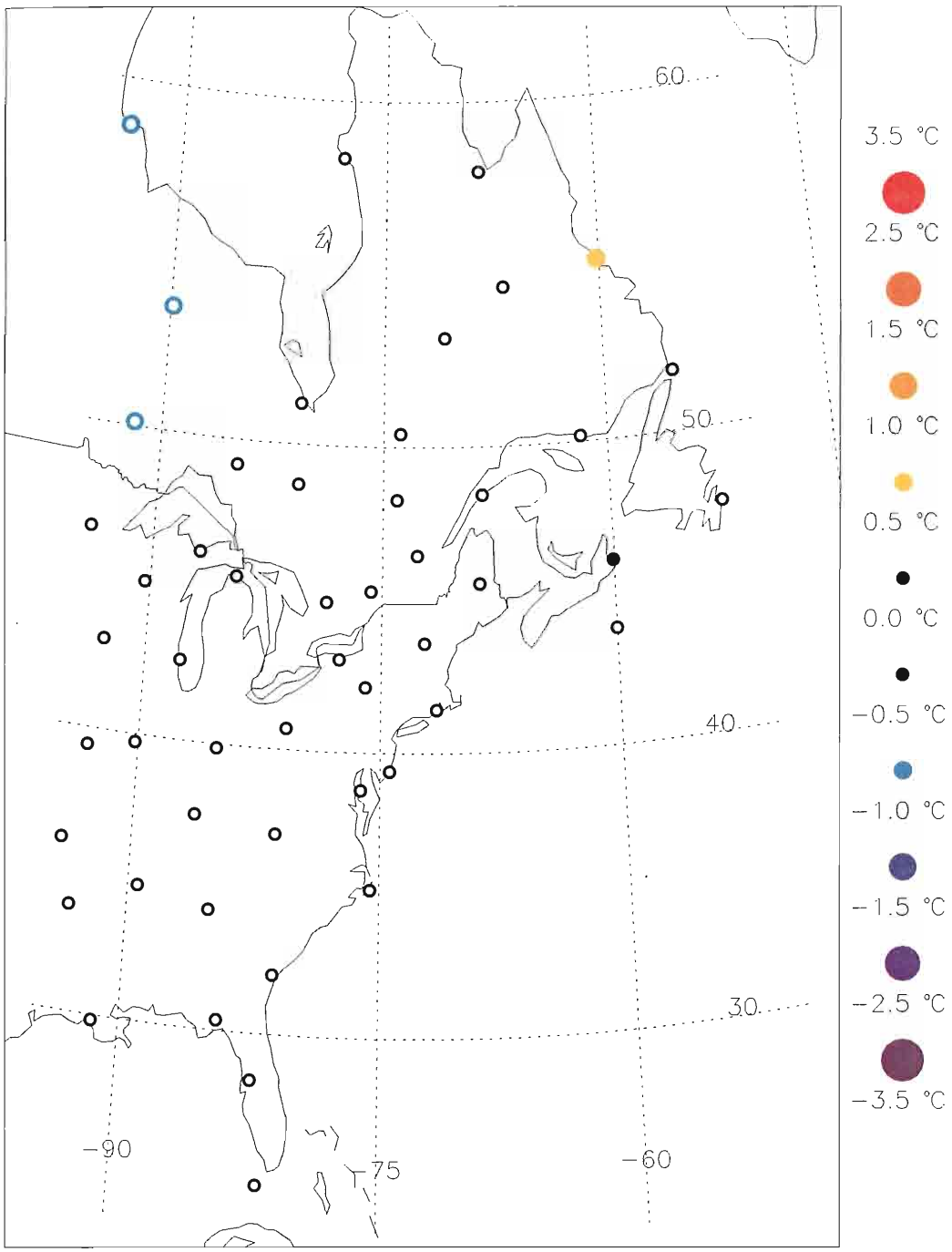

Warm-Neutral NASSTI temperature anomalies during MJJ.

Warm-Neutral NASSTI temperature anomalies during MJJ.

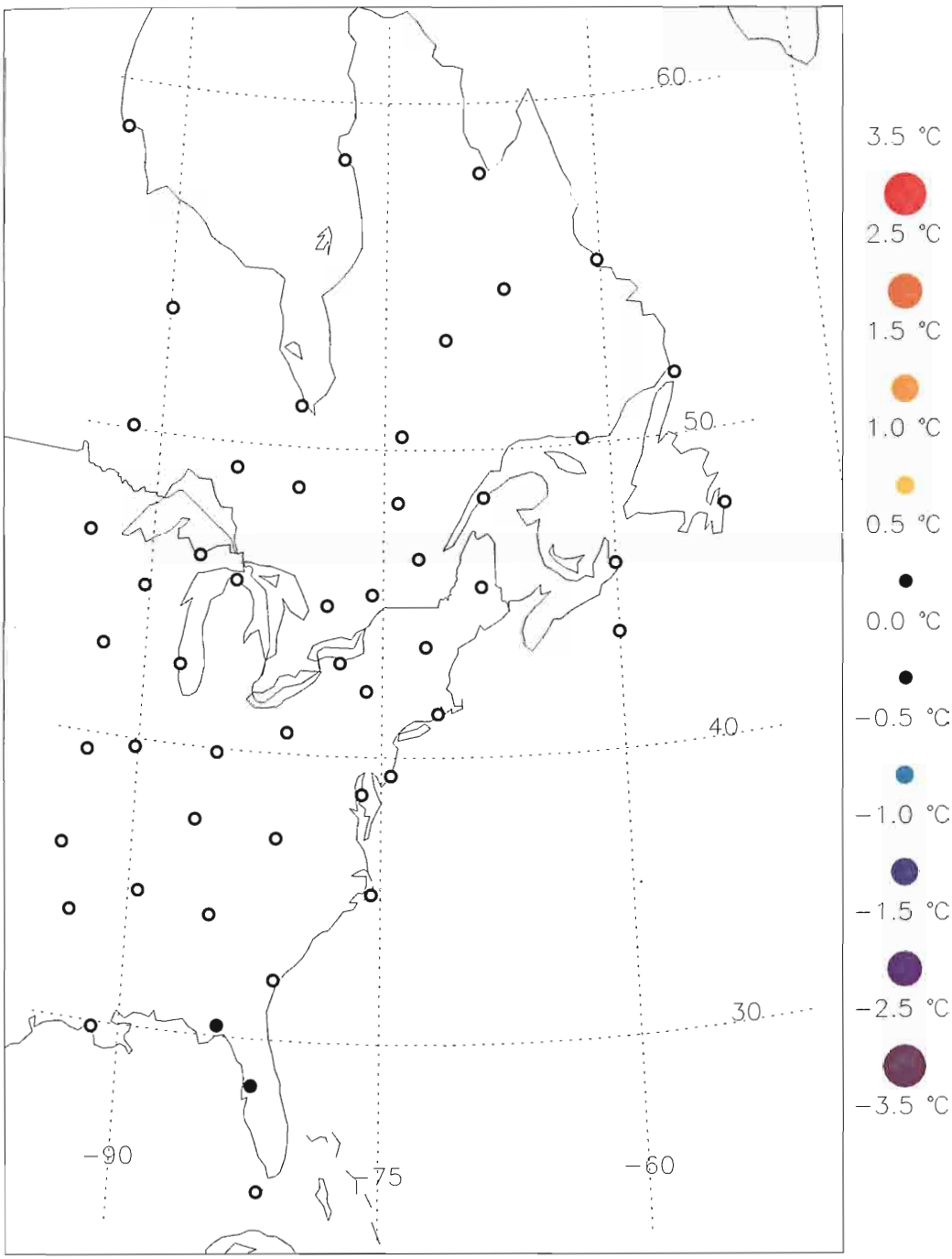

Warm-Neutral NASSTI temperature anomalies during JJA.

Warm-Neutral NASSTI temperature anomalies during JJA.

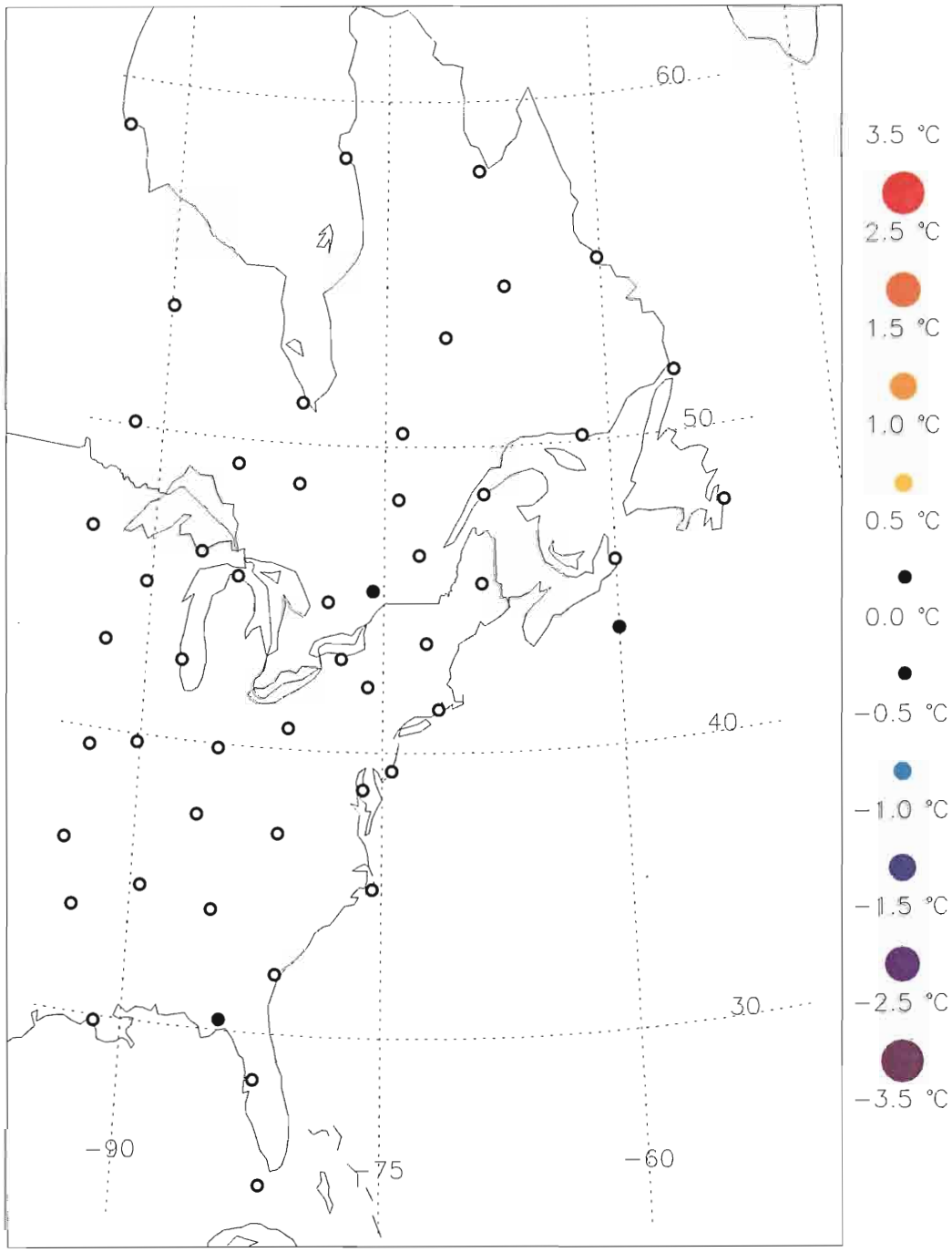

Warm-Neutral NASSTI temperature anomalies during JAS.

Warm-Neutral NASSTI temperature anomalies during JAS.

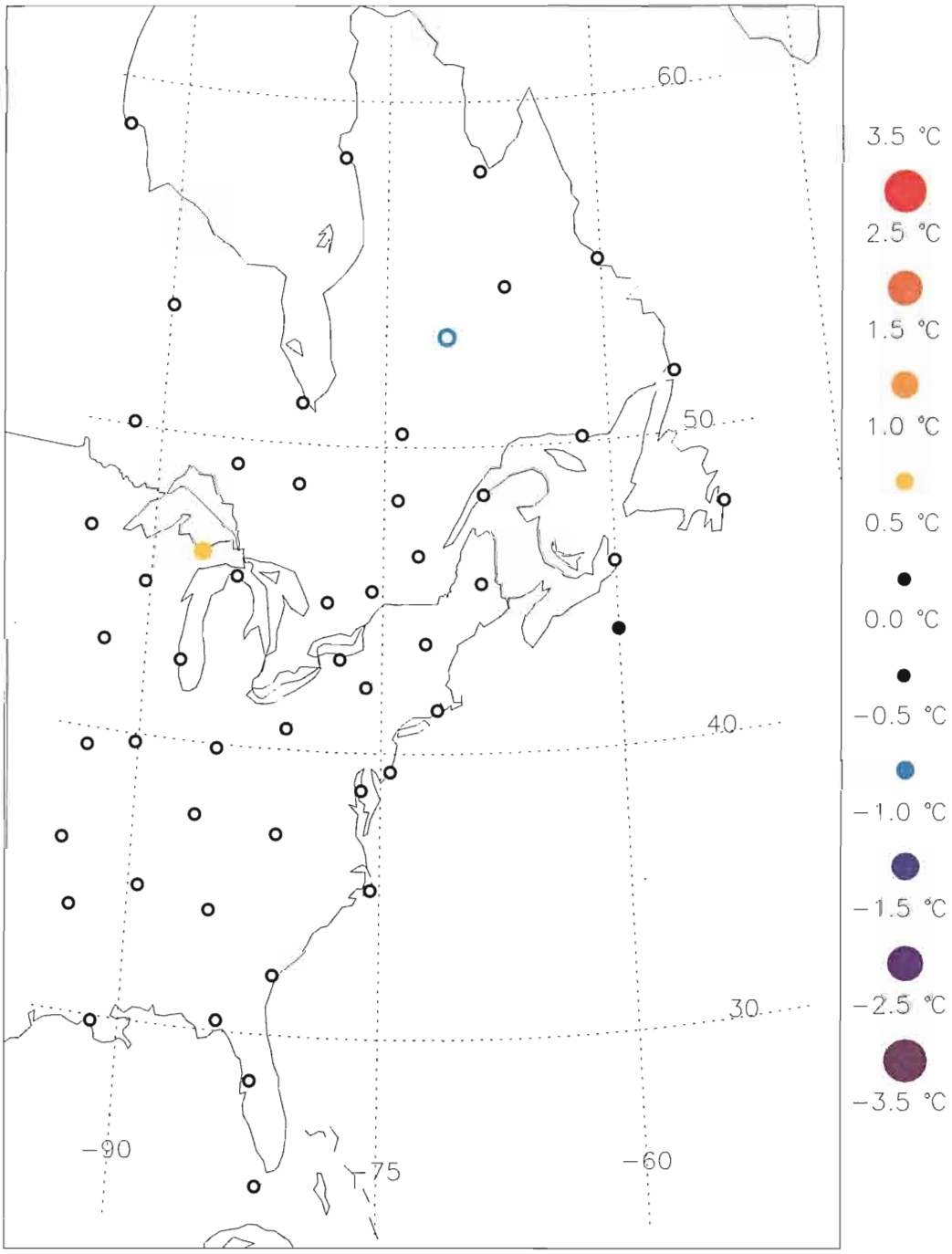

Warm-Neutral NASSTI temperature anomalies during ASO.

Warm-Neutral NASSTI temperature anomalies during ASO.

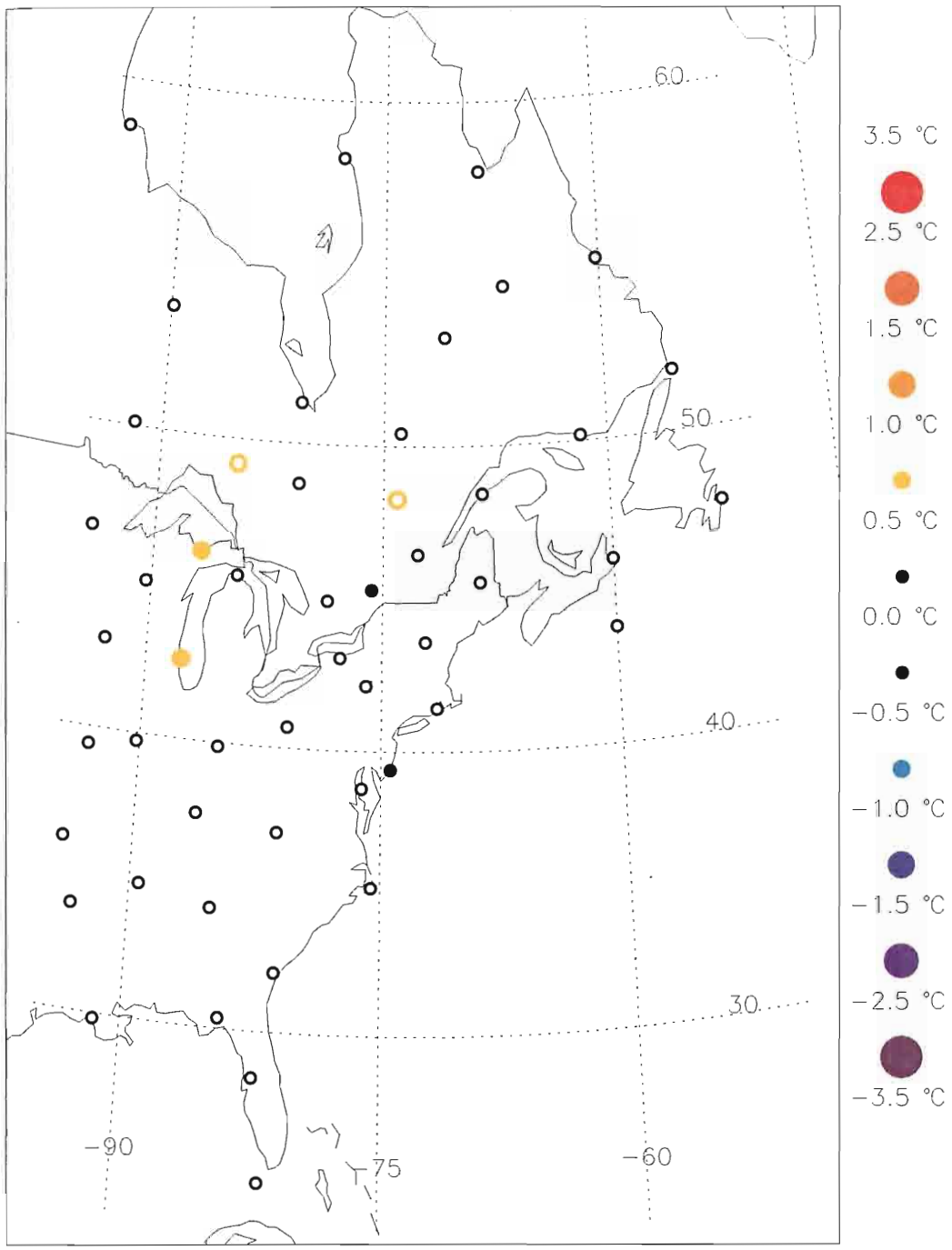

Warm-Neutral NASSTI temperature anomalies during SON.

Warm-Neutral NASSTI temperature anomalies during SON.

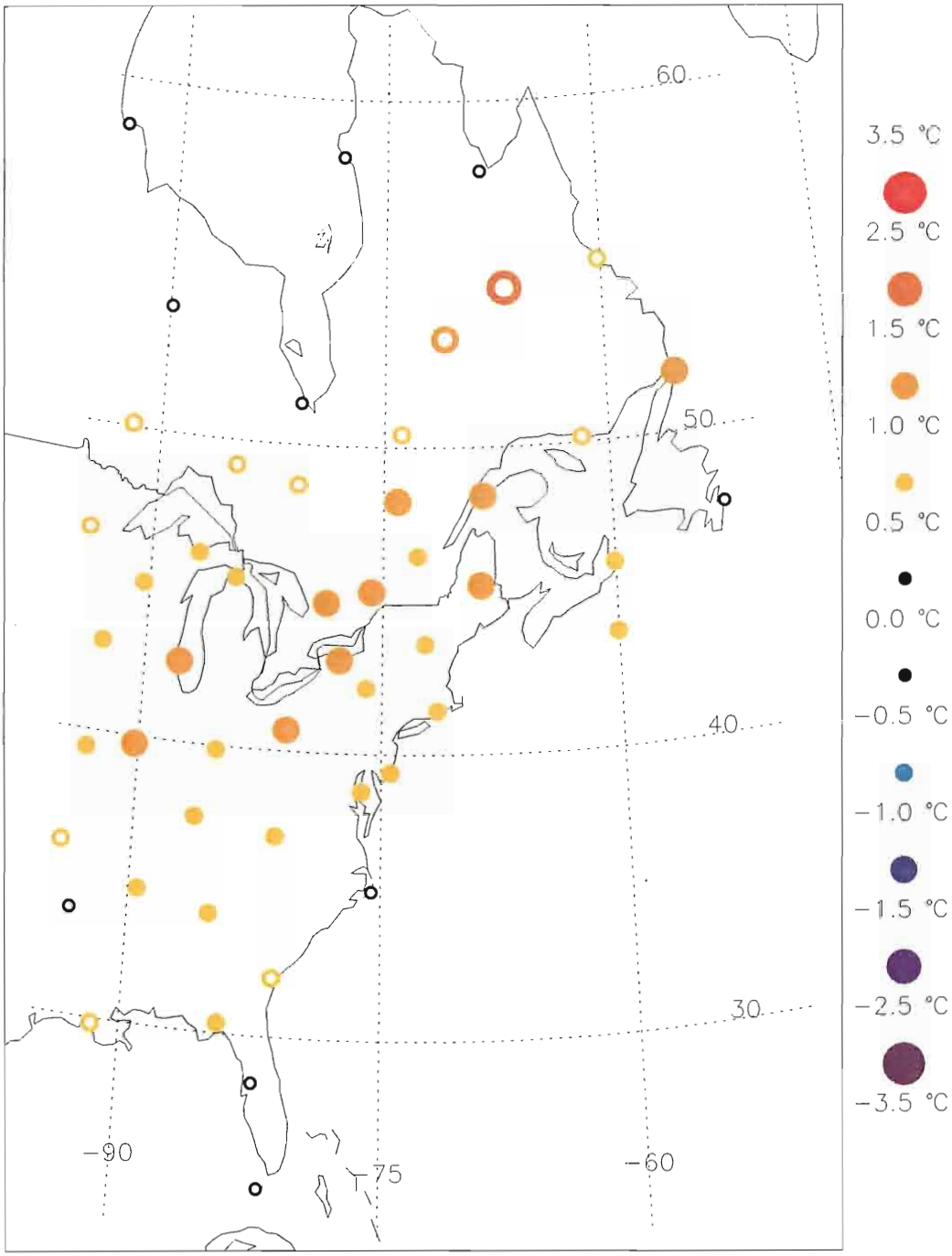

Warm-Neutral NASSTI temperature anomalies during NDJ.

Warm-Neutral NASSTI temperature anomalies during NDJ.

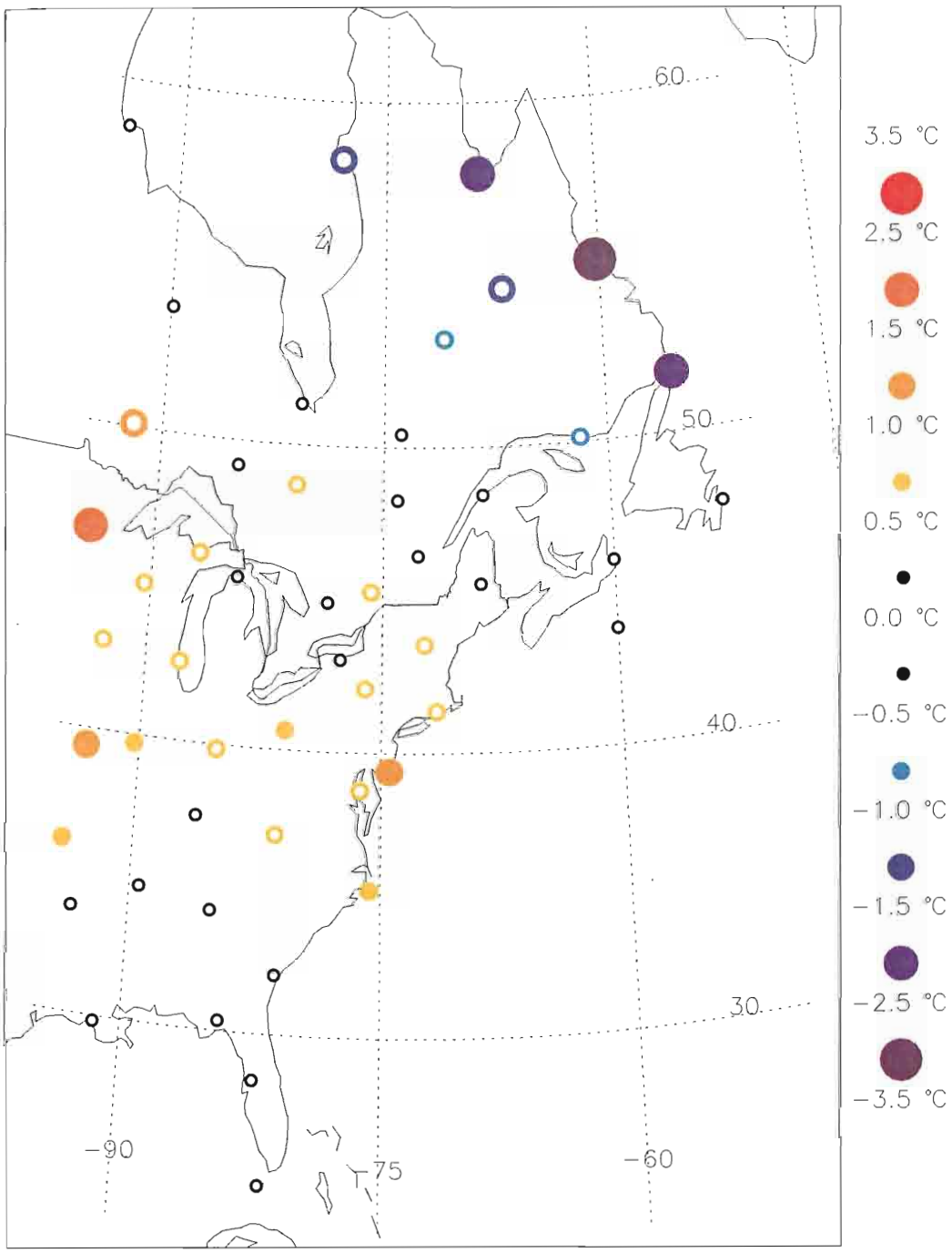

Cold-Neutral NASSTI temperature anomalies during JFM.

Cold-Neutral NASSTI temperature anomalies during JFM.

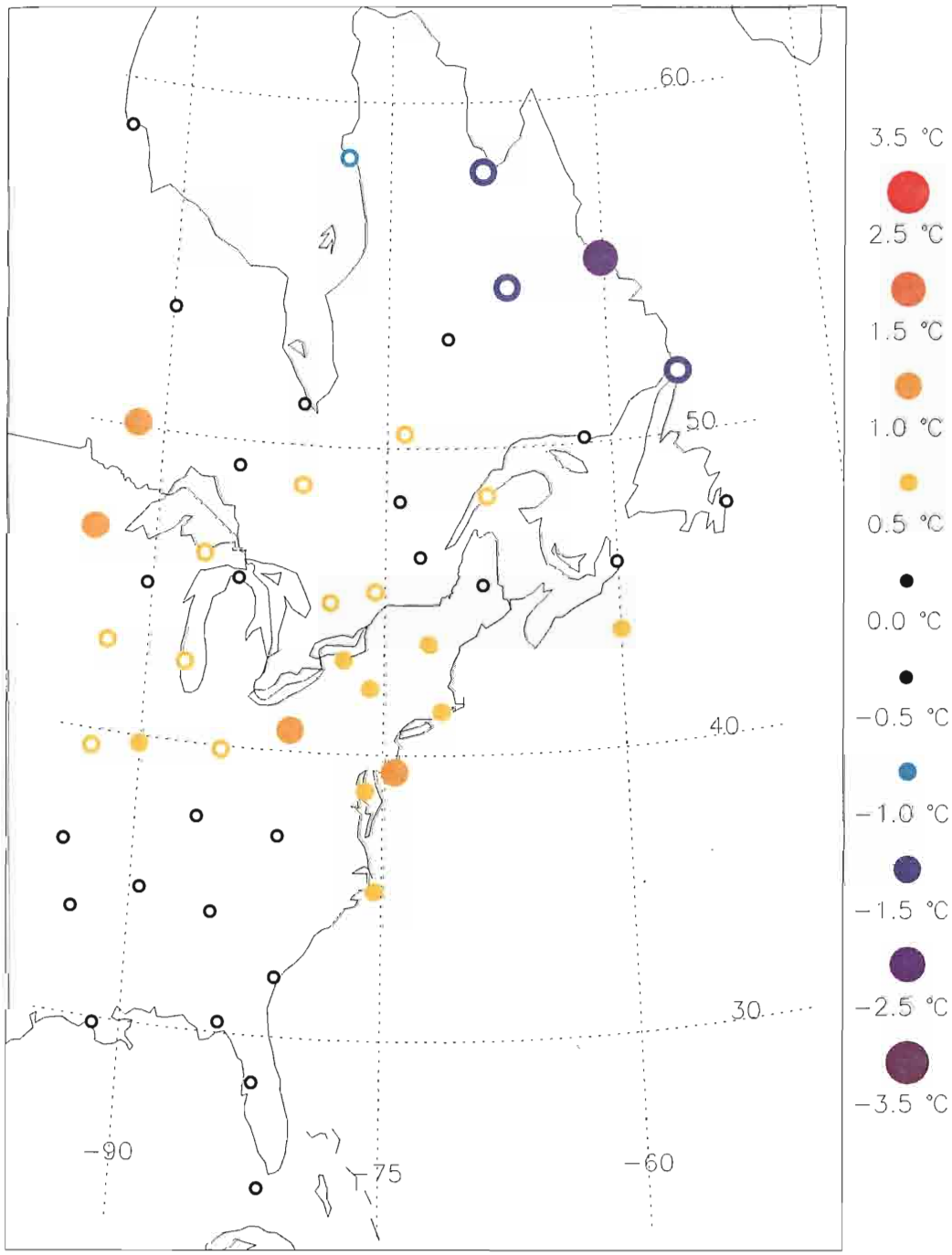

Cold-Neutral NASSTI temperature anomalies during FMA.

Cold-Neutral NASSTI temperature anomalies during FMA.

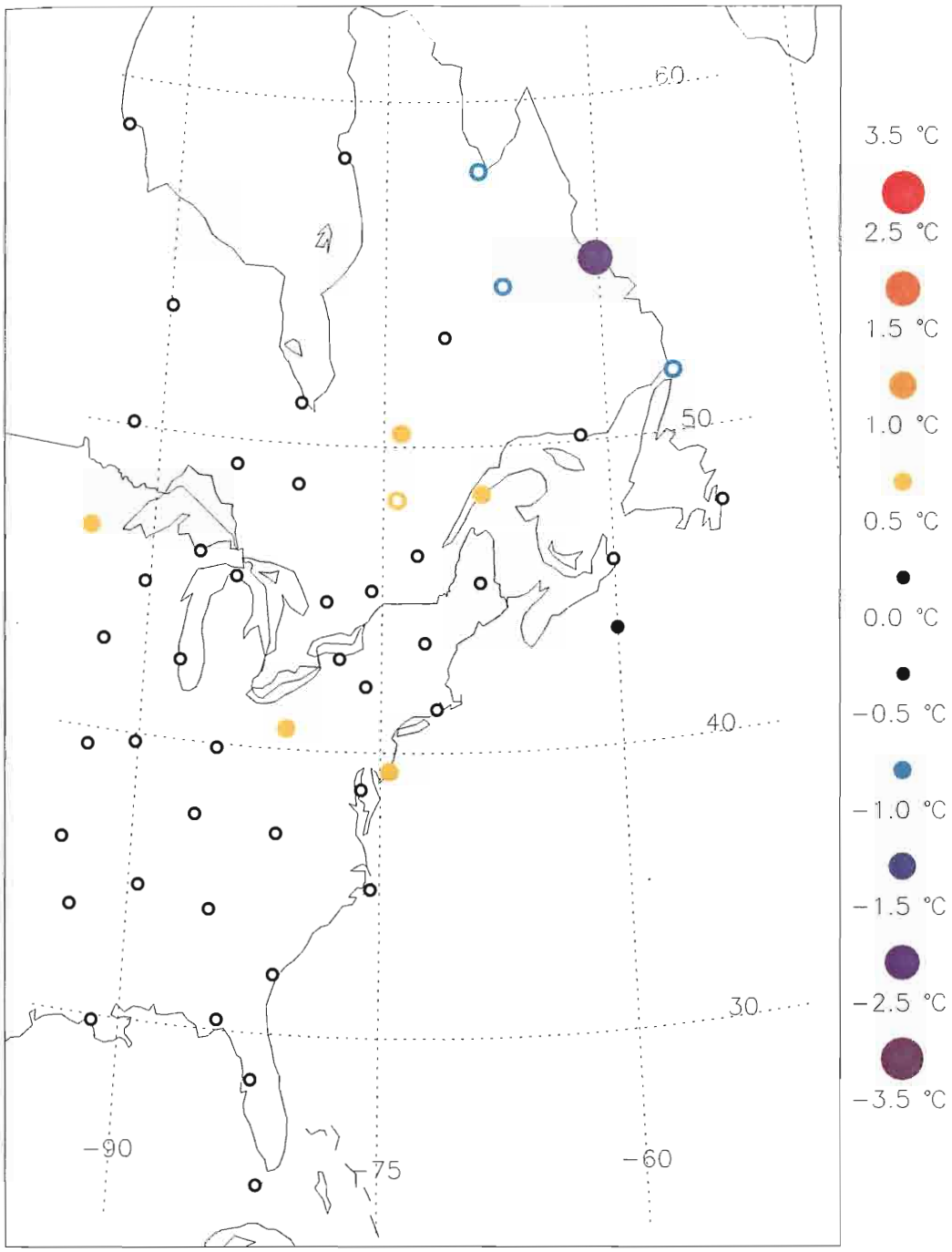

Cold-Neutral NASSTI temperature anomalies during MAM.

Cold-Neutral NASSTI temperature anomalies during MAM.

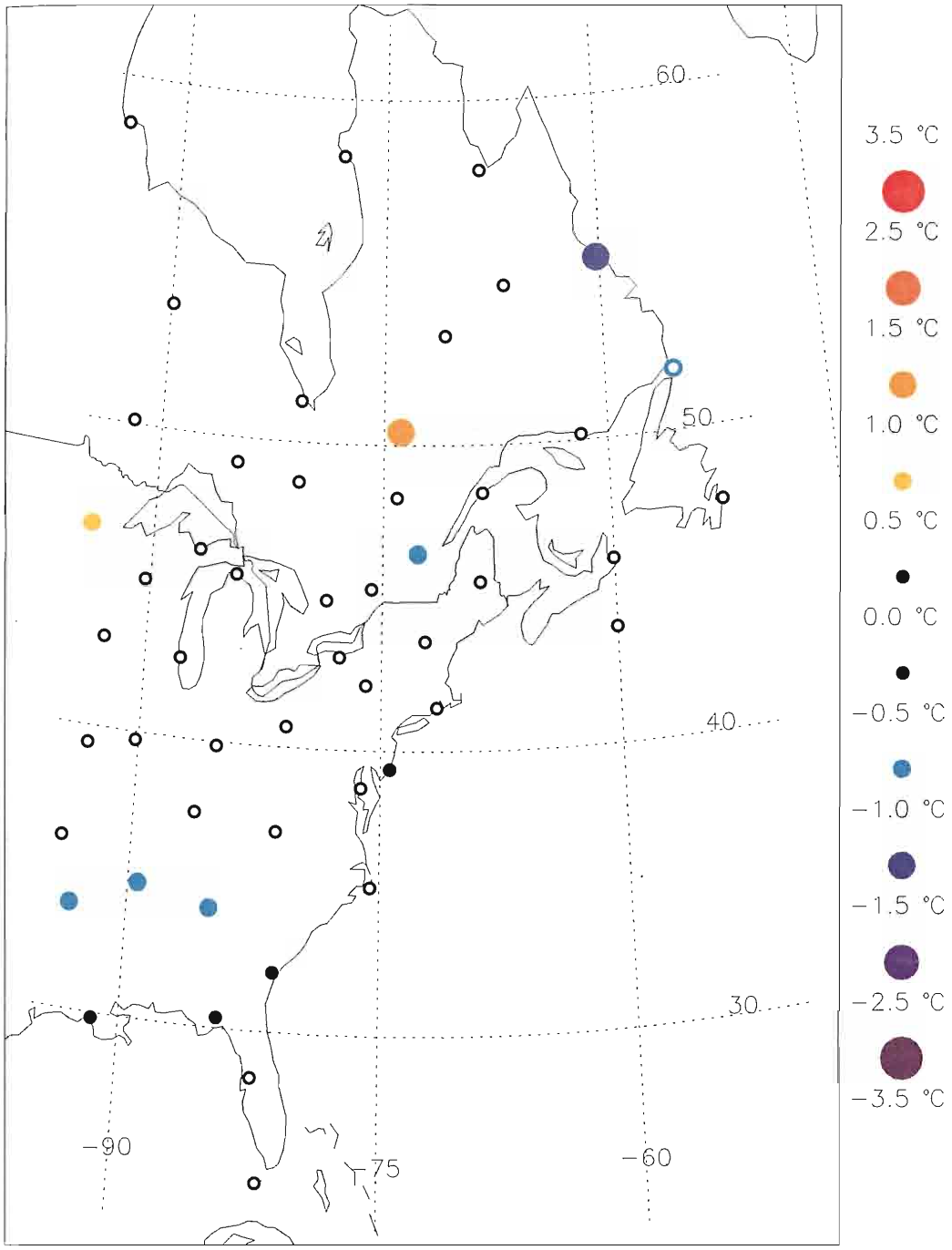

Cold-Neutral NASSTI temperature anomalies during AMJ.

Cold-Neutral NASSTI temperature anomalies during AMJ.

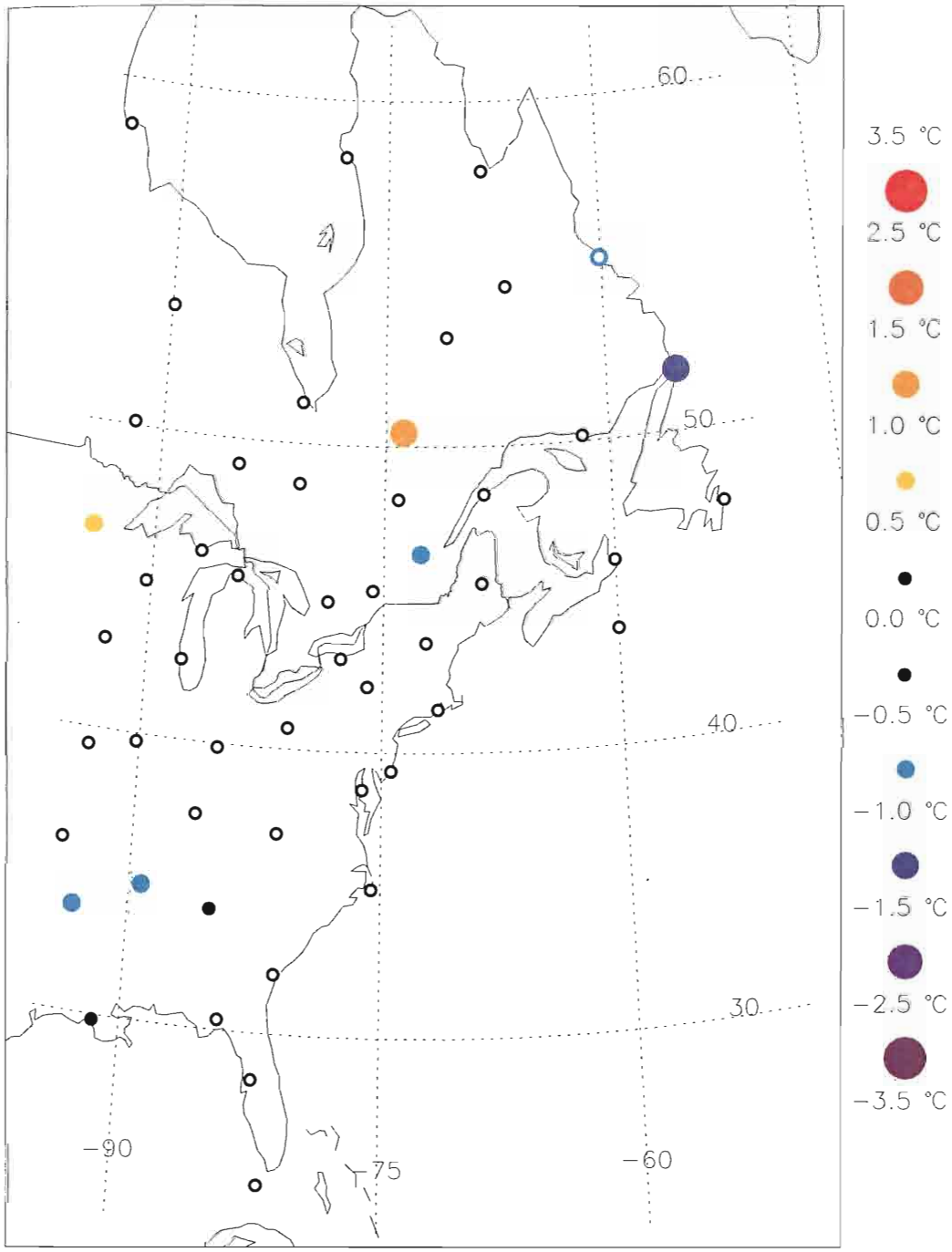

Cold-Neutral NASSTI temperature anomalies during MJJ.

Cold-Neutral NASSTI temperature anomalies during MJJ.

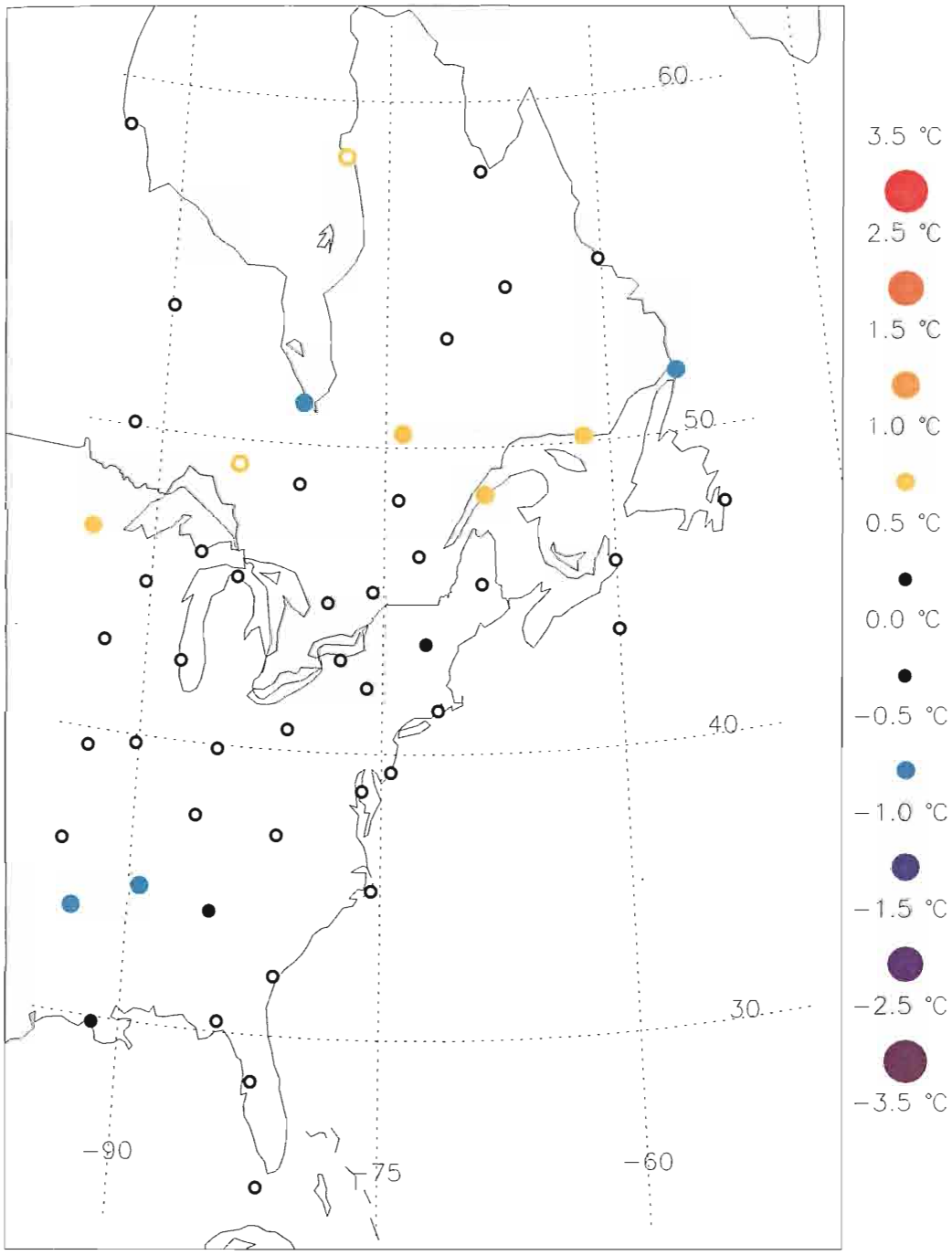

Cold-Neutral NASSTI temperature anomalies during JJA.

Cold-Neutral NASSTI temperature anomalies during JJA.

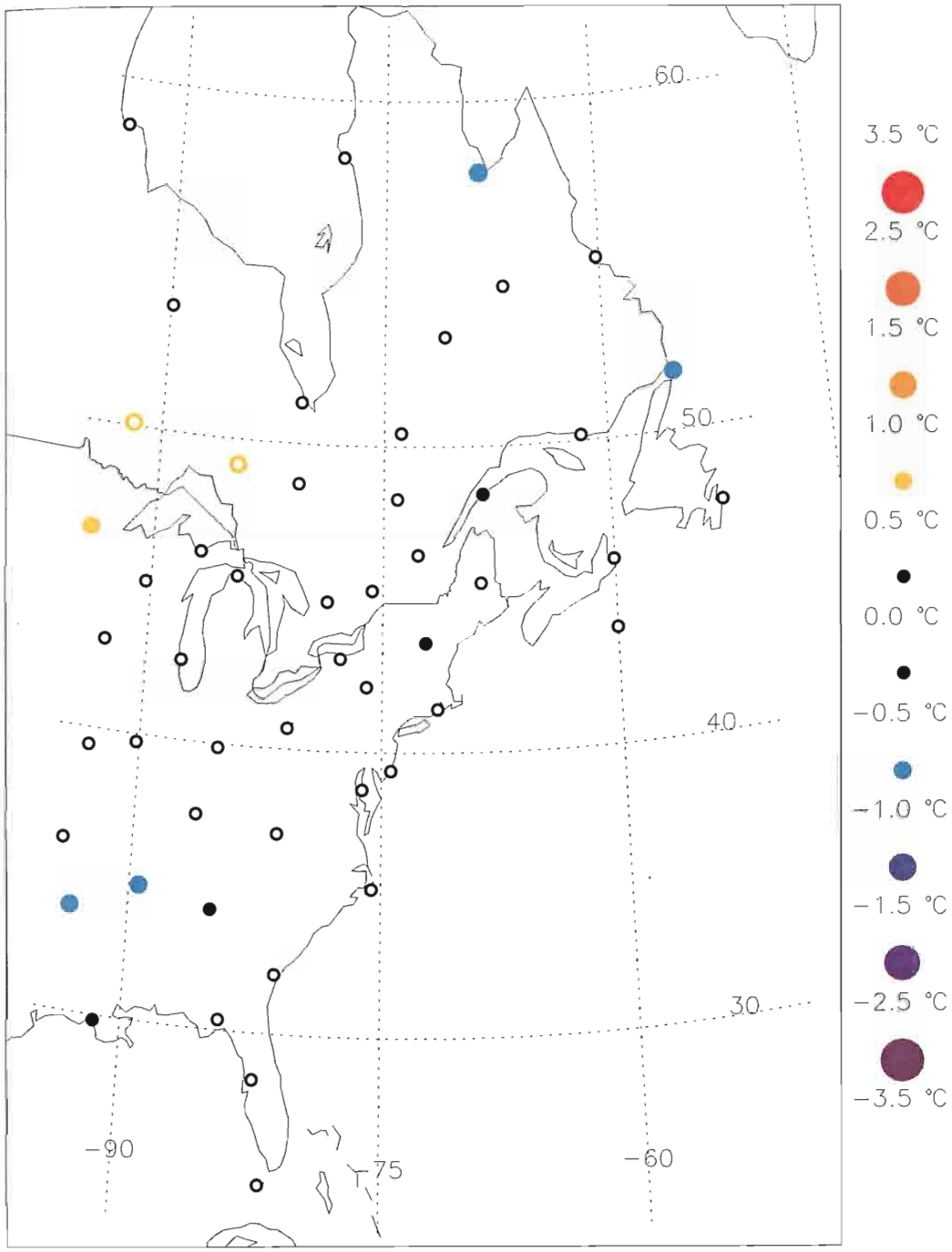

Cold-Neutral NASSTI temperature anomalies during JAS.

Cold-Neutral NASSTI temperature anomalies during JAS.

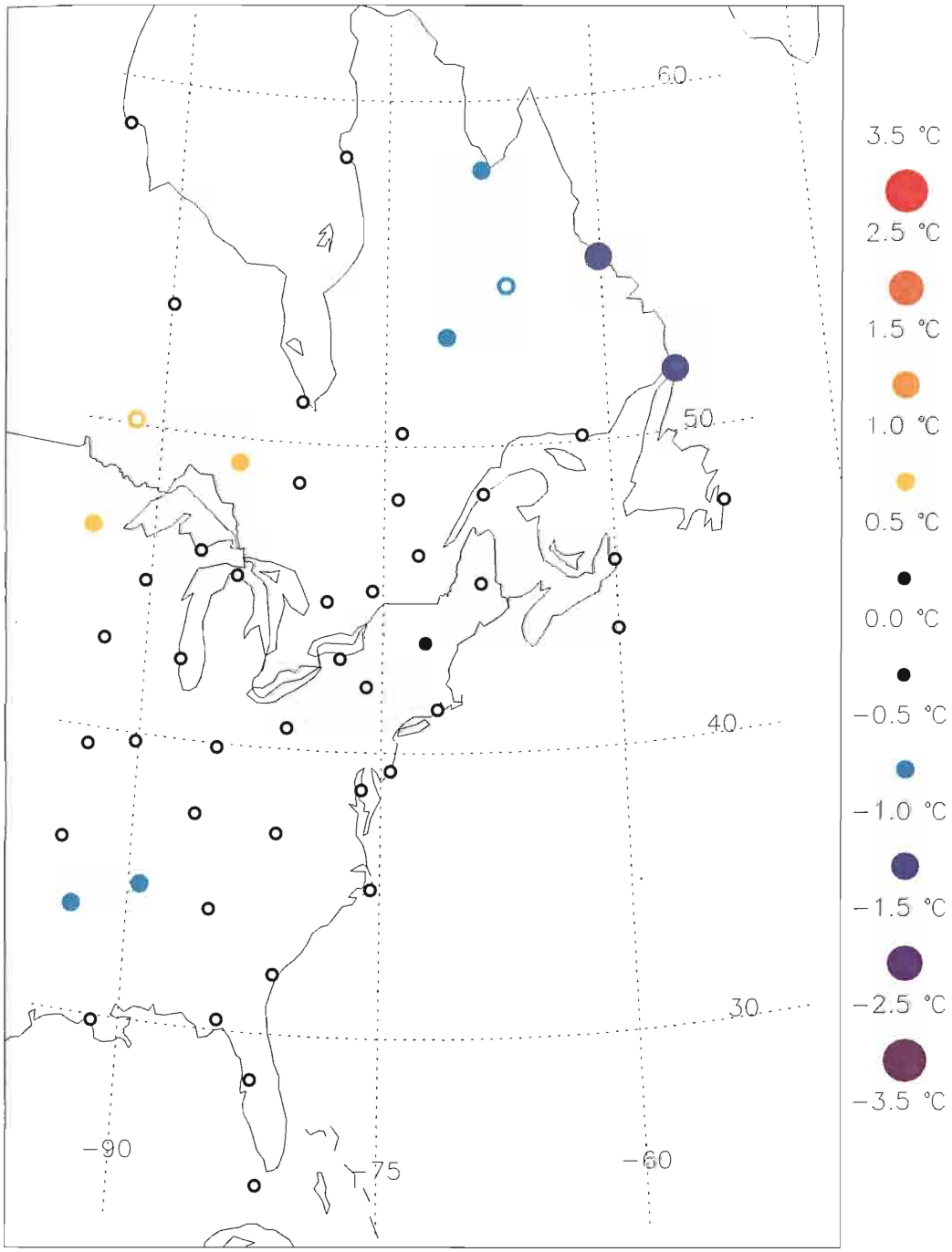

Cold-Neutral NASSTI temperature anomalies during ASO.

Cold-Neutral NASSTI temperature anomalies during ASO.

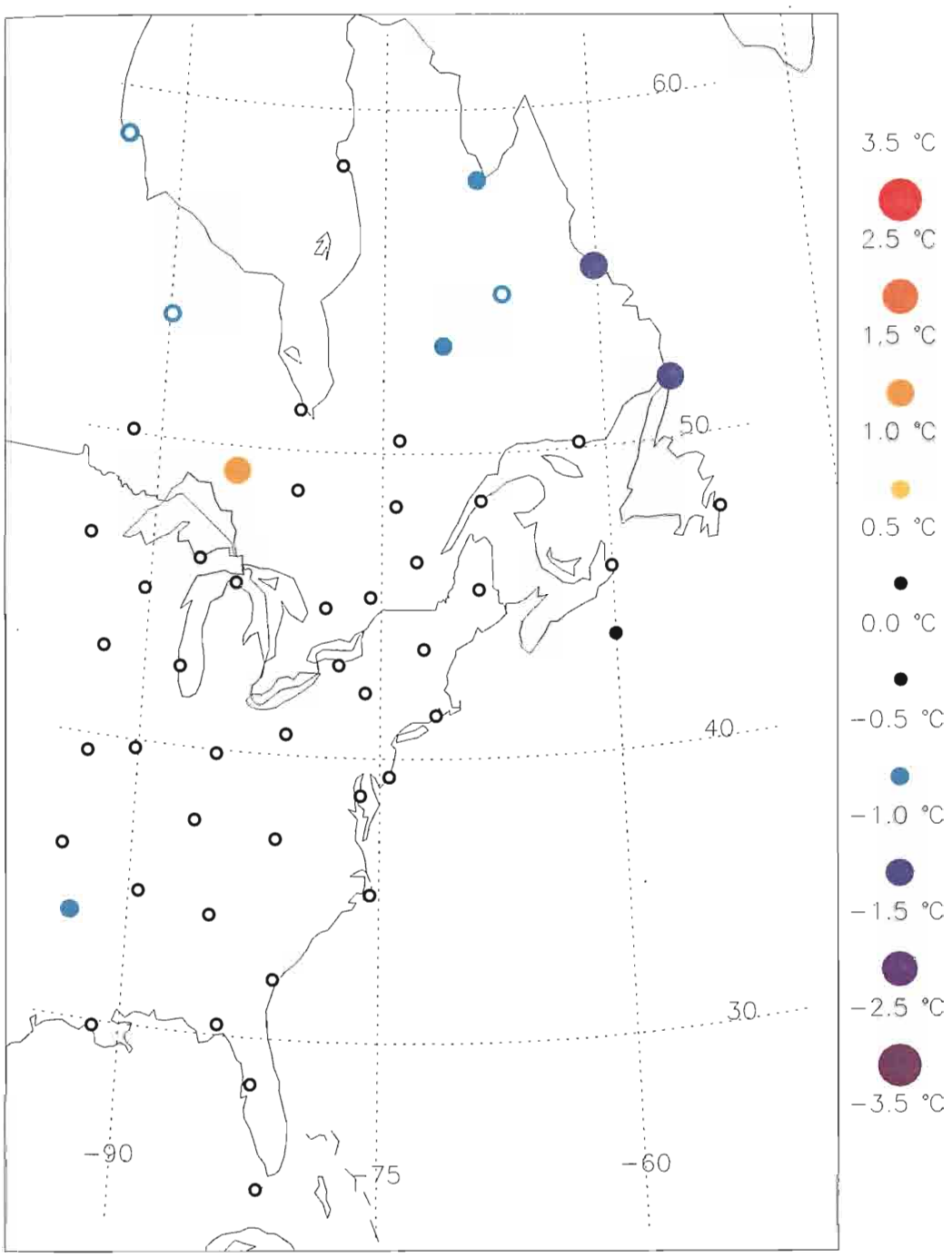

Cold-Neutral NASSTI temperature anomalies during SON.

Cold-Neutral NASSTI temperature anomalies during SON.

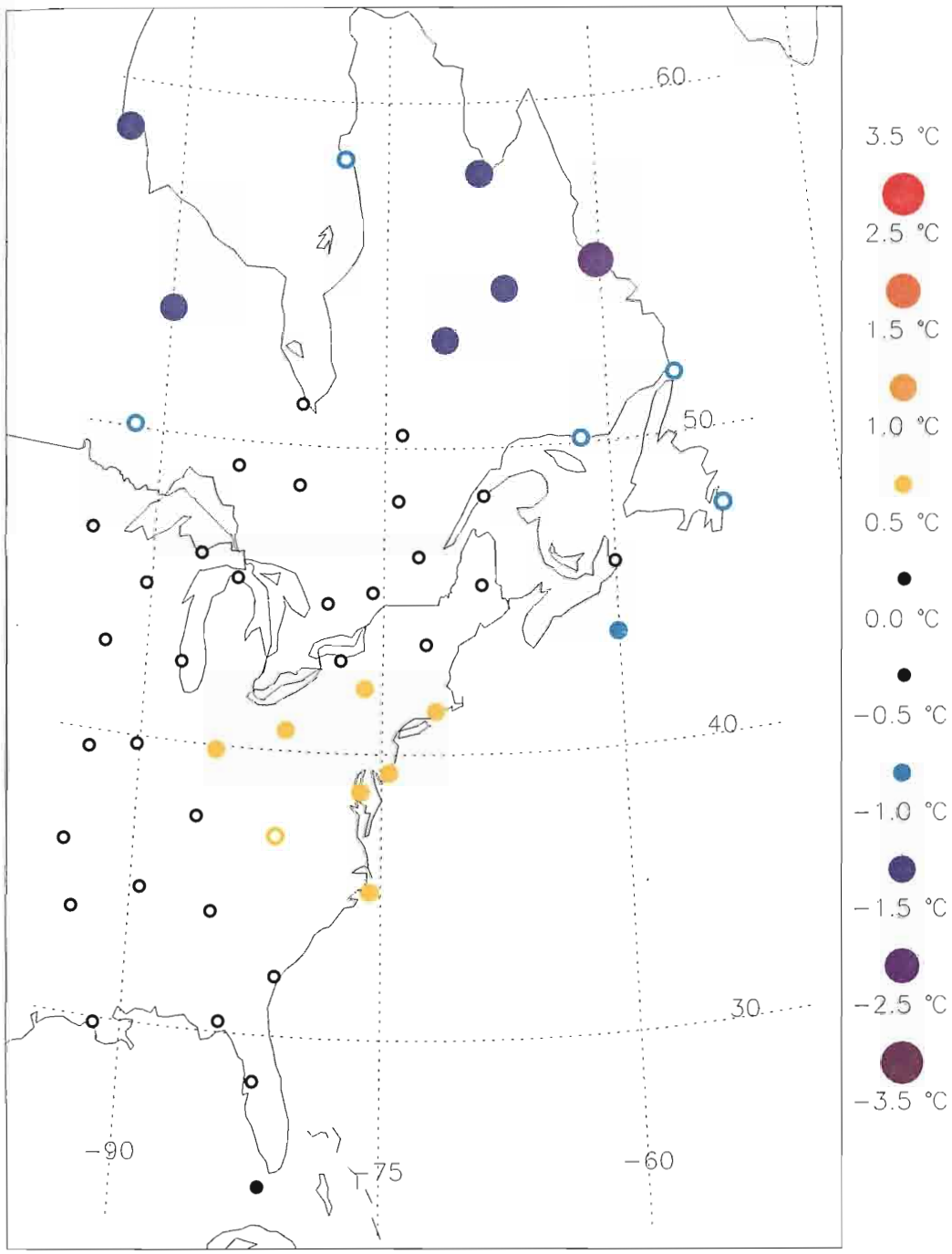

Cold-Neutral NASSTI temperature anomalies during OND.

Cold-Neutral NASSTI temperature anomalies during OND.

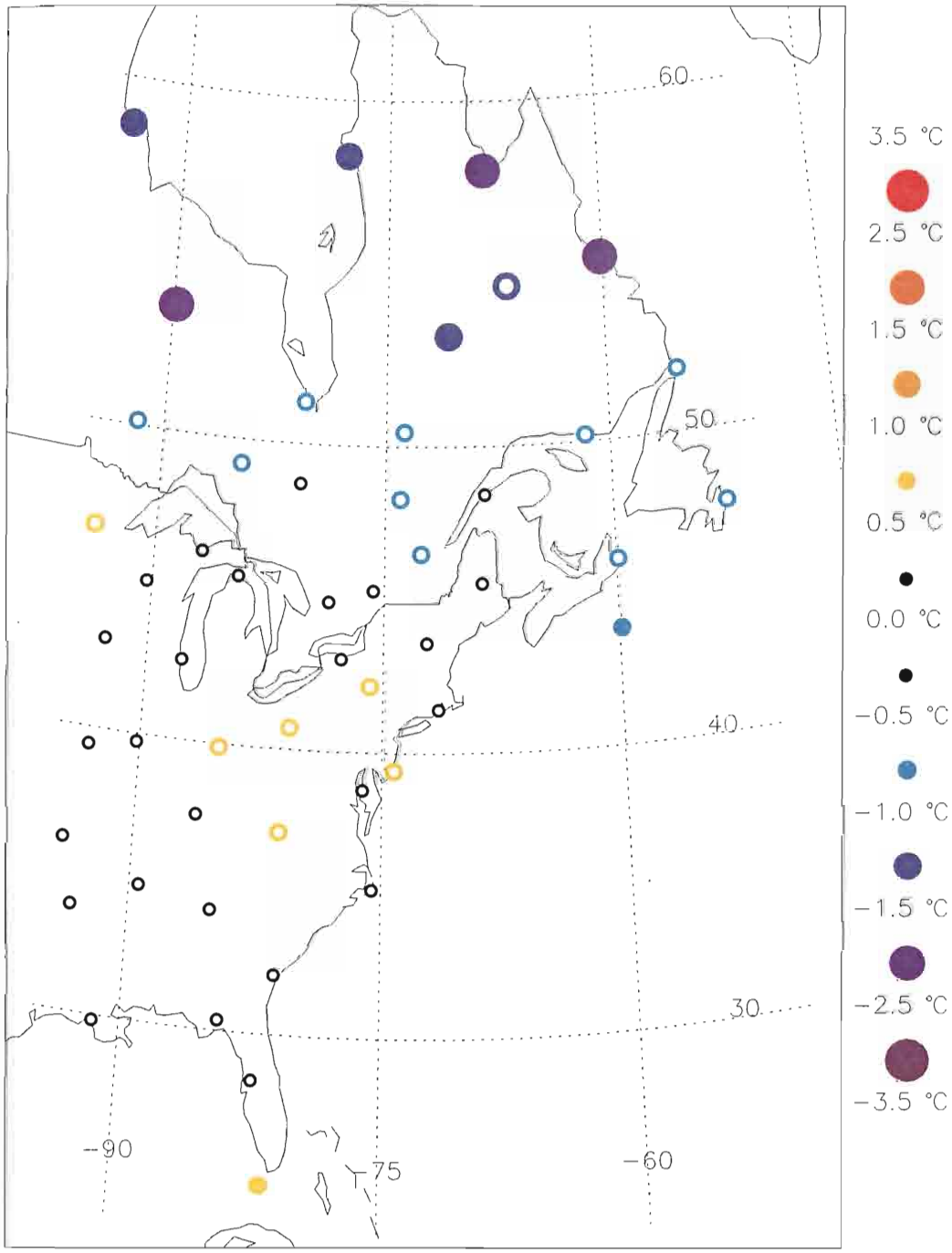

Cold-Neutral NASSTI temperature anomalies during NDJ.

Cold-Neutral NASSTI temperature anomalies during NDJ.

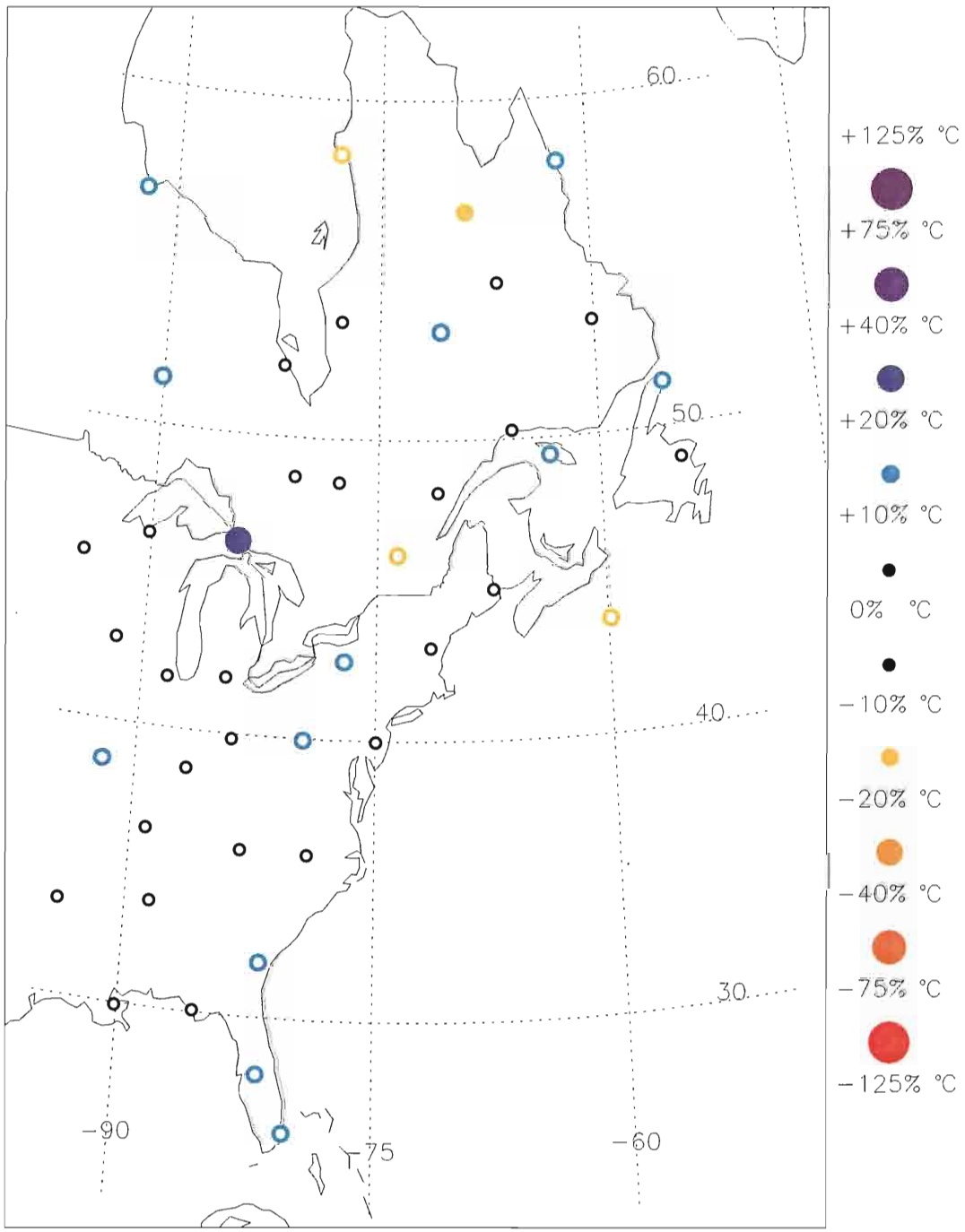

Warm-Neutral NASSTI percent precipitation deviation during DJF.

Warm-Neutral NASSTI percent precipitation deviation during DJF.

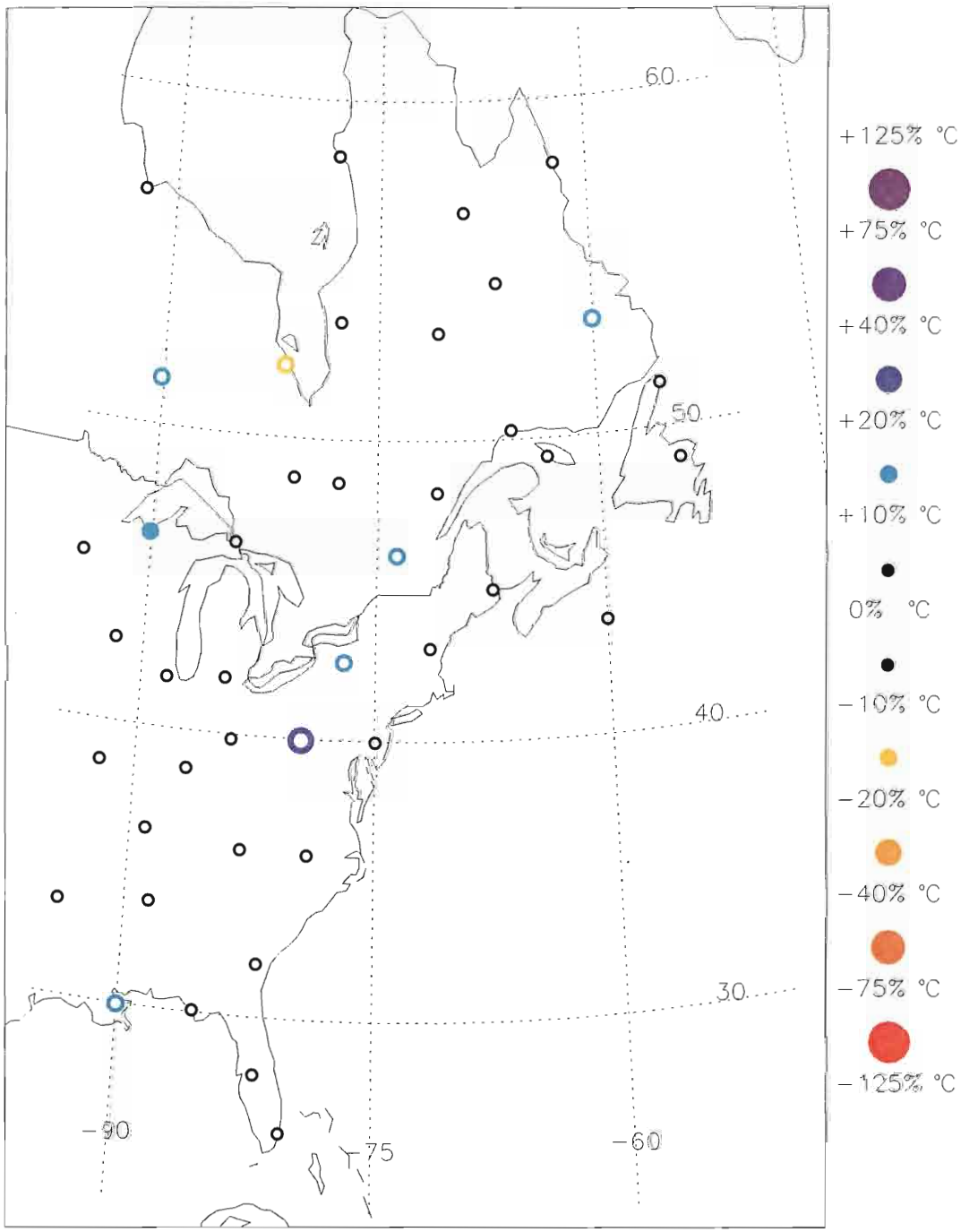

Warm-Neutral NASSTI percent precipitation deviation during JFM.

Warm-Neutral NASSTI percent precipitation deviation during JFM.

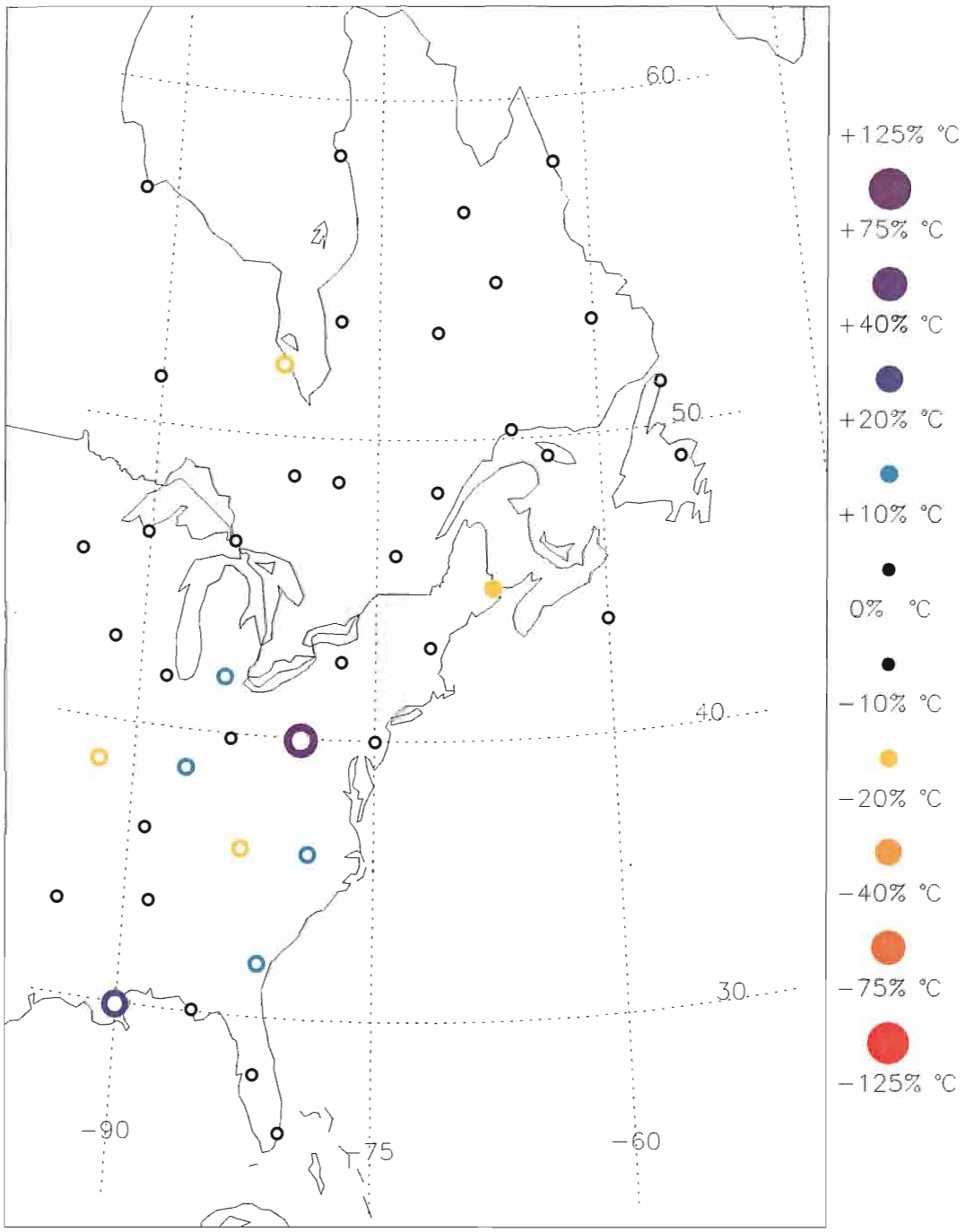

Warm-Neutral NASSTI percent precipitation deviation during FMA.

Warm-Neutral NASSTI percent precipitation deviation during FMA.

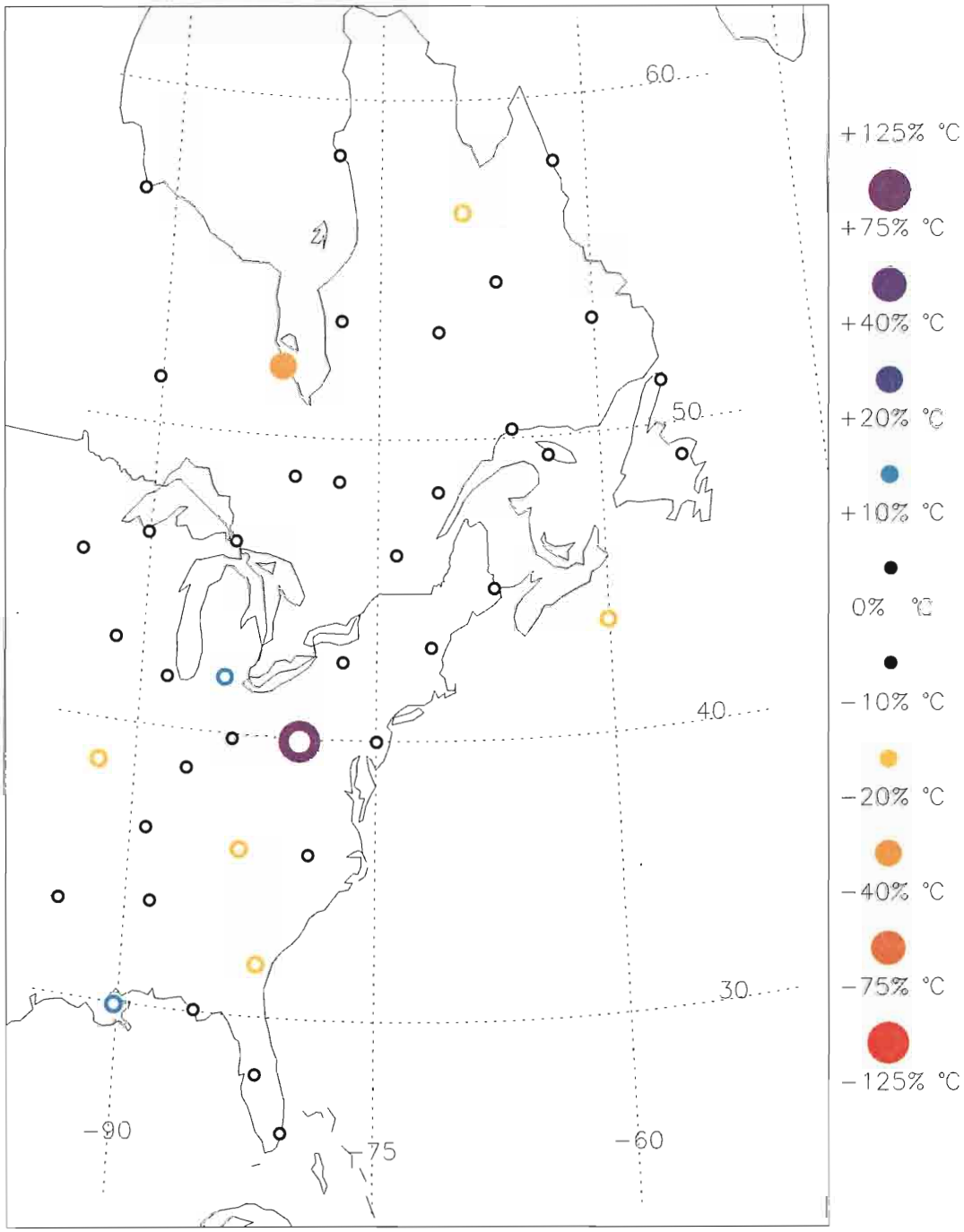

Warm-Neutral NASSTI percent precipitation deviation during MAM.

Warm-Neutral NASSTI percent precipitation deviation during MAM.

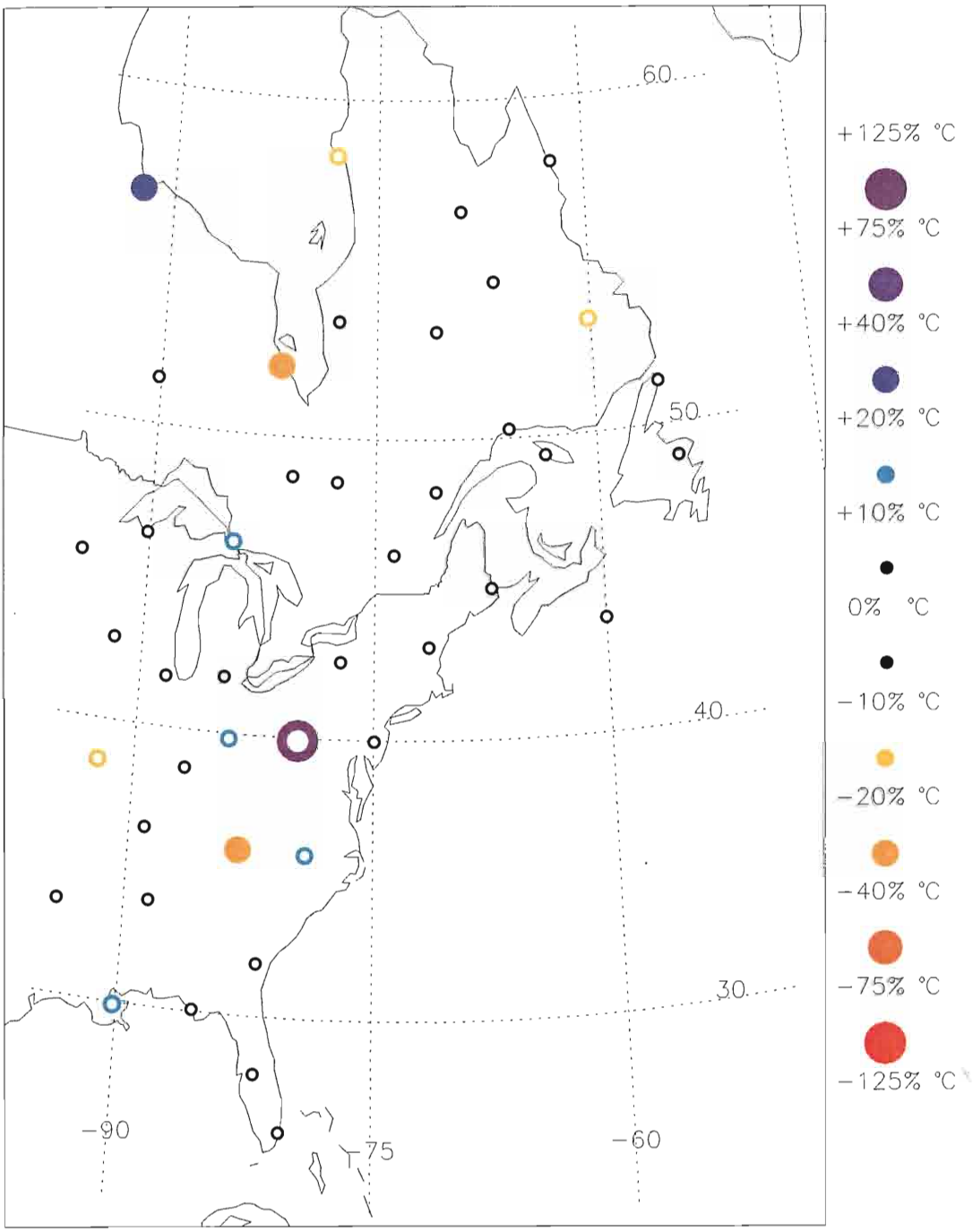

Warm-Neutral NASSTI percent precipitation deviation during AMJ.

Warm-Neutral NASSTI percent precipitation deviation during AMJ.

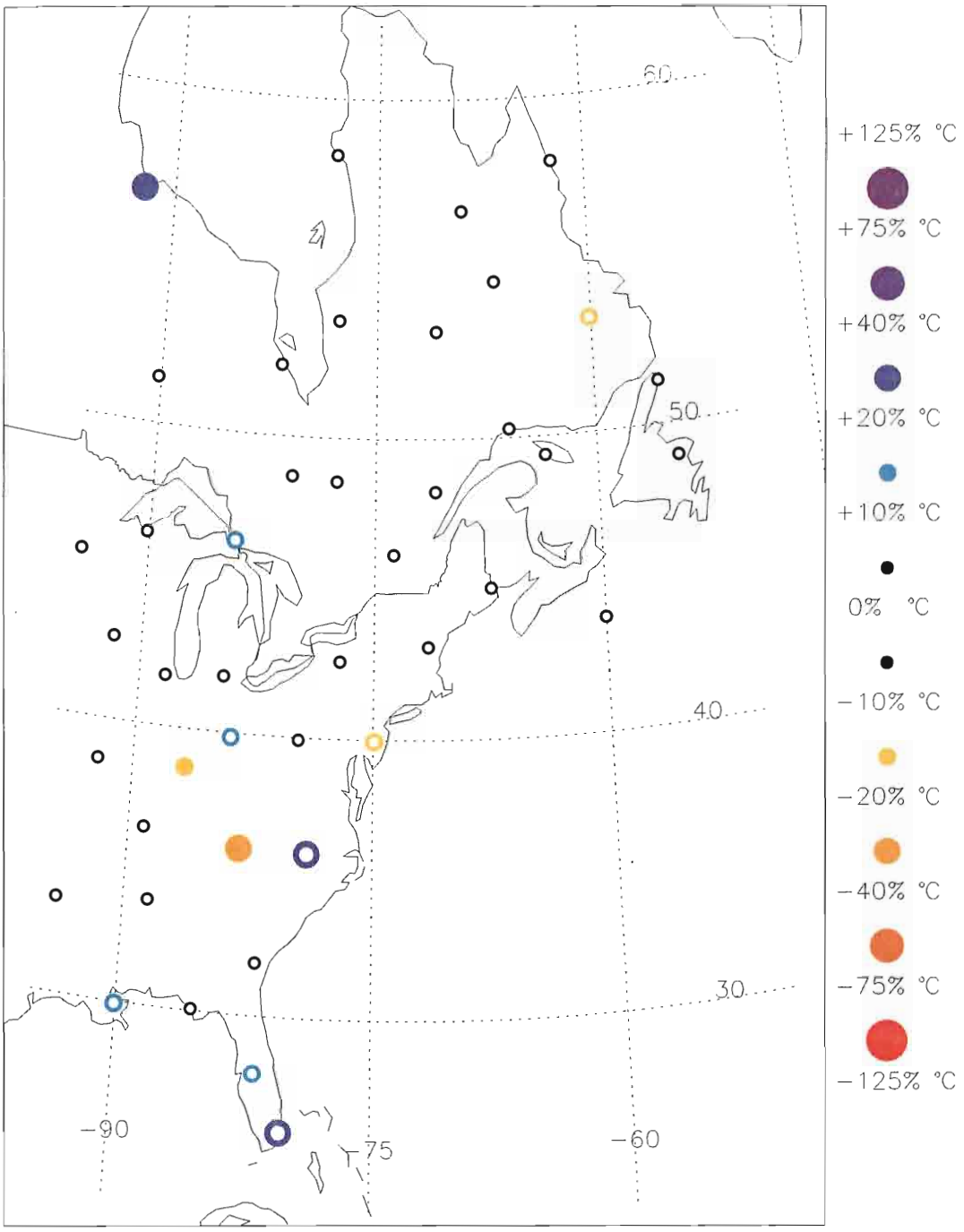

Warm-Neutral NASSTI percent precipitation deviation during MJJ.

Warm-Neutral NASSTI percent precipitation deviation during MJJ.

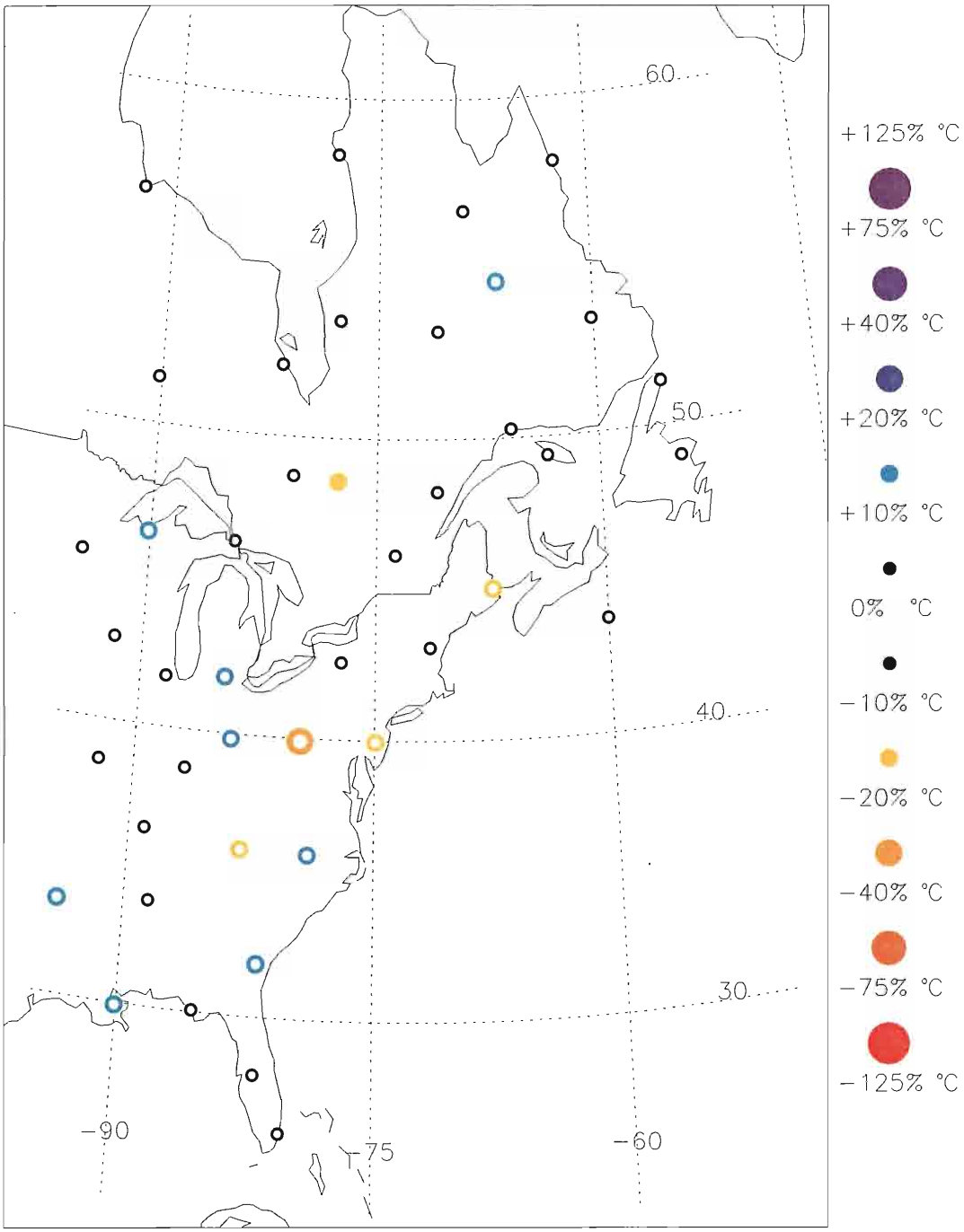

Warm-Neutral NASSTI percent precipitation deviation during JJA.

Warm-Neutral NASSTI percent precipitation deviation during JJA.

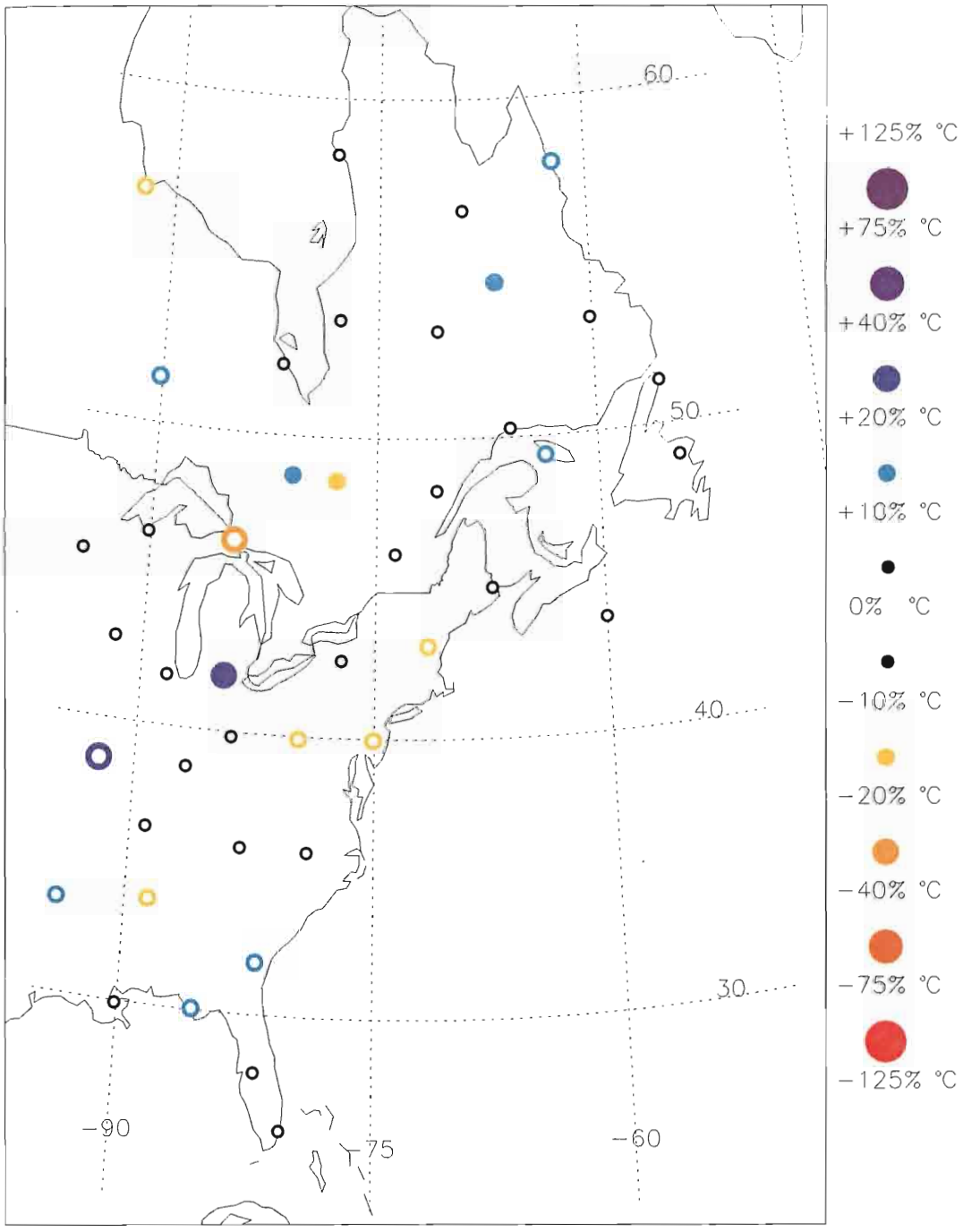

Warm-Neutral NASSTI percent precipitation deviation during JAS.

Warm-Neutral NASSTI percent precipitation deviation during JAS.

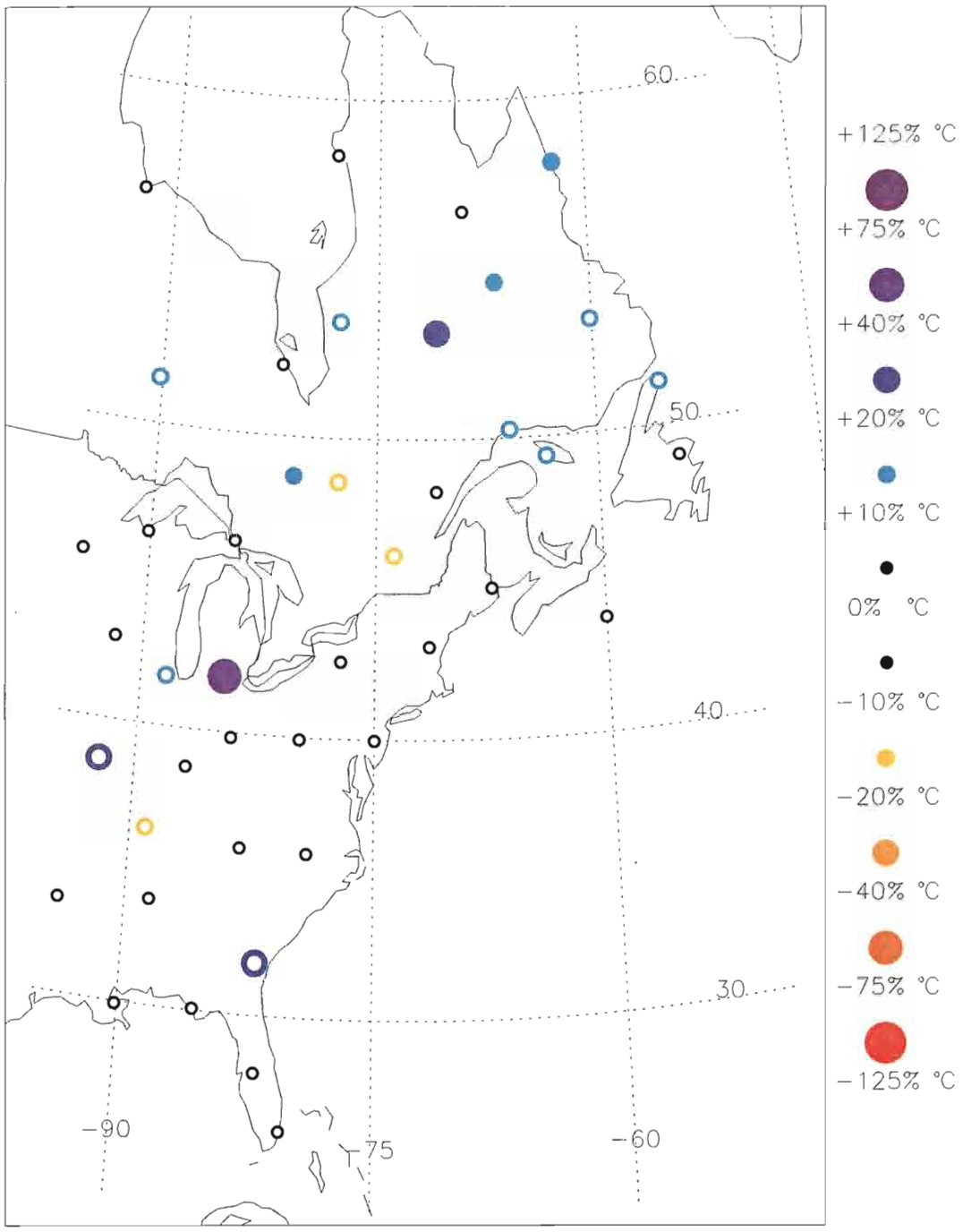

Warm-Neutral NASSTI percent precipitation deviation during SON.

Warm-Neutral NASSTI percent precipitation deviation during SON.

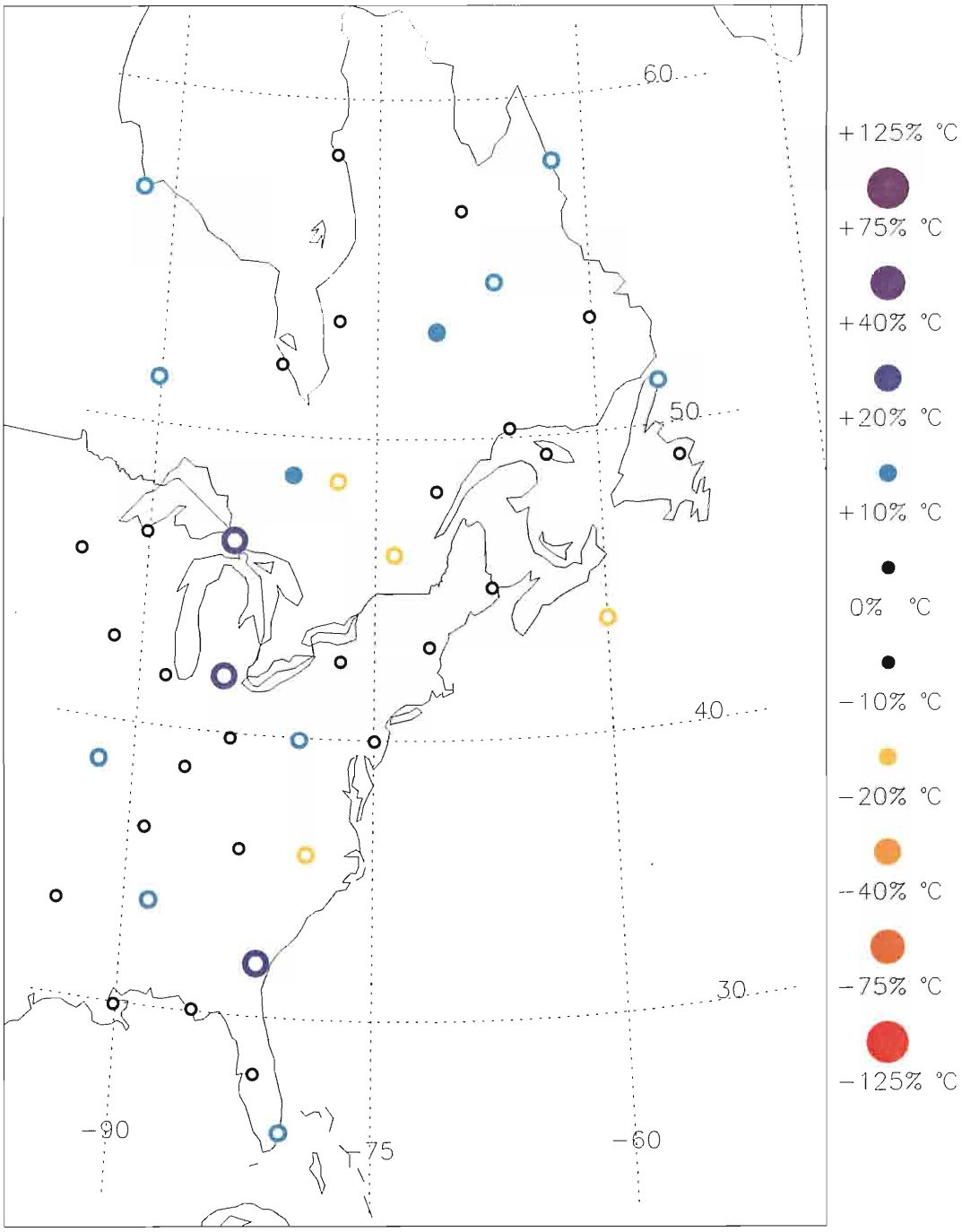

Warm-Neutral NASSTI percent precipitation deviation during OND.

Warm-Neutral NASSTI percent precipitation deviation during OND.

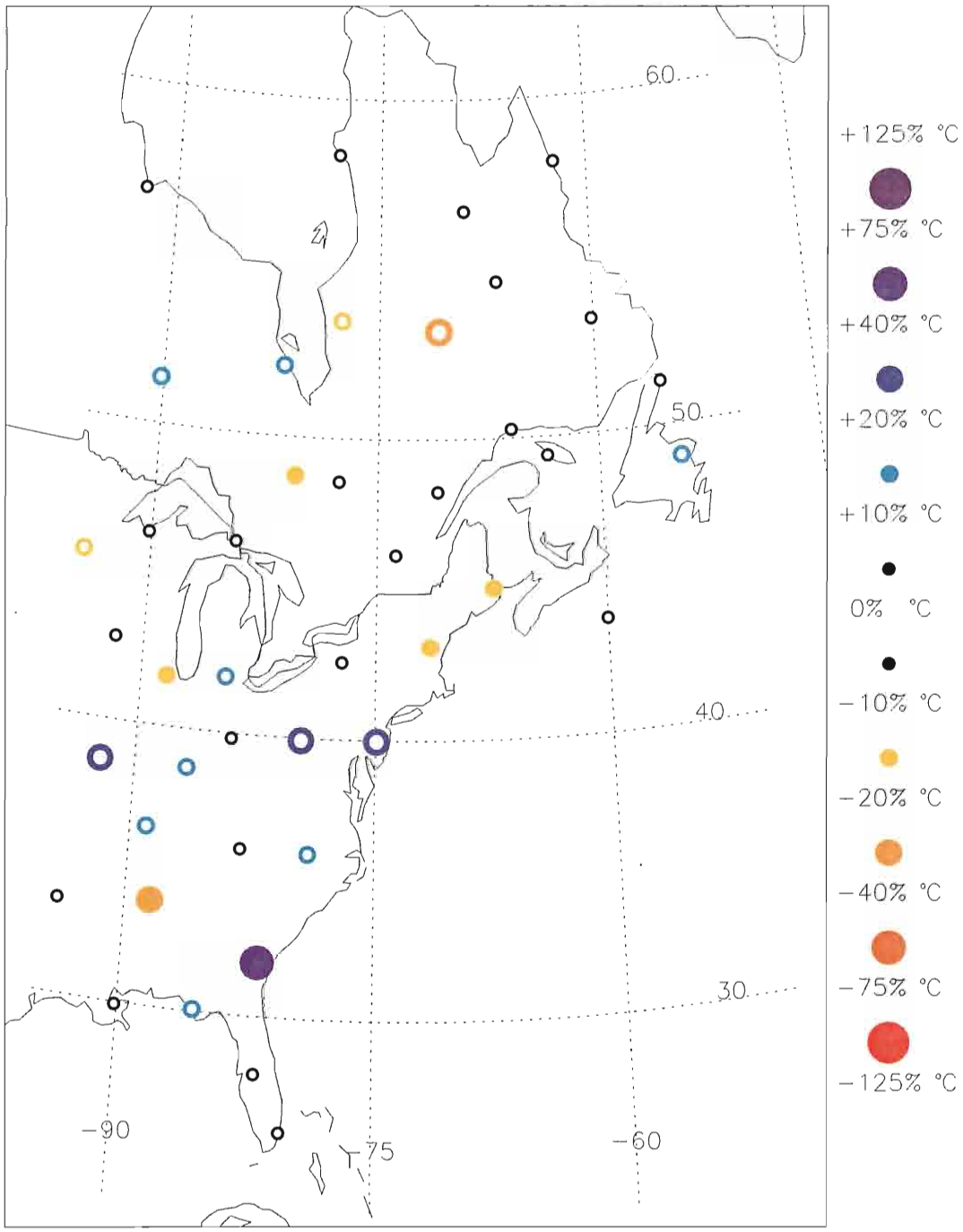

Cold-Neutral NASSTI percent precipitation deviation during DJF.

Cold-Neutral NASSTI percent precipitation deviation during DJF.

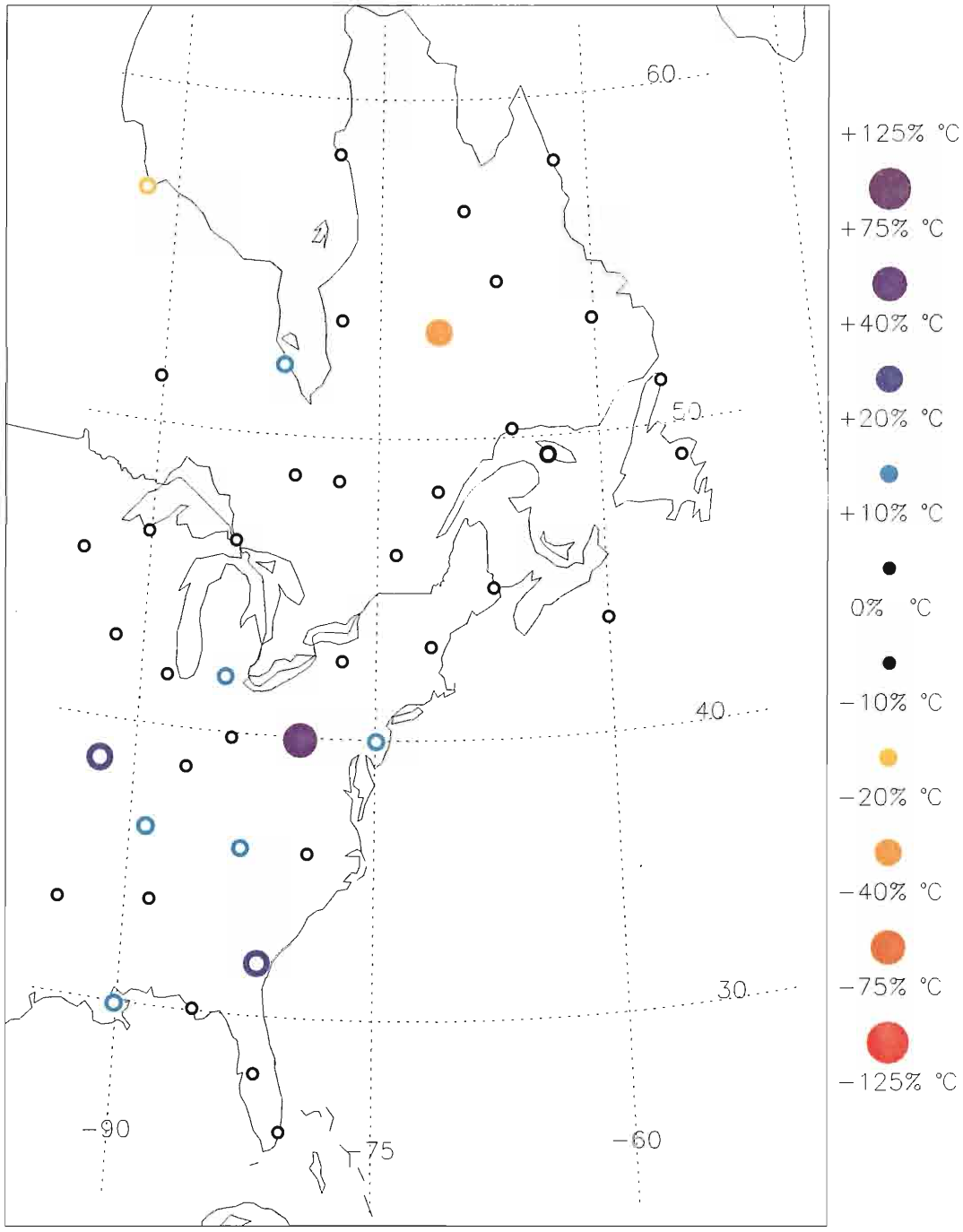

Cold-Neutral NASSTI percent precipitation deviation during JFM.

Cold-Neutral NASSTI percent precipitation deviation during JFM.

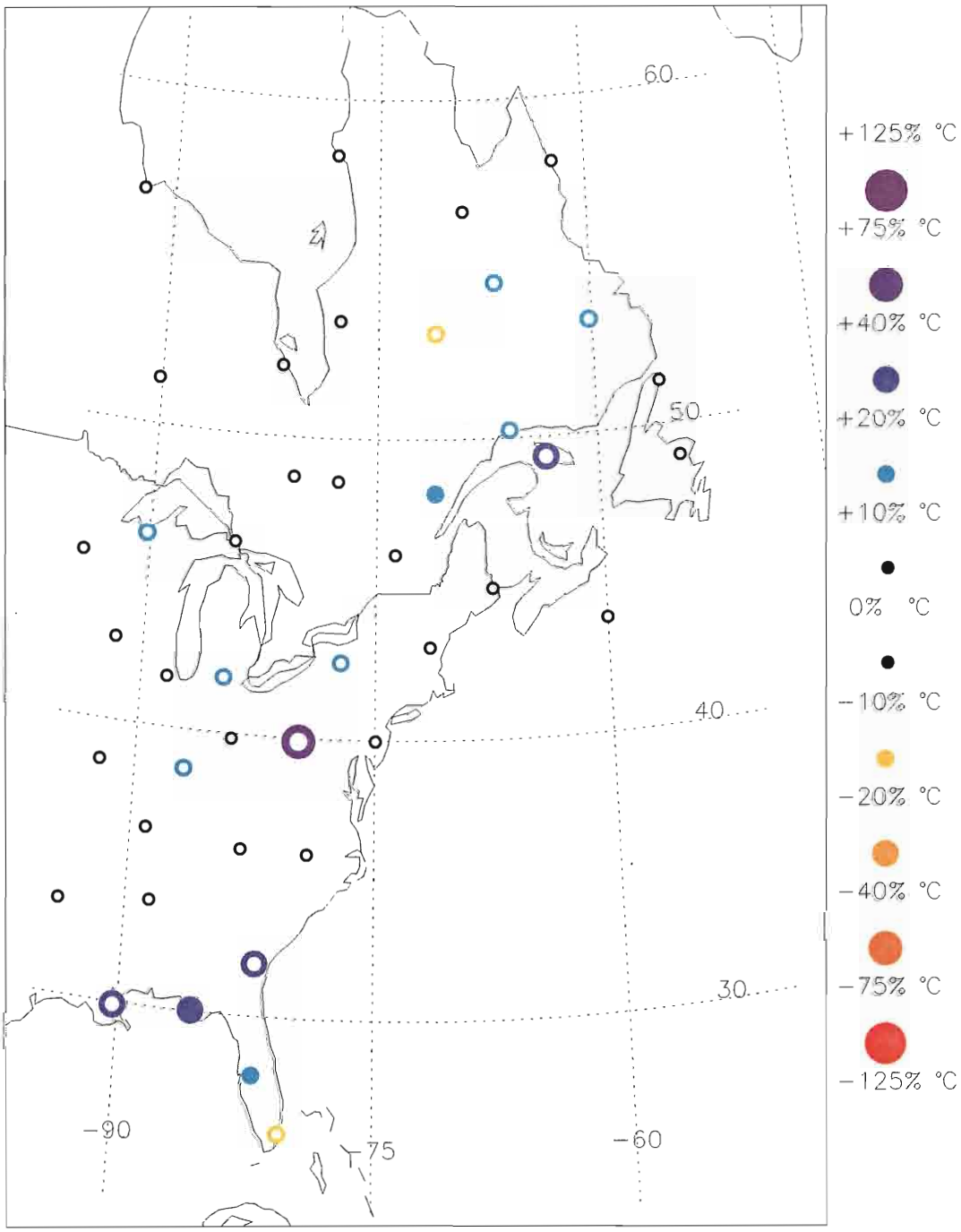

Cold-Neutral NASSTI percent precipitation deviation during FMA.

Cold-Neutral NASSTI percent precipitation deviation during FMA.

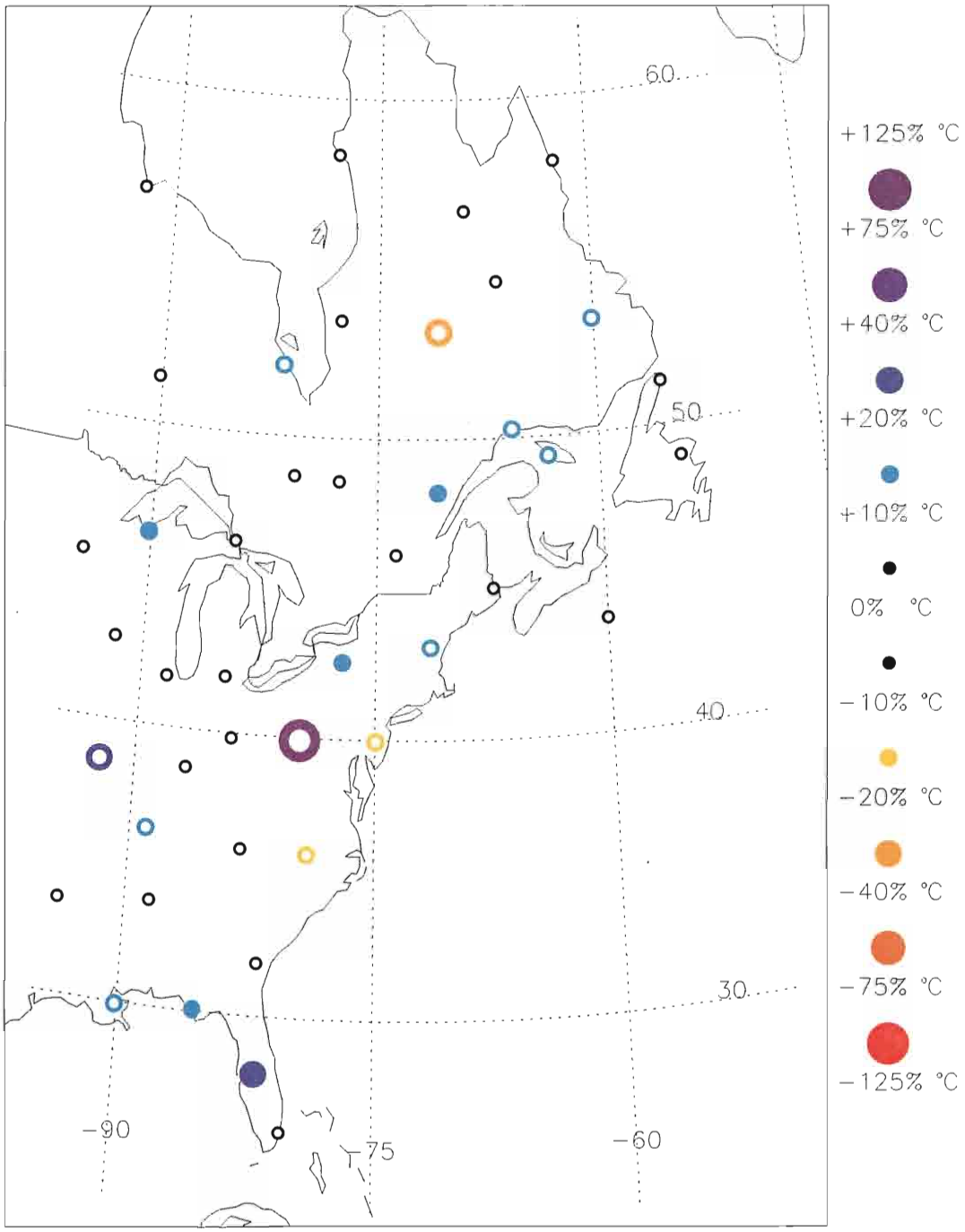

Cold-Neutral NASSTI percent precipitation deviation during MAM.

Cold-Neutral NASSTI percent precipitation deviation during MAM.

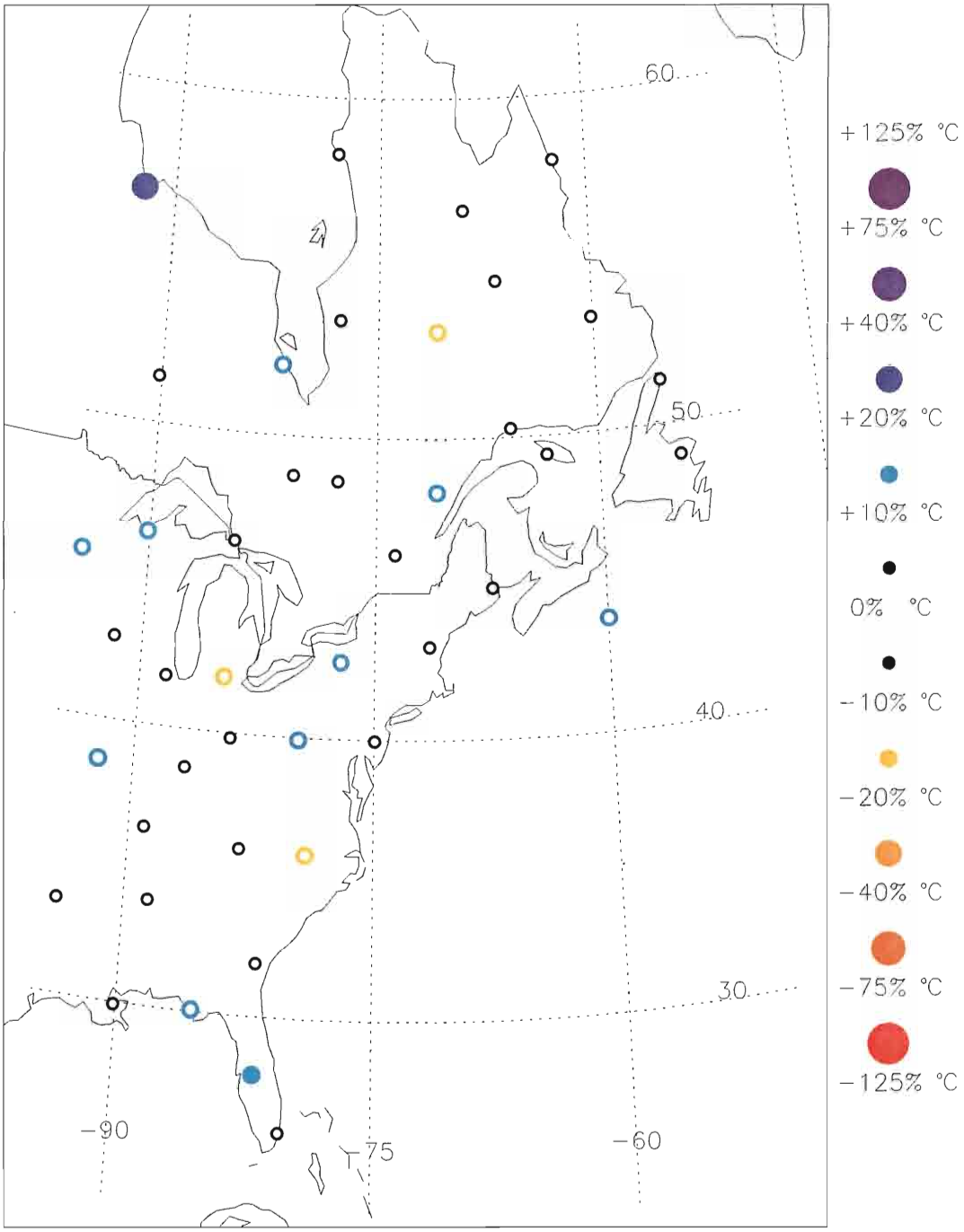

Cold-Neutral NASSTI percent precipitation deviation during AMJ.

Cold-Neutral NASSTI percent precipitation deviation during AMJ.

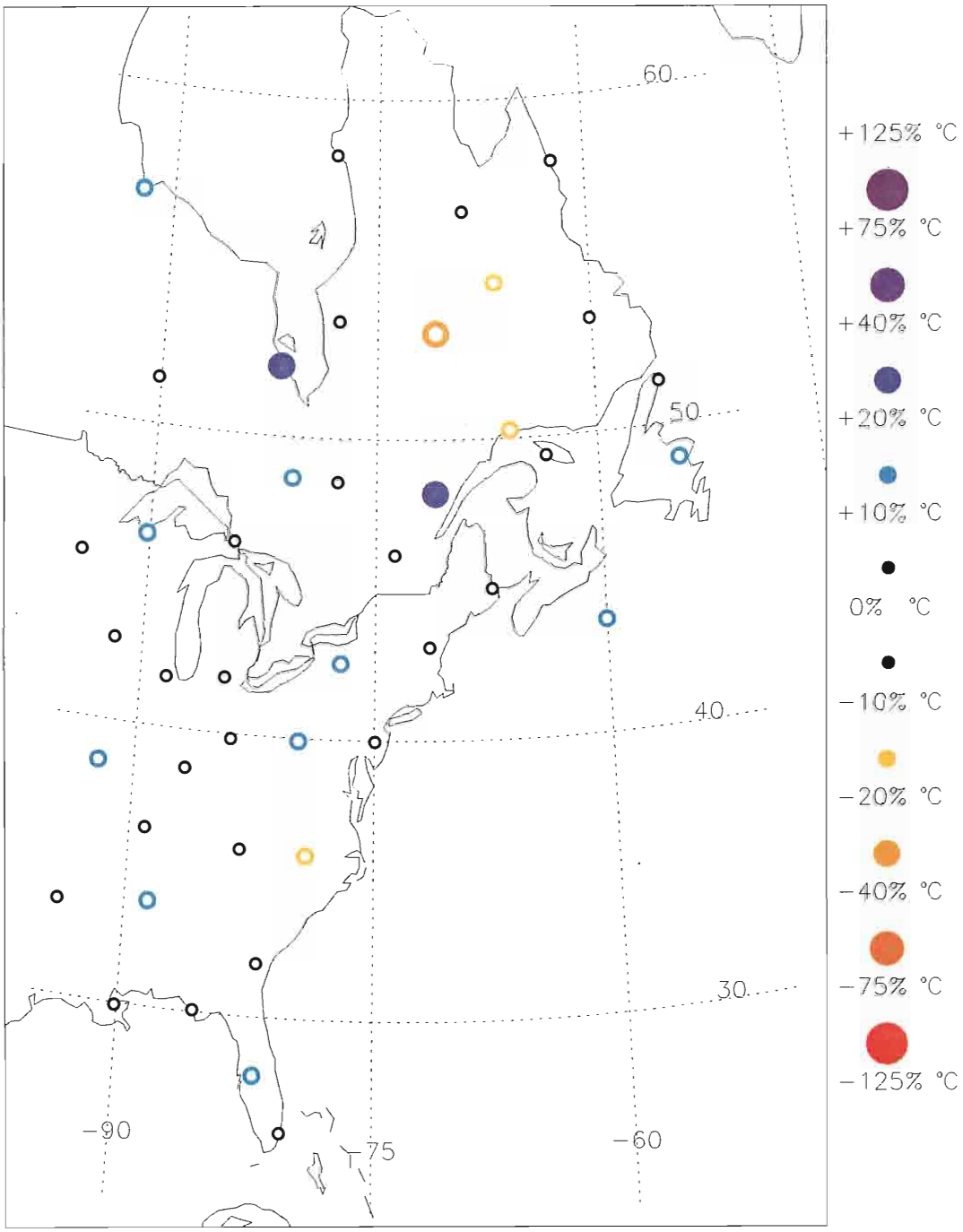

Cold-Neutral NASSTI percent precipitation deviation during MJJ.

Cold-Neutral NASSTI percent precipitation deviation during MJJ.

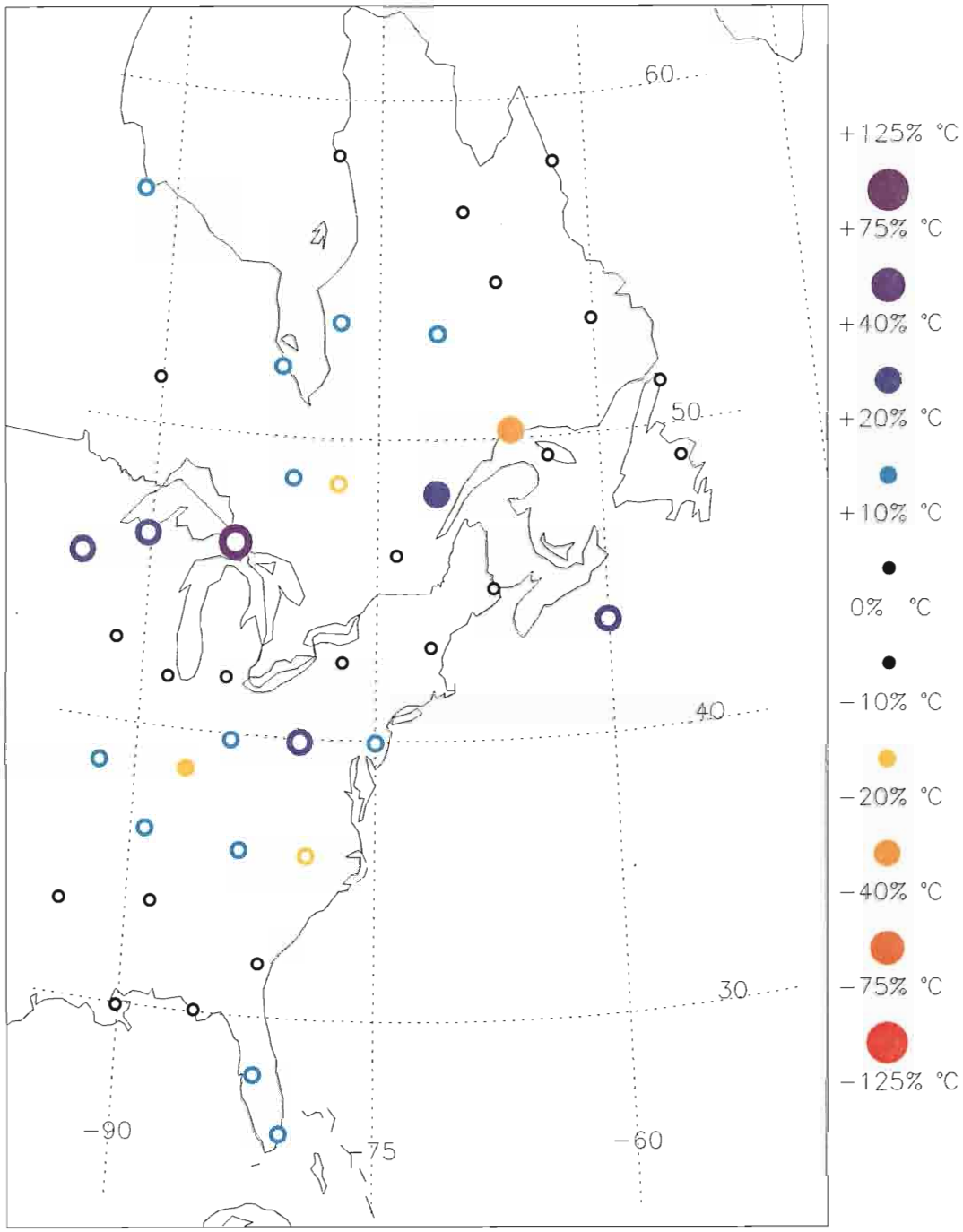

Cold-Neutral NASSTI percent precipitation deviation during JJA.

Cold-Neutral NASSTI percent precipitation deviation during JJA.

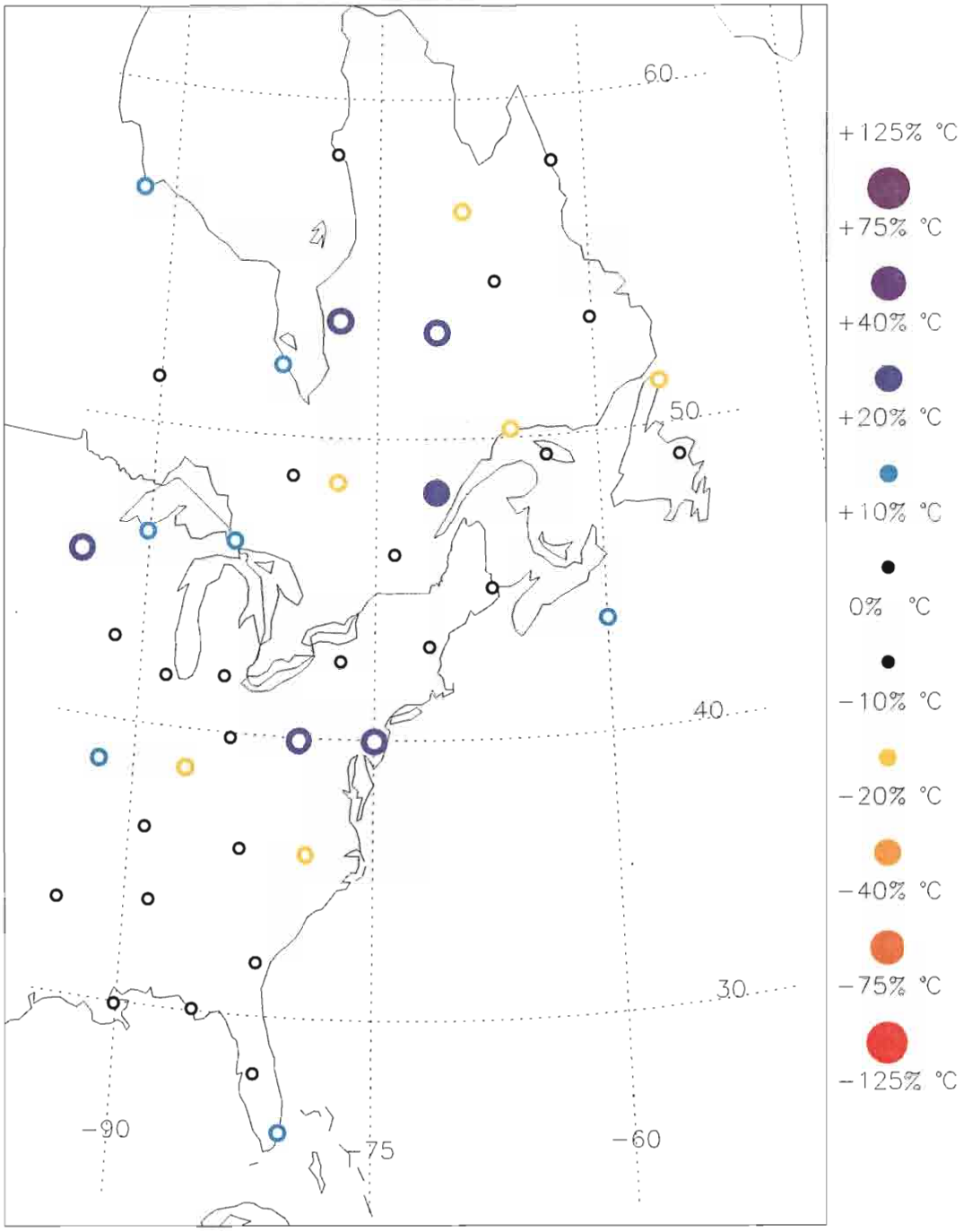

Cold-Neutral NASSTI percent precipitation deviation during JAS.

Cold-Neutral NASSTI percent precipitation deviation during JAS.

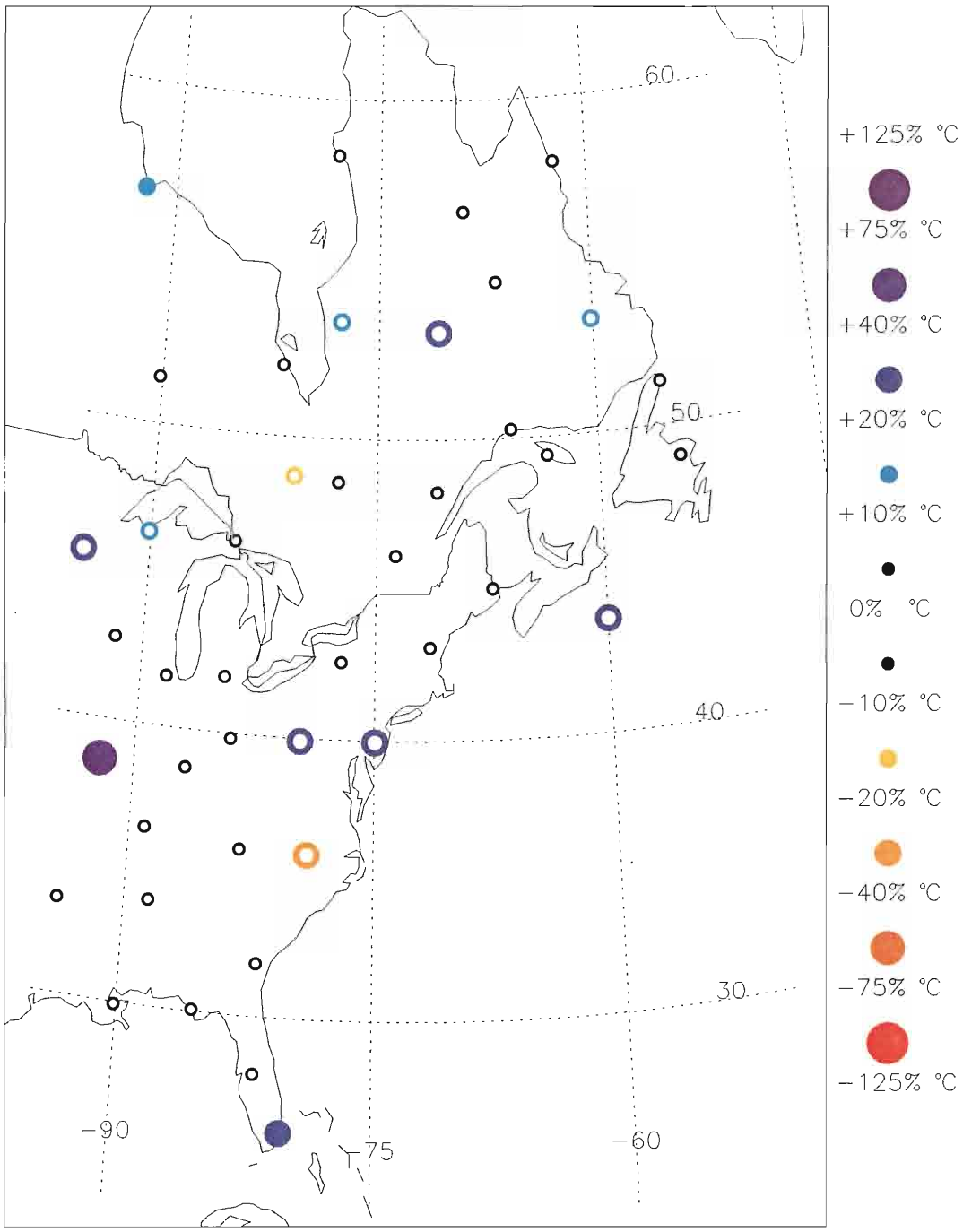

Cold-Neutral NASSTI percent precipitation deviation during ASO.

Cold-Neutral NASSTI percent precipitation deviation during ASO.

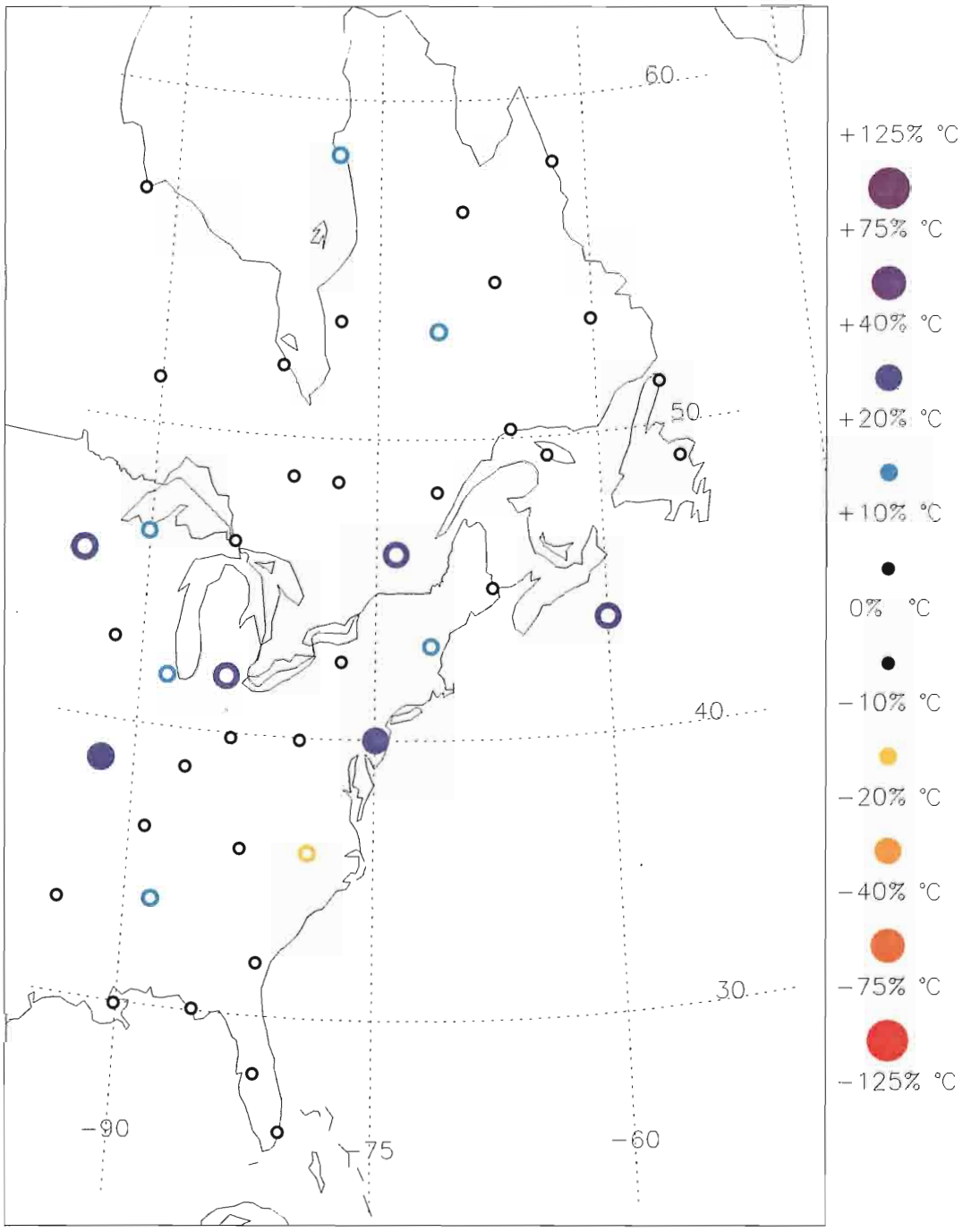

Cold-Neutral NASSTI percent precipitation deviation during SON.

Cold-Neutral NASSTI percent precipitation deviation during SON.

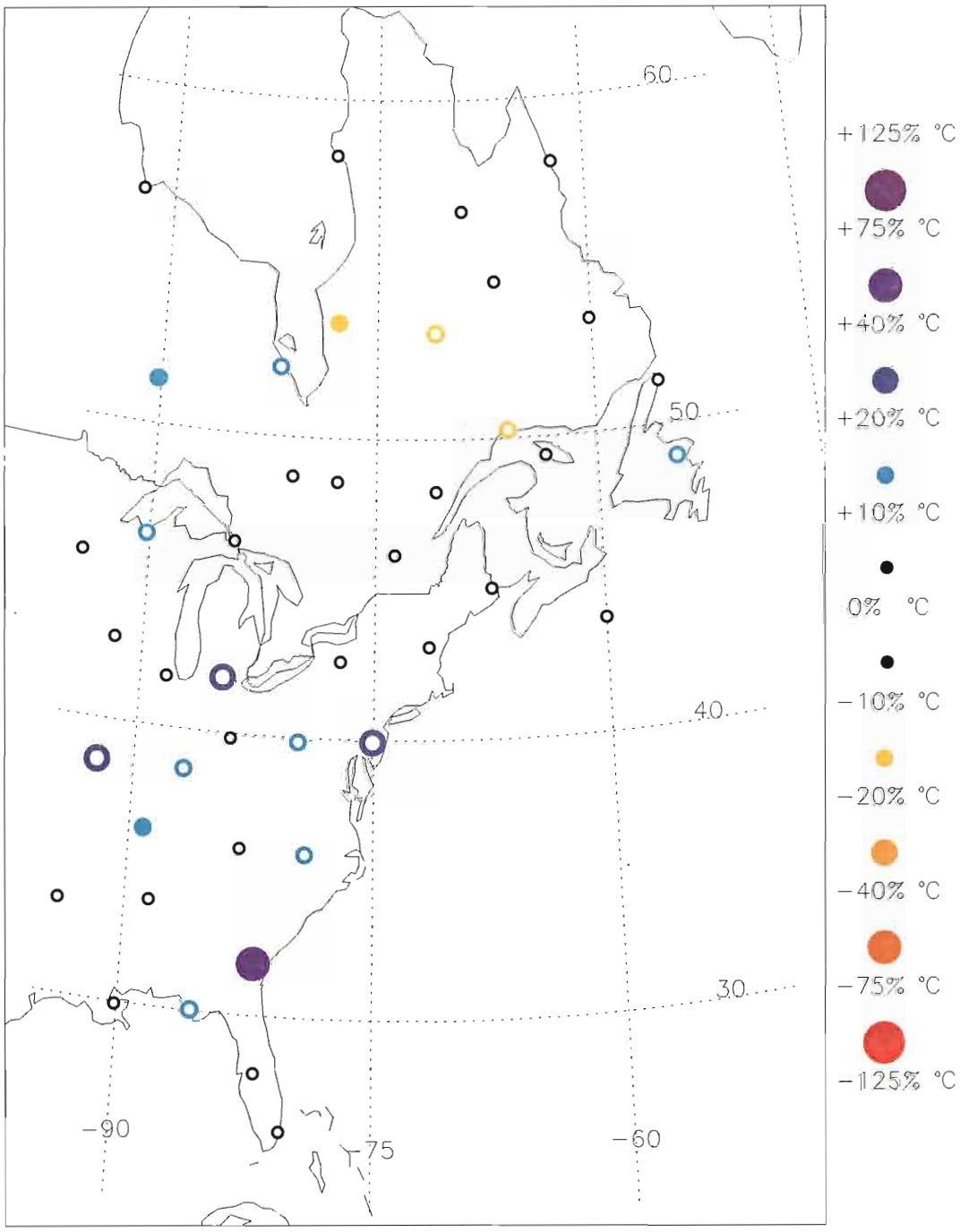

Cold-Neutral NASSTI percent precipitation deviation during NDJ.

Cold-Neutral NASSTI percent precipitation deviation during NDJ.

REFERENCES

Baldwin, M. P. and T. J. Dunkerton, 2000: Propagation of the Arctic Oscillation from the stratosphere to the troposphere. *Journal of Geophysical Research*, **104** (D24), 30,937-30,946.

Bjerknes, J., 1964: Atlantic air-sea interaction. *Advances in Geophysics*, **10**, 1-82.

Delworth, T. L., 1996: North Atlantic Interannual Variability in a Coupled Ocean-Atmosphere Model. *Journal of Climate*, **9**, 2356-2375.

Delworth, T. L. and M. E. Mann, 2000: Observed and simulated multidecadal variability in the Northern Hemisphere. *Climate Dynamics*, **16**, 661-676.

Delworth, T. L., S. Manabe, and R. J. Stouffer, 1993: Interdecadal variations of the thermohaline circulation in a coupled ocean-atmosphere model. *Journal of Climate*, **6**, 1993-2011.

Deser, C., 2000: On the Teleconnectivity of the "Arctic Oscillation." *Geophysical Research Letters*, **27** (6), 779-782.

Deser, C. and M. L. Blackmon, 1993: Surface climate variations over the North Atlantic Ocean during winter: 1900-1989. *Journal of Climate*; **6**, 1743-1753.

Gong, D. and S. Wang, 1999: Definition of Antarctic oscillation index. *Geophysical Research Letters*, **26** (4), 459-462.

Häkkinen, S., 2000: Decadal Air-Sea Interaction in the North Atlantic Based on Observations and Modeling Results. *Journal of Climate*, **13**, 1195-1219.

Higgins, R. W., A. Leetma, Y. Xue, and A. Barnston, 2000: Dominant Factors Influencing the Seasonal Predictability of U.S. Precipitation and Surface Air Temperature. *Journal of Climate*, **13**, 3994-4017.

Hurrell, J. W., 1995: Decadal trends in the North Atlantic Oscillation: Regional Temperatures and Precipitation. *Science*, **269**, 676-679.

Hurrell, J. W., Y. Kushnir, and M. Visbeck, 2001: The North Atlantic Oscillation. Temperatures and Precipitation. *Science*, **269**, 676-679.

Hurrell, J. W., Y. Kushnir, and M. Visbeck, 2001: The North Atlantic Oscillation. *Science*, **291** (5504), 603-605.

Hurrell, J. W. and H. van Loon, 1997: Decadal Variations in Climate Associated with the North Atlantic Oscillation. *Climate Change*, **36**: 301-326.

Jones, P. D., T. Jonsson, and D. Wheeler, 1997: Extension to the North Atlantic Oscillation using early instrumental pressure observations from Gibraltar and South-west Iceland. *International Journal of Climatology*, **17**, 1433-1450.

Kushnir, Y., 1994: Interdecadal variations in North Atlantic sea surface temperature and associated atmospheric conditions. *Journal of Climate*, **7**, 141-157.

Kerr, R. A., 2000: A North Atlantic climate pacemaker for the centuries. *Science*, **288** (5473), 1984-1886.

Mehta, V., M. Suarez, J. V. Manganello, and T. D. Delworth, 2000: Oceanic influence on the North Atlantic Oscillation and associated Northern Hemisphere climate variations: 1959-1993. *Geophysical Research Letters*, **27** (1), 121-124.

Mizoguchi, K., S. D. Meyers, S. Basu, and J. J. O'Brien, 1999: Multi- and Quasi-Decadal Variations of Sea Surface Temperature in the North Atlantic. *Journal of Physical Oceanography*, **29**, 3133-3144.

Parker and Rayner, 2000: Development of the Hadley Centre Sea Ice and Sea Surface Temperature Data Set (HadISST). *Proc. International Workshop on Preparation, Processing, and Use of Historical Marine Meteorological Data, Japan Met. Agency, Tokyo, Japan.*

Peterson, T.C. and R.S. Vose. 1997. An Overview of the Global Historical Climatology Network Temperature Database. *Bulletin of the American Meteorological Society*, **78**: 2837-2849.

Rodwell, M. J., D. P. Powell, and C. K. Folland, 1999: Oceanic forcing of the wintertime North Atlantic Oscillation and European climate. *Nature*, **398**, 320-323.

Shindell, D. T., R. L. Miller, G. A. Schmidt, and L. Pandoflo, 1999: Simulation of recent northern hemisphere winter climate trends by greenhouse-gas forcing. Nature, 399, 452-455

Thompson, D. W. J. and J. M. Wallace, 1998: The Arctic Oscillation signature in the wintertime geopotential height and temperature fields. *Geophysical Research Letters,* **25** (9), 1297-1300.

Thompson, D. W. J. and J. M. Wallace, 2001: Regional Climate Impacts of the Northern Hemisphere Annular Mode. *Science*, **293**, 85-89.

Thompson, D. W. J. and J. M. Wallace, 2001: Regional Climate Impacts of the Northern Hemisphere Annular Mode. *Science*, **293**, 85-89.

Trenberth, K. E. and D. A. Paolino, 1980: The Northern Hemisphere sea level pressure data set: Trends, errors and discontinuities. *Monthly Weather Review*, **108**, 855-872.

Walker, G. T., 1924: Correlations in seasonal variations of weather IX. *Mem. Ind. Meteorol. Dept.*, **24**, 275-332.

Wallace, J. M., 2000: North Atlantic Oscillation/Northern Hemisphere annular mode: One Phenomenon, two paradigms. Quarterly Journal of the Royal Meteorological Society, 126, 791-805.

Wallace, J. M. and D. W. J. Thompson, 2002: Annular Modes and Climate Prediction. *Physics Today*, **55** (2), 28-33.

Woodruff, S.D., 1987: A Comprehensive Ocean-Atmosphere Data Set, *Bulletin of the American Meteorological Society,* **68**, 1239-1250

BIOGRAPHICAL SKETCH

Anthony Arguez was born on January 14, 1978 in Miami, Florida. He is the youngest of five children born to Antonio and Angela Arguez, who came to the United States from Cuba in the 1960s. Anthony spent his entire childhood living in Miami and graduated from Miami Southridge Senior High School in 1996, finishing in the top 1% of his class. In addition to academics, he spent much of his childhood playing baseball and other sports.

Anthony entered The Florida State University (FSU) in 1996 as a sophomore. By 2000, he had obtained Bachelors of Science in Meteorology and in Environmental Studies, graduating Summa Cum Laude and With Honors. As an undergraduate, Anthony began his stay at the Center for Ocean-Atmospheric Prediction Studies (COAPS) as an undergraduate research assistant under the supervision of Dr. James J. O'Brien. Upon graduation, Mr. Arguez continued his education at FSU by enrolling in the Meteorology graduate program under Dr. O'Brien.

While at FSU and COAPS, Anthony has undertaken numerous research projects, covering such areas as the El Nino Southern Oscillation, the North Atlantic Oscillation, the Arctic Oscillation, hurricanes, and tornadoes. He has received several awards while at FSU, including a Presidential University Fellowship and an American Meteorological Society Fellowship. He has also received scholarships from the American Geological

Society Fellowship. He has also received scholarships from the American Geological Institute, the Hispanic Scholarship Fund, and several other organizations.